# Global Optimization Techniques for Dynamic Model Updating of Civil Engineering Structures

**By**

**Faisal Shabbir**

**A thesis submitted in partial fulfilment of the requirements for the Degree of Doctor of Philosophy in Civil Engineering,**
**The University of Auckland, February 2014.**

**Supervised by**

**Dr. Piotr Omenzetter**

**Department of Civil and Environmental Engineering,**
**Faculty of Engineering,**
**The University of Auckland,**
**New Zealand**

# Abstract

Due to uncertainties associated with material properties, structural geometry and boundary conditions and connectivity as well as inherent simplifying assumptions in the development of structural analysis (SA) models, the actual behaviour of structures often differs from model's predictions. On-site measurements may reveal those differences. In model updating, dynamic measurements such as natural frequencies, mode shapes and damping ratios are correlated with their SA model counterparts to calibrate the SA model. The number of measurements available is usually much smaller than the number of uncertain parameters in the SA model, and, consequently, not all uncertain parameters are selected for model updating. In this research, traditional sensitivity-based model updating method and global optimization algorithms (GOAs) are explored on two experimental structures. Three GOAs, Particle swarm optimization (PSO), Genetic algorithms (GA) and Simulated annealing (SiA), have been investigated for their efficiency and accuracy in model updating problems. Initially, the three GOAs were applied to a bookshelf-type laboratory structure and it was found that PSO proved to be computationally more efficient and accurate than the other two algorithms. The PSO was then applied to a dynamically tested full-scale cable-stayed pedestrian bridge. The limitations of sensitivity based method in dynamic model updating of full scale structure are explored. A combination of Sequential niche technique (SNT) with PSO was also proposed to systematically search the full domain and gave more confidence to the analyst by systematically exploring the full search space.

Finally, a damage estimation method was also proposed, using a multi-objective optimization (MOO) technique which simultaneously updated the damaged as well as the undamaged structural model. The technique was applied to a numerical beam model with some noise level to account for the experimental errors. It was found that the proposed method gives

relatively better damage estimation than single-objective optimization (SOO). False detections in undamaged elements were found and a regularization technique was adopted to mitigate false detections.

# ***Acknowledgements***

First, I thank the Almighty Allah, who has blessed me and given me strength to carry out this Ph.D. project.

My profound gratitude goes to my supervisor Dr. Piotr Omenzetter for his guidance and continued encouragement throughout my programme. The preparation of this thesis would not have been possible without his constructive suggestions and discussions during the research.

I would like to acknowledge Graeme Cummings of HEB construction and Ben Ryder of Aurecon for their guidance and help in model testing of the full scale bridge. I also like to acknowledge Graham Bougen and Luke Williams who assisted in this study as their part four project.

I also would like to acknowledge all the staff and post graduate students at the University of Auckland for their support and assistance in this project.

I would like to thank my friends for their continuous support and my family for their patience during my stay at Auckland.

# Table of contents

# List of figures

# List of tables

# List of abbreviations

| | |
|---|---|
| SA | structural analysis |
| FE | finite element |
| GOAs | global optimization algorithms |
| PSO | particle swarm optimization |
| GA | genetic algorithms |
| SiA | simulated annealing |
| SM | sensitivity method |
| SNT | sequential niche technique |
| DOF | degree of freedom |
| SHM | structural health monitoring |
| FRF | frequency response function |
| N4SID | numerical algorithm for subspace state-space system identification |
| MAC | modal assurance criterion |
| MSF | modal scale factor |
| COMAC | coordinate modal assurance criterion |
| EAs | evolutionary algorithms |
| SOO | single-objective optimization |
| MOO | multi-objective optimization |

| | |
|---|---|
| MOEO | multi-objective evolutionary optimization |
| NPGA | niched Pareto genetic algorithm |
| NSGA | non dominated sorting genetic algorithm |
| MOMGA | multi-objective messy genetic algorithm |
| SPEA | strength Pareto genetic algorithm |
| MOI | moment of inertia |

# List of notations

| | |
|---|---|
| ω | modal frequency |
| $\Phi$ | mode shape |
| $P$ | parameter vector |
| $p$ | candidate parameters |
| $R$ | vector of experimental modal outputs |
| $W$ | weighting matrix |
| $F$ | external force |
| $t$ | time |
| $S$ | sensitivity matrix |
| $K$ | stiffness matrix |
| $M$ | mass matrix |
| $y$ | displacement |
| Ω | diagonal matrix of square of the frequencies |
| γ | inertial weight |
| $v_i$ | initial velocity |
| $x_i$ | particle position |
| $c_1$ | cognition component |
| $c_2$ | social component |
| rand | random number between 0 and 1 |
| P (E) | probability of selection |
| E | energy |
| k | Boltzmann constant |
| T | temperature |
| $S_{XY}$ | cross power spectral density |
| $S_{XX}$ | auto power spectral density |

| | |
|---|---|
| $H(\omega)$ | inertance |
| $x^w(t)$ | signal obtained after windowing function |
| $x(t)$ | original signal |
| $w(t)$ | windowing function |
| $x_k$ | state vector at time $k$ |
| $u_k$ | input vector at time $k$ |
| $y_k$ | output vector at time $k$ |
| $A, B, C, D$ | system matrices |
| $\omega_k$ | process noise |
| $v_k$ | measurement noise |
| $U$ | block Hankel matrix |
| $W_p$ | combined block Hankel matrix |
| $Ob_i$ | oblique projection |
| $\Gamma_i$ | extended observability matrix |
| $U$ | unitary matrices |
| $V$ | unitary matrices |
| $S$ | diagonal matrix of singular values |
| $\lambda_i$ | complex eigen values |
| $\Psi_i$ | eigen vectors |
| $f_i$ | modal frequency |
| $\xi_i$ | damping ratio |
| Re | real part |
| Im | imaginary part |
| $k_{xx}, k_{yy}, k_{yx}, k_{xy}$ | resisting forces |

| | |
|---|---|
| $u_x$ , $u_y$ | unit displacements |
| $e_x$ , $e_y$ | stiffness centre eccentricities |
| $m_t$ | translational storey mass |
| $y_{cm}$ | distance to the centre of mass in y axis |
| $x_{cm}$ | distance to the centre of mass in x axis |
| $r$ | radius of gyration |
| α , β | weighting factors |
| $T_{Cab}$ | cable post-tension forces |
| $E_{eq}$ | equivalent modulus |
| E | cable material effective modulus |
| L | horizontal projected length of cable |
| w | weight per unit length of cable |
| A | cross sectional area |
| $K_{y\ Deck}$ | flexural stiffness of the bridge deck for vertical bending |
| $K_{x\ Deck}$ | flexural stiffness of the bridge deck for horizontal bending |
| $K_{t\ Deck}$ | torsional stiffness of the bridge deck |
| $K_{x\ Pylon}$ | pylon flexural stiffness of the bridge |
| $K_{Cable}$ | axial stiffness of all cables of the bridge |
| ∏ | objective function value |
| $G(x,s)$ | derating function |
| $m$ | derating value |
| $r$ | niche radius |
| $d_{xs}$ | distance between current point *x* and best individual *s* |
| ε | random number between -1 and +1 |
| $\alpha_{noise}$ | degree of noise |

subscripts:

| | |
|---|---|
| a | analytical |
| e | experimental |
| j | jth mode number |

superscripts:

| | |
|---|---|
| ' | transpose |
| * | complex conjugate |
| $\ddot{}$ | acceleration |
| $\dot{}$ | velocity |
| + | pseudo inverse |

# Chapter 1. **INTRODUCTION**

## 1.1 Background of the research

A highly developed infrastructure is vital for economic growth in this modern age. The actual behaviour of structures has often been shown to be much different from those considered in a specification-based design approach (Aktan et al. 2007). In addition, the degradation and deterioration of civil infrastructure is unfortunately inevitable due to many factors, including harsh operational conditions, physical aging and natural as well as man-made hazards (Moon and Aktan 2006). Important components of the infrastructure should maintain their service life and be able to perform well in extreme events. It is therefore important to determine the structural characteristics of infrastructural components so as to correctly predict their response (Beck and Jennings 1980). In the recent years, the investigation and characterization of constructed civil engineering facilities has gained much attention (Catbas and Aktan 2002; Catbas et al. 2007; Grimmelsman et al. 2007). A relatively high cost associated with the maintenance of the existing infrastructure is a primary motivating factor. Accurate assessment of the condition of existing infrastructure is therefore imperative to make optimal

decisions for asset management (Salawu and Williams 1995; Catbas and Aktan 2002; Grimmelsman et al. 2007).

For the design and analysis of civil engineering systems, the finite element (FE) method is widely used. Structural analysis (SA) models, based on FEs, of civil structures are usually based on idealized drawings/designs and estimates of material properties, structural geometry and boundary and connectivity conditions, which may not truly reflect the exact behaviour of the as-built system. Field tests can be performed on the full-scale structures to validate the SA models. The dynamic behaviour of structures under external excitation is of major interest to structural engineers, as the experimental responses (such as modal frequencies, damping and shapes) are related to physical properties of the system (mass, stiffness and energy dissipation). Significant differences in the dynamic behaviour of SA models and as-built systems have been noted by various researchers (Friswell and Mottershead 1995; Brownjohn et al. 2001; Schlune et al. 2009) and numerous studies focusing on damage detection and estimation have been carried out using vibration data (Hu et al. 2001; Perera et al. 2009; Huh et al. 2011; Hester and González 2012). These differences can be mainly attributed to a simplification of a complex structure and uncertainties associated with assumptions of materials, geometry, and boundary and connectivity conditions (Moon and Aktan 2006). Dynamic model updating is a process of refining a mathematical model of an actual structure using test measurements.

Dynamic SA model updating is an inverse problem in which uncertain parameters of the SA model are calibrated to minimise the error between the predictions of the SA model and the dynamic behaviour of the actual structure. This can be posed as an optimization problem in which an optimal solution is sought by perturbation of the uncertain parameters of the SA model (Jaishi and Ren 2007; Gladwell and Morassi 2011). Different optimization schemes,

driven by purely mathematical considerations, attempt to minimise the error by variation of parameters of the SA model.

It is important to note that an actual structure has an infinite number of degrees of freedom (DOFs) resulting in an infinite number of frequencies and mode shapes. It is usually not possible to measure as many frequencies and mode shapes as are required for correction of all uncertain parameters of the SA model. This can be attributed to two main reasons: the difficulties in identifying higher modes, and difficulties arising from coarse mode mapping due to limited data acquisition equipment. Therefore the number of uncertain parameters in the SA model can be more than the experimentally available information, such as modal frequencies and shapes (Jaishi and Ren 2007).

Most of the cited literature in model updating (Brownjohn et al. 2001; Jaishi and Ren 2005; Zivanovic et al. 2007) accept a single updated solution, however, it is stated that this may not be a unique solution. Contemporary model updating methods use the sensitivity method (SM) which also gives a single updated solution (Brownjohn et al. 2001) but has a tendency to converge to local minima (Deb 1998). Although model updating using SM-based optimization has been well documented, the application of global optimization algorithms (GOAs) in this field have received limited attention. Most recent studies which report GOAs are for damage detection of laboratory-scaled structures and a few well known signature structures (Perera and Torres 2006; Perera et al. 2009). Their suitability for full scale model updating problems has been relatively less explored. It is worth noting that in the dynamic model updating context, different acceptable solutions can exist, which leads to more uncertainty in the updating results, thus necessitating the need for exploration of the full search space. Motivated by these shortcomings, this research aims to investigate the efficacy of different GOAs for dynamic model updating of full scale structures. Challenges associated with current techniques especially for complex structural systems are

1. Creation of adequate SA models for these structures is not an easy task. Though there are number of guidelines and techniques are available, the selection of element types, proper discretization, boundary and continuity conditions and model updating methods depends largely on the experience of the analyst. Moreover, idealised construction drawings and construction tolerances may further complicate the situation.
2. Environmental factors and working conditions of these structures are not normally reflected in numerical models.
3. Uncertainties arising from signals of the sensors may not be accurately identified due to uncertain input loads, noise in the data, and environmental conditions etc.
4. Effective and efficient algorithms for model updating are needed to match the experimental data with the analytical predictions. The constrained optimization problem may be computationally expensive and depends on a number of uncertain parameters. Moreover, characteristics of these parameters may not necessarily be realistic making physical justification of the result difficult.

## 1.2 Objectives and scope of the research

The general goal of this research is to present a new, robust model updating technique using GOAs to improve understanding of the dynamic behaviour of full scale civil engineering structures by calibration of the analytical models. Detailed objectives of this research are as follows:

- To explore several GOAs, including Particle swarm optimization (PSO), Genetic algorithms (GA) and Simulated annealing (SiA) for calibration of the SA models in dynamic model updating problems,
- To ensure that an optimal solution is reached with increased confidence by exploring

the full search space, and

- To propose a more efficient structural damage estimation method (which is a special case of model updating).

The scope of this study consists of forced vibration testing of a laboratory structure and a full scale bridge structure to acquire global dynamic characteristics of these systems, including natural frequencies, damping ratios and mode shapes. Three GOAs, namely PSO, GA and SiA, have been explored for dynamic model updating. These GOAs are selected due to their differences. PSO uses a velocity equation, GA uses three operators namely selection, cross over and mutation, and SiA uses the Metropolis algorithm for perturbation of the individuals in the search space for minimization / maximization of a particular objective function. To ensure that the optimal solution has been reached, a combination of PSO and sequential niche technique (SNT) is proposed. Also, to enhance the performance of damage estimation procedure, a multi-objective Non-dominated Sorting Genetic Algorithm (NSGA-II) for damage estimation is also investigated. Furthermore, a simple regularization using GOA is also investigated to avoid erroneous damage detections. It was assumed that errors between experimental data and analytical model predictions are due to inaccuracies associated with the modelling parameters, and the global dynamic characteristics such as natural frequencies and mode shapes are used for model calibration of linear systems.

## 1.3 Contributions of the research

The primary contribution of this research is the development of a novel robust model updating algorithm that can be used to identify uncertain physical properties of civil engineering structures by calibration of SA models using experimental dynamic information. A laboratory bookshelf-type structure was tested to determine its dynamic properties and three global modes of vibration were found. An analytical model of the laboratory structure

was updated to assess its physical properties. The three GOAs were applied to obtain an updated solution and their performance compared. It was found that PSO performed better than GA and SiA in terms of accuracy and computational efficiency.

A full-scale bridge was then tested using electro-dynamic shakers to obtain its dynamic properties. Eight global modes of vibration were found, which included two similar vertical modes. A SA model of the bridge was updated using the natural frequencies and mode shapes by the three GOAs to find out its physical properties. PSO was applied for model updating as it is found to be more efficient than other two algorithms. Sensitivity based model updating was also applied to compare its results with PSO based model updating. However, GOAs cannot ensure that the optimal solution of the error function has been reached. The problem was therefore transformed to an exhaustive search using the SNT with PSO. This technique significantly improves the analyst's confidence in the updated results as it gives more information about the search space. Important practical conclusions were drawn from the final updated results obtained for the bridge. For example, the updated results revealed that there is only partial composite action between the cast-in slab and the steel girder, resulting in lower stiffness of the whole deck.

Another contribution of this research is related to damage estimation using model updating. Contemporary approaches to damage estimation compare model updating results for the undamaged and damaged structure acquired separately. A damage detection method which simultaneously updates the undamaged as well as the damaged structure model in a multi-objective optimization (MOO) process is presented herein. A better estimation of damage was obtained with this technique as it effectively uses the experimental data of both the undamaged and damaged structure. However, it has been found that the MOO process also leads to false detections in undamaged elements. Therefore a regularization technique is adopted using PSO which has resulted in successful detection of damage.

## 1.4 Thesis outline

The outline of this thesis is as follows:

Chapter 1 describes the background, objectives, scope and contributions of this research.

Chapter 2 presents a review of the structural health monitoring (SHM), modal testing and model updating methods. Different types of uncertainties encountered in model updating problem have been studied. The role of initial modelling and experimental testing is explained and various methods to correlate experimental and analytical data in model updating are reviewed. Ill-conditioning in the SA model updating technique and its remedies are discussed. Finally some of the successful applications of model updating in civil engineering along with their limitations are discussed.

In Chapter 3, the theory of three GOAs, namely PSO, GA and SiA, which have been used in this research, is discussed in detail. The three GOAs are compared with each other and with the sensitivity based method.

In Chapter 4, modal testing of a three dimensional, bookshelf-type, laboratory structure is presented. An introduction is given to system identification techniques such as spectral analysis, frequency response function (FRF) and numerical algorithms for subspace state-space state space system identification (N4SID) methods. An analytical mass-spring model is derived for the laboratory structure and the three GOAs are compared for obtaining an updated solution of the analytical model. A detailed SA model of the structure is also updated using PSO to study the joints in the structure.

In Chapter 5, modal testing of a full-scale cable-stayed pedestrian bridge is described. Modal characteristics were determined using system identification techniques. An initial SA model is updated using standard SM and PSO. Later SNT with PSO is applied for exploring the full search domain.

In Chapter 6, an introduction to MOO algorithm NSGA-II is given. The MOO procedure is applied to model updating of a numerically simulated beam, and its undamaged and damaged states are concurrently updated to estimate damage. Later a simple regularization technique is adopted to mitigate false detections in the undamaged elements using PSO.

In Chapter 7, a summary of the key results along with recommendations for future work are given.

# Chapter 2. **LITERATURE REVIEW**

## 2.1 Introduction

A literature review, confined to the areas of SHM, modal testing and model updating is presented in this chapter. The review starts with defining the SHM and its role in assessment of structural behaviour. Three basic components of the SHM: sensor system, data processing system and health diagnostic system are explained. The advantages of SHM over other condition assessment methods are presented, with an emphasis on dynamic testing as a well-established methodology for SHM. Following this, the topic of structural identification of civil constructed systems is reviewed and its important components such as initial SA modelling and modal testing, are discussed. The modal testing is further sub-divided into excitation sources, sensing equipment, and data acquisition and processing uncertainties associated with the modal tests are discussed. Methods for correlating experimental and analytical data are then summarised. These methods include correlation between frequencies and mode shapes obtained from experimental and SA model. After this, the basics of dynamic model updating of civil structures are introduced and the goals of optimization are explained in the context of model updating. Common model updating techniques related to

manual model updating, SM-based model updating, and GOAs based model updating are detailed. Important factors in model updating, such as the selection of objective function, updating parameters and robust optimization algorithm, are discussed and problem of ill-conditioning is explained. Lastly, some recent literature related to applications of model updating using SM and GOAs are detailed. Due to the superiority of GOAs over SM, different GOAs are further investigated in this thesis for model updating purposes.

The term finite element (FE) model is a commonly used analogue in the previous research related to model updating. However, the FE models are usually limited to models where restricted displacement of force distributions are required in the formulation of the element properties. Therefore in the context of the work presented in this thesis, the term "structural analysis (SA)" model has been used instead of "FE" model.

## 2.2 Structural health monitoring

SHM is defined as tracking the structural responses, possibly along with inputs, over a sufficiently long duration to determine deterioration, anomalies and damage in a structure, in order to make optimal decisions for asset management (Aktan et al. 1998). More specifically, the responses of the system should be measured under operating and loading conditions in such a way that any operational incidents, damage or anomalies that can affect the serviceability and reliability of the structure are detected (Aktan et al. 2000).

Three major components of SHM are (Li et al. 2007) the sensor system, the data processing system and the health diagnostic system. The sensor system is usually attached or embedded in the structure to measure structural responses such as strain, displacement, stress, acceleration, as well as structural inputs such as wind speed and temperature. Sensors used for measuring structural responses include accelerometers, linear voltage displacement transducers (LVDT), strain gauges etc., whereas sensors used to measure environmental

parameters include anemometers, thermistors etc. A combination of several sensor types can be used to identify the effect of different environmental variations from structural responses. A data acquisition system is normally used to transfer raw data from the sensors to where it is stored for subsequent analyses. Finally, these responses will be interpreted to make critical decisions related to system reliability and load capacity. Diagnostic and prognostic algorithms (De Lautour 2009) based on time series analysis, pattern recognition and modal analysis are commonly used to assess the condition of structures, and to identify damage location and severity.

There are several advantages associated with SHM of infrastructure over other non-destructive condition assessment methods. Non-destructive tests (Jang et al. 2006; Shah and Ribakov 2009; Shah et al. 2011), including magnetic particle, radiographic and ultrasonic testing etc., have several limitations in their application to full-scale structures. For example, they have limited depth of penetration and thus are only able to provide an indication of the local health of a structure, while damage location needs to be known before testing. Also it is very difficult to determine the condition of joints and boundaries. On the other hand, SHM may help in obtaining and identifying the local as well as the global structural characteristics. An efficient SHM system can determine and evaluate serviceability, reliability and the remaining service life of the structure (Auweraer and Peeters 2003).

SHM is generally envisaged to perform the following functions (Aktan et al. 1998):

- Detect damage in a structure at an early stage to ensure optimal structural operation,
- Provide information about the condition of a structure after extreme events,
- Provide prioritization in terms of rehabilitation, maintenance and repair of structures,
- Validate the design assumptions for improving design specifications and guidelines for future structures,

- Monitor repairs to evaluate the effectiveness of the rehabilitation and retrofit processes,
- Obtain a database of records from different structures for research and education purposes, for the innovation of new structural types and application of smart materials.

### *2.2.1 Difference between constructed and manufactured systems*

The fundamental difference between constructed and manufactured system is the level of associated uncertainties. In constructed systems, initial SA models and measured data is frequently subjected to uncertainties associated with our inability to correctly model, understand and predict the behaviour of the system. The magnitude of the aforementioned uncertainties is often many times larger than the random experimental uncertainty.

Much of the research in SHM has been confined to laboratory scale structures and cannot account for the complexity of in situ constructed systems. Unique attributes of constructed systems are heterogeneity, boundary and continuity conditions, intrinsic forces, non-linearity, non-stationarity, uniqueness and changes during their lifecycle. Material properties, dimensions and detailing vary from member to member and within a member, and is further complicated by deterioration in these structures over their lifetime. Constructed systems have complicated soil-foundation interaction and are often non stationary in their behaviour. Continuity conditions of these structures, especially bridges, consist of movement systems which behave differently under different force levels. These systems have complex intrinsic forces due to dead loads, live loads, deteriorations, overloads, damage, staging etc. which are difficult to measure in an absolute sense. Many different types of non-linearities such as yielding, connection slip, friction between interfaces etc. that change in different limit states further complicate the situation. Nearly every constructed system is unique and custom

designed for its intended purpose. Applying results from single structure to a larger population is difficult and challenging due to its uniqueness.

Dynamic testing is a well-established methodology for SHM now-a-days, overcoming the disadvantages and limitations of traditional visual inspection methods. Full-scale dynamic testing results represent structural responses with proper boundary conditions and eliminate any need for scaling. The results from full-scale testing can also provide a benchmark to calibrate structural models and help in developing new mathematical models capable of representing the true behaviour of structures. Dynamic identification of full-scale structures such as concrete and masonry buildings, towers and bridges have been performed by many researchers under different loading conditions. (Ellis 1996; Li et al. 2004; De Sortis et al. 2005; Chen and Zhou 2007). Because of the advantages associated with full-scale testing, many structures have been equipped permanently with monitoring systems capable of measuring their responses under actual service loading and earthquake excitations (Skolnik et al. 2006). The information from such systems is periodically updated to assess the ability of the structure to perform its intended function. Efforts have also been made to compare the results of laboratory scale and full scale structures (Okada and Ha 1992).

## 2.3 Structural identification

Structural identification of large constructed systems typically requires the integration of structural conceptualization, analytical or SA modelling, experimental execution, data processing, model calibration, simulation, interpretation and decisions (Brownjohn et al. 2001). Experimental responses are related to the physical properties of the system and changes in these physical quantities will be reflected as a change in the experimental responses. Therefore in order to identify actual physical characteristics of structures, it is necessary to carry out field tests and measure the resulting responses to correlate and validate

the SA models. Both static and dynamic tests can be carried out on the actual structure for structure assessment. Different important components of the structural identification process are detailed in the subsequent sections.

### *2.3.1 Initial structural modelling*

SA models are mathematical models which provide a means of predicting characteristic responses of structures without actually building them. In SA models, the continuous domain of the actual physical structure (with infinite DOFs) is discretized into small components called FEs. These models have been extensively used in industrial and research applications as they give a reasonable representation of the actual structure. However there are certain inaccuracies and errors in SA models (Moon and Aktan 2006) arising mainly from: 1) incorrect assumptions related to physical properties such as modulus of elasticity of materials and mass densities, 2) discretization errors due to coarse or poor mesh and/or due to faulty assumptions in individual element shape functions, 3) inaccurate approximation of boundary and continuity conditions, 4) inaccurate modelling of joints, and 5) inaccuracies in estimation of spatial characteristics of actual members.

Due to these reasons, it is hard to obtain a SA model which accurately represents the as-built structure and actual structures always differ from their SA models. Especially, the materials and geometric properties of the actual systems can be very uncertain, as well as continuity conditions and coupling effects may not be taken accurately into account in the development of these SA models. As a result, less confidence is usually placed on the SA models leading to higher factors of safety in the design and evaluation process. The SA models, therefore, need to be validated experimentally.

### *2.3.2 Modal testing*

To increase the knowledge and understanding of actual structures, the responses of the structures are observed under a set of known conditions. Vibration testing to determine the experimental modal characteristics of a structure such as natural frequencies, mode shapes and damping is referred as modal testing. This is accomplished by performing a modal test which includes exciting and capturing the responses of a structure by a set of sensors. The experimental setup generally consists of three main components, i.e. excitation, sensing, data acquisition and data processing (Clarence and De Silva 2007).

#### *2.3.2.1 Excitation*

There are three different major types of dynamic tests (Salawu and Williams 1995) depending on the type of excitation used, i.e. forced vibration tests, ambient vibration tests and free vibration tests.

In forced vibration tests, the structure is excited by a known input force. The input excitation to the structure is provided by properly designed excitation systems, which entails application of a known force at particular frequencies or frequency bands of interest (Causevic 1987; De Sortis et al. 2005). This method is based on the fact that if the loading on the structure and resulting responses are known, then the structural characteristics can be more unambiguously determined. By the use of a known forcing function, several uncertainties related to data processing and collection can therefore be avoided. These types of tests also enable achieving higher signal-to-noise ratios in the response measurements (Salawu and Williams 1995). The structures can be excited by shakers or instrumented impact hammers. Two different types of shakers can be used, a linear mass shaker and an eccentric mass shaker. Linear mass shakers can impart a combination of steady state sinusoidal as well as transient state waves, whereas eccentric mass shaker can only impart sinusoidal forcing. Both types of

shakers can be used for horizontal or vertical excitation of the structure. However, the impact hammers can only impart impact force to the structure. Impact hammers can be hand-held, machine-lifted or dropped. Different levels of forces can be generated by using different weights. The advantages associated with impact hammers are that they are fast in their application and tests can be quickly repeated a number of times. Although heavy shakers and heavy drop weights are available, the size of the structure may limit the use of forced type of excitation to full-scale structures. Also, the structure may have to be closed for operations for this type of forcing to reduce the effects of unknown excitations.

In ambient vibration tests, the excitation is not under control and is usually considered to be a stationary random process, which means that the response data from the structure alone can be used to estimate the dynamic parameters. The increasing popularity of this method is because no forcing machinery is required. Ambient excitation can be from sources such as wind, pedestrian or vehicular traffic, earthquakes, waves or similar. For very large and massive structures, ambient excitation is often the only practical choice. Structural identification through ambient vibrations has been successful in numerous cases (Ivanovic et al. 2000; Ventura et al. 2003). However, ambient vibration testing has some important drawbacks, mostly associated with the lack of information on the actual forcing function. Most of the ambient identification procedures assume a white noise excitation, which is at best is only a reasonable approximation, and can be wrong at worst, leading to imprecise or wrong system identification results. A considerable degree of non-linearity exhibited by real structures and a low signal to noise ratio can also complicate the analysis in these tests.

In free vibration tests, the vibration is introduced in the structure by initial inputs only. The structure is disturbed from its initial static equilibrium position and is allowed to move freely (Friswell and Mottershead 1995). No external force is applied to the structure during free

vibration. The energy of the system decays due to material, structural and fluid damping. It is difficult to apply this type of excitation to full-scale structures.

#### *2.3.2.2 Sensing*

The sensing system is composed of transducers aimed to measure the structural responses. A detailed summary of different sensors used for measurement can be found in many text books (Ohba 1992; Wilson 2005; Ecke et al. 2008). Different sensors are used for different measurement purposes such as velocity, displacement, accelerations, temperature, pressure, stress, wind etc. They are categorised on the basis of operating principle or measurand. For modal testing purposes, accelerations are a common choice for short and long term monitoring. Different types of accelerometers are available, such as capacitive accelerometers, piezoelectric accelerometers, strain gauge accelerometers, fibre grating accelerometers, micro-electro-mechanical systems (MEMS) accelerometers and servo accelerometers. The accelerometer measures the accelerations at a specific point of the structure and generates electric signals in the form of voltage to be read by an instrument. Conditioning amplifiers are used to amplify the signals; if the signals become very weak and they can amplify both their magnitude and phase. The sample rate of the dynamic data depends upon the frequency range of the loading and the nature of the structure. Normally the default seismometer is of 100 Hz bandwidth.

#### *2.3.2.3 Data acquisition and processing*

Data acquisition is a procedure in which the data in the form of digital or analogue signals from the sensing mechanism is converted into digital data and stored permanently on a computer. The data processing is a critical step aimed for error mitigation and parameter estimation. Data is checked for errors related to the quantization, aliasing, filtering and leakage in the first phase. Parameter estimation involves identification of the magnitude and

phase of different signals obtained from various parts of the structure and extraction of the modal information that includes modal frequencies, mode shapes and damping characteristics (Ewins 2000). Two different classes of analytical procedures are available, time domain methods and frequency domain methods. The first type determines the structural characteristics directly from the time domain data, whereas the second type converts the data into the frequency domain first, to extract modal information. More details of the time and frequency domain methods used in this study are given in Chapter 4.

#### *2.3.2.4 Uncertainties associated with system identification*

System Identification (Sys-Id) of civil structures has gained a huge attention of the researchers in the modern era of enhanced computational technologies. There are many uncertainties which play a significant role in the Sys-Id process when considering the constructed civil structures. There is a need for proper uncertainty analysis as a part of Sys-Id that supports the decision making such as the management of infrastructure systems, retrofit, and maintenance. The uncertainty is not new in structural engineering as it has been applied in the field of structural safety and reliability analysis for many years. However, the lack of knowledge in areas such as actual loading phenomenon, actual force distribution in structural elements, resulting failure modes, and the structural capacity of civil structures, result in the uncertainties with a Sys-Id process. The types of uncertainties are important to be understood while doing a Sys-Id for civil structures.

There are two major types of uncertainties involved i.e., uncertainties arising due to natural variable phenomena (aleatory uncertainty), and uncertainties arising due to lack of knowledge (epistemic uncertainty). Aleatory uncertainty is associated with the randomness in the environmental factors and natural variations in the system of the structure under consideration. The aleatory uncertainty is described in term of probability and is modelled

with probability theories considering various probability distributions. Although this type of uncertainty cannot be minimized however, more information might help in determining the factors controlling this type of uncertainty. The epistemic uncertainty is due to lack of knowledge. There are two features that can be associated to epistemic uncertainty: 1) potential of inaccuracy meaning that inaccuracy may or may not exist in development of model; 2) incomplete information, which is the basic cause of the epistemic uncertainty. The reason for incomplete information is the uncertainty in either experimental data or modelling technique. The experimental and modelling uncertainties are addressed further.

#### 2.3.2.4.1 Experimental uncertainties

In most of the Sys-Id studies, the structural response data obtained from an experiment is used as a base line to validate the analytical model. The basis of this method is the assumption that the experimental data obtained from a real life structure depicts the actual behaviour of the structure and the analytical model can predict the same values when the various model parameters depict the actual parameters accurately. But it is well known fact that both the experimental data and analytical predictions are not free of errors. As the experimental values act as a baseline in a model updating process, the errors in experimental data create uncertainties about the accuracy of analytical model and therefore effect the engineering decisions followed. In this section the uncertainties induced in data recording and processing are discussed. The uncertainties can come through variations in the mode of excitations, various environmental effects, different boundary and continuity conditions, and data processing.

The difficulties in exciting the large structures have been thoroughly discussed by Wenzel and Pichler (2005). The modern trend towards *mode of excitation* is through the ambient vibration test using primary traffic however as there is no input information in this method, and the results are sometimes questionable. Various factors that can cause high uncertainties

in the obtained results are due to low amplitude of excitation (Brownjohn et al. 1989), difference in excitation techniques (Farrar et al. 2000), placement of excitation source (Catbas et al. 1998), and non-stationary nature of the input (Wilson and Liu 1991). Brownjohn et al (1989) was unable to reasonably identify the lateral mode shapes as the amplitude of excitation in the lateral direction was very low. Different types of loading cause different amplitudes of vibration and Farrar et al (2000) observed significant changes in damping ratios while changing the mode of excitation. Catbas et al (1998) compared different locations for forced excitations and found that the forced excitation near a nodal point of the structure resulted in several poor excitation modes. Wilson and Liu (1991) found it difficult to determine the damping ratios due to the non-stationary nature of input. Hence the mode of excitation should be paid proper attention so as to reduce the uncertainties in the experimental data.

Along with variations in excitation methods, the changes in modal properties can occur due to variations in *environmental factors* such as changes in temperature, wind speed, cloud cover and humidity. Farrar (1997) found 5% changes in structural responses in a 24 hour time attributing changes to temperature variation. Due to freezing asphalt, the first eight eigen frequencies were observed to vary within a range of 14-18% (Peeters and De Roeck 1998). Due to freezing of supports the $2^{nd}$ and $3^{rd}$ eigen frequencies increased up to 50% (Alampalli 1998). Wind also plays some role in varying the eigen frequencies of the structure as it was noticed by Fujino and Abe (2002) that first vertical bending mode decrease significantly with an increase in wind speed. Along with temperature and wind, humidity and cloud cover tend to change the boundary conditions of structures (Aktan et al. 1997).

*Boundary and continuity conditions* of constructed structures are very hard to perceive and there is a lot of uncertainty involved. Brownjohn (2003) observed that there was 50% increase in the modal frequency of a bridge due to the rotational restraint at the abutment.

Soil structure interaction is very important when creating an analytical model for a structure as it was observed that modal parameters varied for isolated and fixed base conditions (Luco et al. 1988). Even without any shear connections, the bridge behaved like a composite structure due to chemical bond (Catbas et al. 1998). The movement mechanisms of the bridge were considered fully constrained in order to come close to real values (Catbas et al. 2007).

There are a lot of uncertainties present in the outcomes after *data processing*, as many thousands of data points are reduced to modal frequencies, modal shapes and damping ratios through Sys-Id. For Sys-Id there are more than ten algorithms proposed in the last 30 years and which are used to identify various structure properties. Various studies have been performed on Vincent Thomas Bridge, San Pedro, California which has a continuous real time monitoring system (Lin et al. 2001) to identify modes of ambient vibration tests and data from 2003 Big Bear earthquake. Various frequencies for earthquake induced and ambient vibrations almost agree with each other but there were significant differences in absolute values for indexed modes.

#### 2.3.2.4.2 Modelling uncertainties

Civil engineers are engaged in modelling of physical behaviours of constructed as well as proposed systems for the past several decades. Two categories exist for analytical methods: non physics based and physics based models. Non physics based models includes the application of techniques related to probabilistic reasoning, fuzzy logic, statistical driven models, Markov chains etc. Physics based models are based on laws of mechanics, continua models and discrete geometric models, and are preferred as parameters have clear physical meanings.

FE models have gained popularity in civil engineering applications. Although initial FE models were developed to solve the problem of modelling the stressed skins in swept-back

aircraft wings, it soon found applications in structural and continuum analysis for constructed as well as mechanical systems (Clough and Wilson 1999). FE models have become powerful tool for simulation and prediction of dynamic behaviour of systems with growing computational technologies. Now-a-days, linear, deterministic and stationary SA models, based on FEs, are mostly used for constructed systems.

Due to discretizations and idealizations, different errors in the continuum models are inevitable. If SA model is not able to conceptualize force distributions, loading mechanisms, and kinematic capabilities, the analytical predictions may be far from the actual results. Effort should be made to correctly model the initial SA model so as to correctly eliminate the modelling error. Preliminary models are usually generated from idealised drawings, material tests, site inspections as well as previous studies done on similar structures. Therefore construction tolerances and exact materials properties can hardly be correctly modelled in the initial SA model. Depending on the objectives of the Sys ID process, different idealizations of the same structure may be idealized with sufficient accuracy. A satisfactory SA model should be capable of simulating and predicting geometry, stiffness and inertia, boundary and continuity conditions, load path distributions, and kinematics relationships.

It is always challenging to convert a real world problem having infinite DOF into a SA model. It can be mainly attributed to modelling errors inherent in SA models in addition to experimental uncertainties as discussed earlier. Possible sources of modelling errors include discretization errors, conceptualization errors and parameter errors. Discretization errors are a result of improper shape functions and mesh coarseness. Since constructed systems have infinite DOFs whereas a SA model realization is a discrete numerical model, therefore the existence of these errors is inevitable resulting in deviation of the eigen values. If the initial SA model has large discretization errors, the updating solution tries to compensate that error and may deviate from the original solution (Chen 2001). Even if the magnitude of the

discretization errors is small, the updated solution may deviate from the actual result. Different authors have attempted to address the problem of discretization errors. A possible solution to discretization errors was presented by Mottershed et al. (1995). Mesh density parameters have also been included in an attempt to refine the mesh in updating (Link and Conic 2000) and different mass distribution approach has been tried for alleviating these mesh errors (Chen 2001).

Parameter errors basically highlight the 'as-built' characteristics of the constructed systems such as geometry, material properties, degradation, construction tolerance, environmental actions and load effects. These characteristics may cause deviation of the updated solution from the original solution. Most of the studies carried out in the context of model updating are aimed to correct these types of errors in the analytical model to make a true realization of the structure. Parameters chosen for the model updating purposes should be sensitive otherwise the updating result may deviate far from the original model. Different parameter location techniques have been investigated to reduce the number of parameters (Link 1991; Maia et al. 1994; Baker and Marsh 1996).

The constructed systems are high redundant systems with large number of structural and non structural members and their force distributions, loading mechanisms, boundary and continuity conditions and joint conditions are rarely understood in a precise manner. As a result, SA models usually employ physical laws, mathematical manipulations and other behaviour assumptions resulting in conceptualization errors. As a result, loss of a physical feature from the structure's true behaviour makes a model incapable of predicting the correct response. These type of errors have been neglected in the process of model updating although different researchers have mentioned their importance (Mottershead and Friswell 1993; Sanayei et al. 2001; Chen and Ewins 2004).

Since a large number of simplifications and assumptions are usually made in the development of SA models, the resulting errors may appear in various forms. In very large structures, the SA model may be a representation of a limited portion of the whole structure. Geometric simplification in complicated elements can also lead to modelling errors. Dimensional reduction in the form of simplified 1D or 2D models may make it difficult to correlate the higher modes of interest and can lead to more uncertainty in the prediction of these structures. Other critical mechanisms such as damping are almost impossible to simulate accurately which further add to these errors. Boundary and continuity conditions are also difficult to model with confidence. Non-stationarity and non-linearity may further compounds the situation. Catbas et al. (1998) reported that the Seymore bridge had intermittent contact with the boundaries resulting in different bridge behaviours in the operating limit state and they incorporated idealised support conditions to address this phenomenon.

Epistemic uncertainties can be reduced with more information. Many researchers have encountered epistemic modelling errors in the development of initial SA models and one or more rigorous cycles of Sys-ID were needed to identify and address them. Ambient vibration tests were conducted by Black and Ventura (Black and Ventura 1999) on Crowchild Trail Bridge in Canada. Four different types of models i.e. distributed beam, 2D uniform beam, 2D plane and 3D model were developed for the bridge and compared with experimental modal properties. Limitations and strengths of each of the models were reported. Ren et al.(2004) investigated Tennessee River bridge using ambient vibration testing. Two different models i.e. 3D model with shell elements and a simplified model using equivalent beam models were investigated. It was found that both models were able to depict the vertical and longitudinal modes. However, the transverse modes gave closer prediction with the simplified model when compared to the detailed 3D model.

Ambient vibration studies on Brooklyn bridge (Grimmelsman and Aktan 2005) revealed that the excitation sources of the tower was not only comprised of wind and minor ground movements but also transmitted motions from the suspension bridge due to traffic. Repeated modal vectors have been identified and posed tremendous difficulty in correct estimation of bridge properties.

Attempts have been made to address the modelling uncertainties. Saanayei et al (2001) investigated the influence of modelling errors through numerical simulations with respect to measurement type and its location, error function and location of uncertain parameters. Recognition and mitigation of the problem remain unresolved. A vector projection method was proposed by Chen and Ewins (2004) to check the idealization errors, and applied it on numerical examples on an aero engine. However, in the case of civil engineering constructed systems, large differences in measured and analytical DOFs can make it very difficult to localize conceptualization modelling error accurately. Robert et al. (2005) investigated a set of analytical models for system identification of a highway bridge to recognise the controlled modelling error.

Vibration based Sys-ID process is a highly under-determined system with incomplete and imprecise information at both the experimental as well as initial SA model level. In many cases, a number of physically reasonable and different models are capable of correlating the experimental data with that of analytical predictions. It was pointed out by Avitable (2000) who demonstrated this with the help of sensitivity analysis on a simulated model. A systematic study has been carried out by Pan et al. (2010) for mitigation of epistemic uncertainty in Sys-ID problem on a long span steel arch bridge. A 3D model was updated using ambient vibration data. A series of incorrect modelling assumptions related to continuity conditions of vertical elements along the main arch and via duct spans has been

identified. The use of sensitivity analysis along with engineering intuition and judgement were used to mitigate a priori modelling uncertainty.

## 2.4 Methods for correlating experimental and analytical responses

To assess the quality of the analytical model with respect to experimental data, correlation is normally the first step. It is a usual practice to correlate the analytical model results with experimental results to see if the analytical model is in reasonable agreement and can be updated in a reasonable way (Friswell and Mottershead 1995). In dynamic modal updating, the modal data of the SA model is compared with modal data obtained from the experiment. The following are the commonly used techniques to correlate the analytical and experimental data (such as frequencies and mode shapes) for model updating.

### *2.4.1 Correlation of experimental and analytical frequencies*

The most commonly used approach is to compare the natural frequencies obtained from experiment and SA model. The percentage difference ε between these two can be calculated as

$$\varepsilon = [(\omega_{aj} - \omega_{ej})/\omega_{ej}] \text{ x } 100\ \% \qquad \textbf{2.1}$$

where ω represents modal frequency, and subscripts a and e refer to analytical and experimental jth modal frequency, respectively. This percentage difference is calculated for each mode of interest.

### *2.4.2 Correlation of experimental and analytical mode shapes*

A mode shape is a pattern of vibration at a specific natural frequency executed by a mechanical system. Different frequencies are associated with different mode shapes, thus

correlation of mode pairs is paramount for correlation of the natural frequencies. If the mode shapes are not in correlation to one another, there is no point of comparing frequencies. A thorough investigation should be carried out to match correlated mode pairs correctly. Different methods for this correlation are now discussed further.

The first method of correlation of mode shapes is to plot each element of mode shape vector, analytical and experimental, on an x-y plot. Each individual point relates to a specific DOF of the structure and it is desirable that all the points lie on the straight line passing through the origin with a slope of ±1 for a perfect correlation. The slope of this line can be found by modal scale factor (MSF) (Allemang and Brown 1982) given for each mode as

$$MSF_j = \frac{\Phi'_{aj}\,\Phi_{ej}}{\Phi'_{ej}\,\Phi_{ej}} \qquad \textbf{2.2}$$

where $\Phi_{aj}$ is the jth analytical mode shapes, $\Phi_{ej}$ is the jth experimental mode shape and " ′ " represents transpose of the mode. MSF can also be used for scaling of similar experimental and analytical modal vectors which may not have similar distribution of mass.

Modal assurance criterion (MAC) (Allemang and Brown 1982) is often used for comparing mode shapes during model updating process. The MAC assurance criterion is given by the formula

$$MAC(j) = \frac{\left|\Phi'_{ej}\,\Phi_{aj}\right|^2}{\left(\Phi'_{ej}\Phi_{ej}\right)\left(\Phi'_{aj}\,\Phi_{aj}\right)} \qquad \textbf{2.3}$$

MAC does not require the stiffness and mass matrices, and is relatively easy to apply for automatic pairing of mode shapes. A MAC value of 0 for two given modes shows that there is no correlation between the modes and a value of 1 indicates perfect correlation. For MAC, the analytical and experimental mode shapes must have the same number of elements. If the

measurements on the actual structure are made exactly at the nodes of the SA model, the MAC formula can be directly applied to mode shapes without any need for rescaling of experimental and analytical mode shapes. Those modes that have a high MAC value (greater than 0.9) are considered to be well-correlated modes, whereas those modes which have a low MAC value (less than 0.05) are considered as uncorrelated modes.

Another criterion which came from the basic concept of MAC is known as coordinate modal assurance criterion (COMAC) (Lieven and Ewins 1988). While MAC compares the analytical and experimental data mode-wise, COMAC considers each individual degree of freedom (DOF), summing over all modes of interest. The COMAC formula is given by

$$COMAC(j) = \frac{\sum_{r=1}^{m} \left| \Phi_{a.jr} \, \Phi^{*}{}_{e.jr} \right|^2}{\sum_{r=1}^{m} (\Phi_{a.jr})^2 \sum_{r=1}^{m} (\Phi_{e.jr})^2} \qquad \textbf{2.4}$$

where $r$ is a correlated individual mode pair, m is the total number of available mode pairs and * represents the complex conjugate of the mode shape. A COMAC value close to 1 shows a very good correlation and a value near to 0 indicates little correlation.

A static force balance procedure is given by Wada (1980) for the jth analytical and measured mode shape by the following expression

$$F_{ej} = K_a \Phi_{ej} \qquad \textbf{2.5}$$

$$F_{aj} = K_a \Phi_{aj}$$

where $j$ represents the mode number and $K_a$ represents analytical stiffness matrix.

The high unbalanced force values highlight the parts of the structure that need updating. This method is not widely used in practice as it requires structural stiffness matrices and

experimentally obtained mode shapes that may need scaling and expansion to match with SA model mode shapes.

## 2.5 Structural model updating

Creating a good SA model which correctly represents the actual structure is not easy (Brownjohn et al. 2001). There is a degree of uncertainty in assessing the actual properties of the materials used as well as the most realistic representation of the element stiffness in the development of an analytical model (Yu et al. 2007). The main reasons for the differences between the SA model and the original structure can be attributed to modelling and parametric errors. Modelling errors are associated with the simplification of a complex structure, whereas parametric errors are associated with incorrect estimation of the material's properties, geometry and boundary conditions. Dynamic model updating is a branch of structural optimization which calibrates the SA model by comparing the modal properties of the built structure with those of the SA model predictions. The principle of modal updating process is that the system matrices such as stiffness, mass and damping are modified with respect to the experimental modal data, i.e. natural frequencies, mode shapes and observed damping.

There are two types of model updating procedures based on modification of system matrices, iterative and one-step procedures. Iterative procedures are based on updating the parameters (such as material and geometry properties of members), whereas the one-step procedures directly make the changes to the whole stiffness and mass matrices. The updated matrices using the one step procedure can exactly reproduce the experimental modal properties but generally are not able to maintain structural connectivity, thus having less physical significance than iterative procedures (Brownjohn et al. 2001). In this thesis, iterative

methods have been used for their superiority. For iterative procedures, the candidate parameters for updating describing the geometry and material properties can be written as

$$P = p1, p2, \dots\dots, p_n \quad \textbf{2.6}$$

where subscript 1,2….n indicates the candidate parameters.

Let $R_e$ represents the vector of experimental modal outputs and $R_a$ represents the modal output vector obtained from an initial SA model. Both $R_e$ and $R_a$ are considered to be a function of parameter vector $P$. The difference between these two, often called the residual vector, is given as

$$\delta R_a = R_e - R_a \quad \textbf{2.7}$$

An objective function can be defined as a norm of the residual vector

$$f(P) = \delta R_a{}' \delta R_a \quad \textbf{2.8}$$

Minimization of this function will maximize the correlation of the experimental and analytical model. To account for the larger importance of some of the residuals compared to others, a weighting matrix $W$ can also be used with this residual vector

$$f(P) = \delta R_a{}' W \delta R_a \quad \textbf{2.9}$$

In civil engineering model updating problems, the discrepancies between frequencies and mode shapes are minimized by solving a least square problem.

The equation of motion of linear elastic systems is given by the formula

$$M\ddot{y}(t) + C\dot{y}(t) + Ky(t) = F(t) \quad \textbf{2.10}$$

where $M$, $C$ and $K$ are system matrices for mass, damping and stiffness, respectively, $\ddot{y}(t)$, $\dot{y}(t)$ and $y(t)$ represent acceleration, velocity and displacement, respectively, and $F(t)$ is the external force applied to the system at a given time *t*.

When the system has relatively small damping ratios (if the damping is proportional), the eigen value problems can be solved to determine frequencies and mode shapes ignoring the damping matrix

$$(K - \Omega M)\, \Phi = 0 \qquad \textbf{2.11}$$

where Ω is a diagonal matrix of square of the frequencies.

The next step is to define residual vectors for the experimental and analytical values in terms of experimental frequencies and mode shapes. The residual vectors lead to objective functions which can contain different criteria for finding out the discrepancies between experiment and SA model such as differences of frequencies, model coordinates, MAC, COMAC and others (Wu 1999). It is the goal of optimization to minimize the error residual to determine a set of physically justifiable parameters $P$.

Due to many candidate parameters for the updating of the SA model, several different combinations of the parameters can lead to acceptable results. There may be one set of uncertain parameters values which gives an acceptable convergence of the error residual and gives a reasonable justification for the deviation of experimental and analytical results. The challenge of finding such a set of suitable parameters necessitates the need of optimization. It is difficult to determine all the natural frequencies and mode shapes experimentally, as the original structure has an infinite number of DOFs. As the number of measurements available is usually much smaller than the number of uncertain parameters, and, consequently, not all

uncertain parameters are selected for model updating, different solutions may exist in the solution space for a specific error function.

The attainment of a correct solution is a challenging optimization problem. There are two main concerns for solving model updating problems, the capability of the algorithm and the complexity of the search domain (Horst et al. 2000). The capability of the algorithm is related to its ability in detecting the global solution and its computational efficiency in finding the global minimum. The complexity of the search domain is related to the number of parameters involved in the search process. The increase in the number of parameters leads to an increase in the dimensionality of the search domain, which may further complicate the problem. Thus structural updating is essentially a search process and a suitable optimization techniques should be explored to deal with it. Common model updating techniques, to find a set of suitable parameters, in the context of model updating of civil structures are now detailed.

### *2.5.1 Manual model updating*

This approach basically involves manual changes in the updating parameters, usually with the help of parameter sensitivities, via trial and error approaches (Jaishi and Ren 2005). Most influential parameters to the experimental responses are selected in this case, assisted by engineering intuition, and varied to globally calibrate the model. A reasonable starting model is normally necessary in this case. The most influential parameters in full scale structures typically include connectivity and boundary conditions, material properties, elastic modulus and kinematics of the system.

### *2.5.2 Sensitivity method*

Contemporary methods of structural updating in buildings and bridges include the use of a SM to improve the correlation between analytical and experimental modal properties (Brownjohn and Xia 2000; Yu et al. 2007). SM lies in the category of local optimization

techniques and the solution largely depends on the starting point or initial values (Kalyanmoy and Deb 2007). These methods take advantage of the solution space characteristics by calculating gradients and converge quickly to (possibly local) maximum or minimum values. A good guess of an initial point is necessary so as to converge to the global minimum. However, this has limited their use to smooth and uni-modal objective functions. The SM computes the sensitivity coefficients defined as the rate of change of a particular response with respect to a change in a structural parameter, mathematically expressed as

$$\boldsymbol{S_{kl} = \frac{\partial R_k}{\partial P_l}} \qquad \textbf{2.12}$$

where $S_{kl}$ is the sensitivity matrix, $\partial R_k$ represents the kth structural response and $\partial P_l$ represents lth parameter to be updated. The sensitivity matrix can be calculated by using perturbation techniques, finite differences or by direct derivation (Friswell and Mottershead 1995). In the formulation of SM, the experimental responses are expressed as a function of analytical responses and a sensitivity matrix (Zivanovic et al. 2007). This is done by Taylor series expansion and, ignoring higher terms, as

$$R_e = R_a + S(P_u - P_o)$$

$$\Delta R = S\Delta P \qquad \textbf{2.13}$$

$$\Delta P = S^{+}\Delta R$$

where $\Delta P = P_u - P_0$

and $\Delta R = R_e - R_a$

$R_e$ and $R_a$ are values of the vectors of analytical and experimental structural responses respectively. $P_u$ is a vector of updated parameter values, $P_0$ is a vector of current parameter values and "+" sign indicates pseudo inverse.

The main difference between the various sensitivity schemes is the method used to calculate the sensitivity matrix. For experimental sensitivity, modal parameter derivatives can be calculated by using orthogonality relations. However, analytical sensitivity analysis require the use of mass and stiffness matrix derivatives and are less sensitive than experimental sensitivity matrices due to large perturbations in the parameters and due to noise in the data.

A methodology is presented by Ricles (1991) in which a sensitivity based matrix update method which takes into account variations of mass and stiffness, mass location, changes in mode shapes and natural frequency, and statistical confidence factors for structural parameters. A hybrid approach has been used where modal parameter sensitivities are calculated from the experimental data and matrix sensitivities are calculated from the analytical model. Sanayei and Onipede (1991) also used results of static load tests for updating the stiffness parameters of the SA model. An element level sensitivity based technique is used to minimize the residual between the applied forces and the forces produced after application to the model stiffness matrix.

One of the most widely used and computationally simplest filtering algorithms is the Least Mean Squares (LMS). The steepest descent method is used by the algorithm and an estimate of the gradient is used instead of the actual value to simplify the calculations. The LMS technique possesses better noise rejection properties. Adaptive LMS (Geoffrey Chase et al. 2005) is employed in SHM as it takes advantage of this filter's ability to adaptively model noisy signals to update the structural parameters in comparison to the base model. A series of coupled adaptive filters are used for this purpose in a real time application. Unlike most of the other SHM applications in civil engineering, the adaptive LMS can be used directly to assess non-linear changes in stiffness and can be applied to highly non-linear structures. The mean square error is minimized by adjusting the coefficients from sample to sample. The

method is advantageous over the usual procedures involving the modal data (i.e. natural frequencies and mode shapes) as it can be applied in real time applications.

A real time convex integral based method was also presented by Singh-Levette (2006) that employs non-linear and linear baseline models, and compares them with measured accelerations and low frequency displacements. The method can successfully identify time varying, pre and post yield stiffness and corresponding displacements components for non-linear models. However, for linear baseline models, the method identifies only the time varying stiffness and is still capable of identifying the presence of structural damage. In the context of this research, a linear baseline model was adopted for model updating considering measured experimental frequencies and mode shapes. The initial linear SA model stays the same during the process of updating and an inadequate initial model may result in a meaningless updated model.

### *2.5.3 Global optimization algorithms*

GOAs, which are part of evolutionary algorithms (EAs), are stochastic search-based methods and are promising techniques for finding the global minimum in difficult optimization problems (Kalyanmoy and Deb 2001). They are generally independent of the solution space (Tebaldi et al. 2006; Tu and Lu 2008) because they work on a population of points in parallel, whereas the traditional search techniques such as SM work only on a single point at one time. Thus the tendency of traditional search techniques converging to a local minimum in the search space can be addressed by using GOAs. This makes the GOAs much more robust in the case of an ill-behaved solution space.

These techniques are particularly efficient for finding the minimum of objective functions having constrained variables and a large number of dimensions. This makes them more suitable to use in model updating problems with different objective functions such as those

based on frequencies, mode shapes or MACs. Therefore, global techniques find the global minimum out of local minima and often give better results where local optimization techniques perform less favourably (Deb 1998). Drawbacks of global optimization techniques are that they do not take advantage of characteristics of the solution space such as steepest gradients and they have a slow rate of convergence. The three GOAs used in this research, namely PSO, GA and SiA, are discussed in detail in Chapter 3.

## 2.6 Factors for consideration in model updating

Generally, in model updating problems, not only is a good correlation required between experimental and analytical results, but also the updated parameters should have physical significance. The success of model updating is dependent on three key factors, setting up of objective function, selection of parameters and a robust optimization algorithm (Ward and Heylen 1997). A proper objective function is necessary to effectively minimise the difference between the experimental and analytical results. Selection of parameters is an important issue as there may be many sets of parameters that can produce acceptable results. It requires a deep insight into the types of uncertainties involved, and trial and error approaches are usually used along with engineering intuition to select the parameters. Only those parameters that have physical meaning should be selected. Sensitivity analysis can also be used to select the most influential parameters to the experimental results. A robust optimization algorithm is required to find the minimum in the search space. The algorithm should be able to find a global minimum out of many local minima with precision and accuracy. The outcome of a model updating application to a constructed system should be an analytical model that can replicate the actual mechanical characteristics of the built structure with a good level of confidence.

## 2.7 Ill-conditioning of the model updating problem

As mentioned earlier, the number of measurements usually taken during full scale structure testing is limited. The sensitivity matrix S may become rank deficient when either of the following requirements are met (Friswell and Mottershead 1995):

1. One or more columns of the matrix can be expressed as linear combinations of other columns
2. Insufficient information has been collected from the experiments to enable the parameters to be estimated uniquely.

In other words, when the columns of the matrix are linearly related with each other, then the problem becomes ill-conditioned. Practical constraints restrict the number of measurements while the structural systems might have higher number of potentially uncertain areas. The number of system parameters to be identified becomes higher than the mode shapes and natural frequencies that are independently measured from vibration data sets. Also if the measurements are taken near the node of a mode, this effect will be worsened. If the estimation of many uncertain parameters as compared to experimental data is attempted, the columns of the matrix again become linearly related except for measurement noise. To get a unique solution from the equations set, the usual requirement is to over determine the problem. By the inclusion of few insensitive parameters during the updating process, the determinant of the model updating equation equals zero. Simultaneously, if there are few linearly dependent columns in the sensitivity matrix, the determinant in the said equation set is again zero, hence the uniqueness of the solution is not obtained. When the dynamics of a structure have similar effects from two different parameters, then the columns are almost linearly dependent. Consequently, ill-conditioning of the updating process can be avoided by incorporating only the most important parameters so that these residues are highly sensitive

with respect to structural parameters. Inclusions of insensitive parameters, in the identification process should be avoided.

Several studies have been conducted for vibration based model updating. It has been found that the modal data alone cannot identify changes in the mass and stiffness matrices simultaneously (Baruch 1997). The relationship between identifiable parameters in a sensitivity based updating method depends on measured resonant frequencies plus the number of modes times the number of DOFs (Gola et al. 2001).

Yeo et al. (2000) described discontinuity and non-uniqueness of the solution in SA model updating procedure in detail. Two vector spaces of measured vibration responses and the system parameters are used to explain the cause of the instabilities. In the case of an ill-conditioned system and with measurement noise, the system parameters in different sets can produce the same set of responses at distinct locations of the search space; hence the solution cannot be affirmed as unique. Three remedies are introduced to overcome the ill-conditioning of the problem i.e. (i) modification of the space of the system parameters; (ii) modification of measured data and (iii) modification of the error function.

The first two remedies are about the relationship between number of parameters and measured data. The first remedy calls for a reduction in the number of uncertain parameters for model updating. The most commonly used approach is grouping similar elements into one parameter (Zhang et al. 2000). Another approach to decrease the number of parameters is by use of a damage function (Abdel Wahab and De Roeck 1999). Efforts to increase the number of independent vibration responses have been made in pursuit of the second remedy (Zang et al. 2006) by using laser vibrometry or by testing the structure in different configurations (Li and Brown 1995). In the bulk of practical cases, the number of unknown system parameters is still greater than the measurable independent vibration, hence the reduction in the number

of parameters to be identified is proposed. Defining one unknown parameter for a cluster of number of similar elements is a basic approach to handle such problem (Zhang et al. 2000). The number of unknown parameters in the SA model updating process is significantly reduced by the application of this approach. The composition of cluster can vary and primarily depends on the precise engineering judgment of the individual. There are more refined schemes for grouping system parameters. Hjelmsted and Shin (1996) presented an approach to reduce the number of system parameters by introducing a grouping of elements on an adaptive parameter basis. Araki and Miyagi (2005) worked out a simple technique for grouping of parameters and subdivision mentioned as above by recasting the problem into combinatorial optimization and developing a procedure of mixed integer nonlinear least squares solution. This technique increases the problem size and is reliable for a limited number of damaged sites identification. A damage function has also been used to reduce the number of unknown parameters as an alternate approach (Abdel Wahab and De Roeck 1999; Teughels et al. 2003). In these two papers, the damage pattern of reinforced concrete beams is characterized by the damage function of three parameters. This leads to conclusions that the major difficulty in getting adequacy of a SA model updating problem for vibration based system identification is its ill-conditioning. However, use of the damage location information can be made to considerably alleviate the ill-conditioning of the problem, hence reducing the number of unknown parameters.

Diverse inverse problems have been attempted by adopting the third remedy, called a regularization technique (Schnur and Zabaras 1990; Lee et al. 2000; Yeo et al. 2000). Regularization techniques make use of the prior information to get an additional check for the minimization problem by modifying the error function. The unknown parameters are assumed to be closer to the known nominal values. The solution space, for example, is directly reduced by setting the upper limits in close proximity to the baseline characteristics.

It is done by incorporating a weighted norm of the parameter changes to keep the parameter changes small. The most usual form is known as the Tikhonov regularization (Teughels et al. 2003), as it was introduced to resolve the ill-conditioning of systems with the aim to control the condition number of the problem. The condition number of an objective function with respect to a parameter measures the change in the output value to a small change in the input argument. This is an indicative of how sensitive is a function to perturbations in the data especially in inverse problems. A low condition number is said to be well conditioned whereas a high condition number is said to be ill-conditioned. The problem can be further regularized by insertion of structural parameters having imposed inequality constraints.

Addressing the ill-conditioning using a regularization technique is a topic of interest in SA model updating problems. Sensitivity based regularization techniques have been explored in this context by various researchers. Ahmadian et al. (1998) addressed the problem by incorporating side constraints and used singular value decomposition, cross validation and L curves for determination of regularization parameter. The L curve approach and the generalised singular value approach are used reliably to get updated parameters with physical understanding. Weber et al. (2007) investigated structural damage detection with Tikhonov regularization and Weber et al. (2009) introduced consistent regularization for a non-linear model updating problem. Further studies of regularization techniques in model updating include Titurus and Friswell (2008) and Mottershead et al.(2011). In these studies, the sensitivity based updating with a special focus on optimization of the response prediction and a priori information about the uncertain parameters has been investigated with the help of an additional regularization criterion.

## 2.8 Examples of applications of model updating to civil structures

### *2.8.1 Model updating using sensitivity method*

Zivanovic et al. (2007) investigated the Podgorica foot bridge with an aim of describing the complete model updating process for civil engineering structures. A detailed SA model of the bridge was made using the modelling software ANSYS (1999). The initial model showed discrepancies in the correlation with the experimental modal results and underestimated the frequencies by up to 29%. A SM-based model updating software FEMtools (FEMtools 2004) was used for model updating. A first attempt of model updating based on SM had produced some physically meaningless results. This confirmed the conclusions drawn in an earlier study (Brownjohn and Xia 2000) that, when large differences are present between analytical modal properties and their experimental counterparts, the initial SA model might not be updated using SM. This is mainly because, when large differences are present, the key assumption that a relationship between errors in responses and changes in the parameters could be expressed only by the linear first term of the Taylor series expansion (Equation 2.17) may unreasonably change some of the updating parameters. The authors decided to manually update the analytical model first. A trial and error approach was used for manual model updating and it was found that the introduction of flexible supports at the girder ends in the longitudinal direction improved the correlation and successfully reduced the maximum frequency errors between experimental and analytical results to only 4%. After manual model updating, an automatic model updating was performed using SM. Twenty four parameters were selected for updating related to stiffness of the spring supports, modulus of elasticity of deck, slab and column plate, the density of deck and water pipe, and the height of the column plate and deck. These factors had been allowed to change in different ranges during automatic model updating and the maximum range was from -50% to +50%. Finally, a

physical justification of the updated parameters was provided so that a meaningful model updating attempt could be justified. Similar observations were made in Brownjohn et al. (2001) where the Safti Link bridge was updated using the SM. Manual updating was done prior to updating by SM.

Many other studies have been performed using the SM for different types of full scale civil engineering structures (Zhang et al. 2001; Wu and Li 2004; Jaishi and Ren 2005). Skolnik et al. (2006) has updated a permanently instrumented UCLA Doris and Louis Factor building. The building suffered damage during the 1994 Northridge earthquake. The authors have used the stick column approach to update the structure based on SM. Floor updating has also been tried using SM. A lively open plan office floor occupied by the office equipment has been dynamically tested by using linear shakers and updated (Pavic et al. 2007). ANSYS (ANSYS 1999) was used as a modelling tool and the SA model was later updated by SM to match the experimental values to those of the analytical model. The model updating was proved to be successful. A multi-start SM-based method named coupled local minimisers (Teughels et al. 2003) has also been investigated for model updating of a beam using pair wise synchronization constraints.

Although SM is a fast method to obtain the updated results, its outcomes can have no physical significance. The SM is essentially a local optimization technique and its solution can converge to a local optimum. The model has to be manually updated in some cases and even after manual model updating; the search of a globally optimal solution in a particular search space is not ascertained.

### *2.8.2 Model updating using global optimization algorithms*

Several GOAs have received interest in studies related to dynamic model updating problems. Perera and Torres (2006), Raich and Liszkai (2007),Tu and Lu (2008) and Perera et al.(2009)

studied GAs, Levin and Lieven (1998) used both GA and SiA, and Saada et al. (2008) used PSO for model updating problems.

GA was used (Perera and Torres 2006) for assessment and damage detection of a simulated beam structure and an experimental beam structure. Multiple damage scenarios were studied along with the effect of different noise levels on a simulated beam structure. Later, GA was applied to a laboratory beam structure to verify its effectiveness in the damage detection and its assessment. Raich and Liszkai (2007) presented an advanced GA and applied it on simulated beam and frame structures for improving the performance of damage detection. A GA based MOO scheme was developed by Perera and Ruiz (2008) to detect and assess the damage in simulated structures as well as a signature bridge structure. The initial two dimensional model of the bridge was used for damage detection and model updating. The bridge frequencies were successfully identified for the first three flexural modes. However due to the simplification of the SA model, the torsional modes were not matched. Perera et al.(2009) also compared different multi-criteria GA for damage detection and estimation of simulated structures and simple laboratory beam structure.

In another study (Levin and Lieven 1998), both SiA and GA were investigated to update a numerical model of a cantilever beam and an experimental wing plate structure. A new blended SiA algorithm was also proposed to improve the model updating results. An adaptive real parameter hybrid of SiA and GA (He and Hwang 2006) was also successfully implemented for detecting multiple damage occurrences in beam structures to improve the convergence speed and solution quality. Saada et al. (2008) used PSO for model updating of a beam structure, whereas a hybrid PSO-Simplex method was proposed for model updating of a ten-bar truss and a free-free beam (Begambre and Laier 2009). The new method proposed performed well for model updating of the numerically simulated structures. PSO and GA (Perera et al. 2010) were also applied in a multi-objective context to damage

estimation problems with modelling errors. Marwala (2010) applied different GOAs to a simple beam and an unsymmetrical H-shaped structure and found that PSO gave better results when compared to other GOAs.

Coupled local minimiser (CLM) method, applicable to global optimization of a function, was proposed by Teughels et al. (2003) for detection of multiple minima in a model updating problem. A population of local minimisers set up a cooperative search mechanism and were coupled using synchronization constraints during search process. CLM was successfully applied to SA model updating problem in which damage was detected in a reinforced concrete beam. Two different minima exist for the objective function considered and method was able to successfully detect both of them. Bakir et al. (2008) also proposed an improved CLM technique to correctly identify damage in a complex structure. The improved CLM method was compared with Levenberg–Marquardt algorithm, Sequential Quadratic Programming and Gauss–Newton methods and it was found that improved CLM technique gave better results.

In another study by Zarate and Caicedo (2008), multiple admissible solutions to model updating problem was identified using a Modelling to Generate Algorithm (MGA). A full scale Bill Emerson Memorial bridge model was updated and different plausible solutions were detected. The authors selected the solution which has physical justification and has a higher objective function value instead of the global minimum.

A novel EA which is able to identify local and global optimal solutions was also proposed by Caicedo and GunJin (Caicedo and Yun 2011) which was accomplished by intruding two new operators in GA. The algorithm was used on a simulated numerical example of American Society of Civil Engineering Structural Health Monitoring Benchmark structure where two parameters were updated. A random white noise was added to the acceleration records which have created multiple local minima. Two minima were correctly detected by the proposed

algorithm in which the local minimum has a lower objective function value and the global minimum has a higher objective function value. The proposed technique detects the multiple minima but does not guide the analyst to decide which is the correct solution.

However it can be noticed that most research efforts have been made towards the damage detection and the assessment of simulated structures or simple laboratory scale structures. The focus of those studies was not on exploration of the full search space. Scarce studies have reported algorithms for multiple alterative solutions. Moreover, updating of full scale structures still remains a challenging and relatively indistinct topic. GOAs have received less attention, especially for complex updating problems. Many different sets of parameters in the initial SA model and different types of modal data available from the experiment may lead to potentially different solutions. Even if the modal values and their analytical counterparts match reasonably well, the right solution is left to the judgment and experience of the analyst.

## 2.9 Summary

This chapter presents an introduction to SHM especially related to a vibration based method. The differences between the complex constructed civil engineering systems and manufactured systems are detailed. Different components of structural identification such as initial SA modelling and modal testing are explained. Two different types of uncertainties i.e. aleotary and epistemic are introduced. Epistemic uncertainty is found to be more appropriate for numerical models, as it can be corrected with better knowledge of the system. Methods for correlation of experimental data with analytical data are then detailed. SA model updating in the context of this thesis is explained. It was concluded that factors for model updating problem should be carefully selected so that the problem may not become ill-conditioned. Lastly, examples from both SM and GOA methods show that the assurance of obtaining the globally optimal solution in dynamic model updating of civil structures with confidence,

accuracy and computational efficiency using a suitable optimization algorithm remains an interesting and important area of research to which the present study makes a contribution.

# Chapter 3. GLOBAL OPTIMIZATION ALGORITHMS

## 3.1 Introduction

In an optimization problem, the set of all possible solutions constitutes a search space. The main task is to find a solution that fits best among all the solutions in terms of an objective function value. If it is possible to find out all the possible solutions, then the problem of finding the best solution among all solutions does not pose much difficulty. But if the search space is too large or complex, it becomes infeasible to find all the possible solutions, so some specific techniques should be applied to find the optimal solution. GOAs are meta-heuristics, which means that they make few or no assumptions about the problem to be optimized and can handle large or complex spaces of solutions. These methods do not use the gradient information of the problem and can handle complex problems that are irregular, multimodal, noisy and time-variant. They are basically population-based algorithms and offer an attractive alternative to conventional optimization techniques. In this chapter, Section 3.2 explains the goals of optimization and Section 3.3 describes the three GOAs ---PSO, GA and SiA--- used in this research.

## 3.2 Optimization

Optimization plays an essential role in various areas of industry, science and engineering. The main function of the engineer is to design new, efficient or less expensive systems and to improve the operation of existing systems. Different optimization tools are now being used in the field of civil engineering for designing and monitoring of civil structures. There can be many goals of the optimization search process (Horst et al. 2000). One of the basic goals is to find the global optimal solution in the search space which minimises the value of the objective function. Another important goal is faster convergence. Faster convergence is desired when it is expensive to compute the objective function and its gradients; however, this may increase the chances of the solution being trapped in local minima. Another goal could be to produce a range of diverse solutions across the search space. When the solution space contains several minima with relatively similar objective function values, it may be desirable to be able to select a solution from amongst many possible solutions in the search domain. It depends on the experience of the analyst to select his goals with respect to any particular problem.

One of strongest theoretical results were given by Wolpert (1996), namely *no-free-lunch* theorem which states that *"any two algorithms are equivalent in terms of their performance when it is averaged over all problems instances and metrics".* In other words, if one algorithm X outperforms the other algorithm Y in some specific problems, the other also exactly outperforms the first one in some other problems. This theorem is applicable for finite search space and where the algorithm does not revaluate the points already searched. Applicability of this theorem in practice is an ongoing discussion. However, its main conclusion holds that special characteristics of a problem are key to the selection of the most suitable algorithm. Therefore, efforts shall be made for specific problem to reveal these

elements; otherwise choice of a particular algorithm may be suboptimal. There are various optimization algorithms available depending on the type of their exploring capabilities, so it is necessary to investigate the optimum algorithm for specific purposes to achieve acceptable performance.

## 3.3 Global optimization algorithms

### *3.3.1 Particle swarm optimization*

PSO (Kennedy and Eberhart 1995) is a population-based stochastic optimization method that tries to improve the solution iteratively with respect to a given measure of quality. The concept of PSO was developed based on the swarming behaviour of fish, bees and other animals. These are the natural systems where collective behaviours of a population are observed producing self organised-synchronised collision free movements to the target. These aggregated behaviours exhibit certain traits of intelligence through collaboration and competition between the individuals. Early development of PSO by Keneddy and Eberhart (1995) employed the main rules of nearest neighbour velocity and acceleration at distance to simulate swarming behaviour of the agents in search of food.

The basic idea is that if one of the members sees a desirable path for the most fertile feeding locations, the rest of the swarm should follow. PSO, a population based algorithm, exploits a population of solutions within the search space. Population of solutions is called swarm where as each individual of the population is called a particle. Each particle in the swarm should be influenced by the rest of the swarm to increase the diversity but also be able to independently explore its own vicinity to a certain extent. PSO moves the particles in the search space based on simple mathematical formulae. Movement of the particles is influenced by its local best position and also by the best position of the whole search space,

resulting in better and better solutions as the algorithm proceeds. It is expected that this moves the whole swarm to a global optimal solution.

Two factors mainly contribute to swarm intelligence: group knowledge and individual knowledge. This is achieved by the particles that have a position and a velocity vector in multidimensional space, where each position coordinate represents a parameter value. The particles can have continuous or discrete values. PSO calculates the fitness of each particle from its fitness function. These particles flying in 'n' dimensional space have two reasoning capabilities: the memory of their own best position in consecutive generations called *pbest* and knowledge of the swarm's best position normally called *gbest* as shown in Figure 3.1. The velocity of each particle towards its *pbest* and *gbest* locations is adjusted by the formula

$$v_i(t+1) = \gamma v_i + c_1.\mathrm{rand}_1.\big(\mathrm{pbest}(t) - x_i(t)\big) + c_2.\mathrm{rand}_2.\big(\mathrm{gbest}(t) - x_i(t)\big) \qquad \textbf{3.1}$$

where $\gamma$ is the inertial weight, $v_i$ is the initial velocity, $c_1$ and $c_2$ are the cognition and social components, and $\mathrm{rand}_1$ and $\mathrm{rand}_2$ are random numbers between 0 and 1.

Due to the velocity given by Equation 3.1, the position $x_i$ of each particle is updated in each iteration by the following formula

$$x_i(t+1) = x_i(t) + v_i(t+1) \qquad \textbf{3.2}$$

Different important components of the Equation 3.1 and Equation 3.2 are discussed in the following sub-sections.

#### *3.3.1.1* pbest and gbest

In PSO, the velocity is adapted in an iterative sense to allow particles to reach at any point in the search space. There are two important portions of the above Equation 3.1: one relates to the global position, which defines the swarm exploratory behaviour; the other relates to the

local best position, which defines the swarm exploitative behaviour (Konstantinos and Vrahatis 2010). Exploratory behaviour is related to the search of the broader region of the search domain, and exploitative behaviour is related to the local search, where a given particle tries to get closer and closer to the (possibly local) minimum. An important property of pbest in the velocity equation is that it remembers the previous steps of its particles. In terms of memory, each particle stores the best location it has ever visited during previous iterations. Likewise, the algorithm also estimates the best location of all the particles in a generation in the form of gbest, which is also crucial information. Thus, the velocity equation is essentially an information exchange mechanism in which particles mutually communicate their experience during the search.

#### *3.3.1.2 $\gamma v_i$ component*

The inertial movement of the particle is preserved by the previous velocity term "$v_i$" in Equation 3.1. This property of the algorithm prevents it from biasing towards the best positions in a specific generation, which could be possible if the algorithm is trapped into a local minimum (for example if both best positions lie in the vicinity of a local minimum). This component helps in avoiding the stagnant behaviour of particles when their previous and next positions coincide with each other. In that case, the two stochastic terms related to gbest and pbest may vanish in Equation 3.1 and the particle would stay at its position for several iterations until a new position is found by another particle. Also, the previous velocity term serves as a perturbation for the global best particle and helps in establishing effective convergence.

A large value of inertia weight $\gamma$ favours a global search and a small value favours a local search. Thus a large value of inertia can be used in the first iterations, which gradually decreases as optimization runs to concentrate the particles near the global minimum in the

last few iterations. A linearly decreasing inertia weight ‘w’ can be mathematically expressed as

$$\gamma = w_{up} - (w_{up} - w_{low})\, t/T_{max} \qquad \textbf{3.3}$$

where $w_{up}$ and $w_{low}$ are upper and lower bounds of w, t is the generation counter, and $T_{max}$ is the maximum number of generations.

### *3.3.1.3* $c_1$ *and* $c_2$ *component*

To avoid premature convergence, the parameters $c_1$ and $c_2$ in Equation 3.1 should be carefully selected. The value of these two parameters can bias the new positions of the particles towards pbest and gbest thus affecting the magnitude and spread of the search (Konstantinos and Vrahatis 2010). A high value of these parameters leads to better global exploration of the whole search space in relatively distant regions whereas a low value promotes a more refined local search around the best positions found. Also if $c_{1<} c_2$ , movement towards gbest would be favoured and if $c_{2<} c_1$ , movement towards pbest would be favoured. This aspect is particularly useful if some information regarding the search space is available.

It is important in most of the optimization problems that the search particles lie within the search space during subsequent iterations. Therefore, bounds are imposed on the position of the particle $x_i$ in Equation 3.2. So in the simplest case, if a particle moves out of the search space after the application of Equation 3.2, it is immediately brought back to the boundary value. Furthermore, an important aspect of swarm explosion, which is an uncontrolled increase in the magnitude of velocities leading to the movement of particles out of the search space, can be addressed by limiting the velocity. To address this, the velocity of the particles can be clamped to avoid taking extremely large steps from their current position. Therefore, before the application of Equation 3.2, each velocity should be checked to follow the

restriction of maximum velocity thresholds for each component. This ensures that particles remain in the search space and their values are kept within the maximum and minimum bounds.

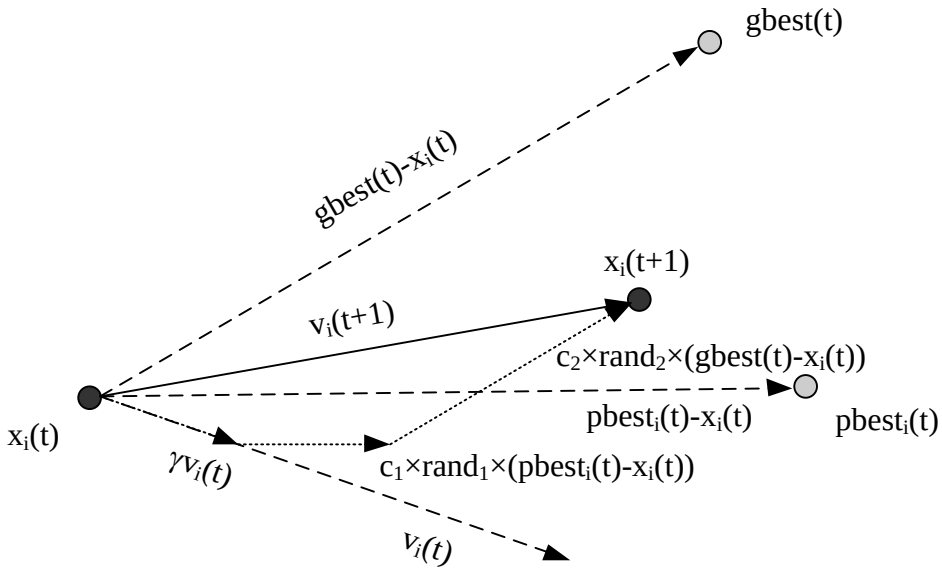


**Figure 3.1 Pictorial view of swarm behaviour with particle and velocity update**

The implementation of PSO compared to the other optimization techniques is relatively faster and cheaper as there are few parameters to adjust and it can be used for a wide range of applications (Knowles et al. 2008). Both theoretical and empirical studies have been undertaken to help in selecting proper values of the parameters (Trelea 2003; Zheng et al. 2003; Pedersen and Chipperfield 2010). To improve optimization performance of basic PSO, numerous variants are continually introduced. Attempts were made towards hybrid approaches of PSO with other optimization algorithms (Abdel-Kader 2010; Niknam and Amiri 2010), adaptation of behavioural parameters (Zhan et al. 2009) and reduction of premature convergence problems (Zhao and Wang 2010; Yang et al. 2011).

### *3.3.2 Genetic algorithms*

GA (Holland 1975) mimic the process of natural evolution according to Darwin's theory. GA works on a population of potential solutions based on the principle of survival of the fittest to produce better and better solution. A new approximation of the solution is created by selecting individuals according to their level of fitness and then bred together using the operators working on the concept of natural genetics. As the generation proceeds, the whole process leads to the development of better suited individuals as compared to the individuals they are created from.

Each individual is encoded as strings usually called a chromosome. A population of candidate solutions are randomly generated. A standard form of representation is in the form of array of bits (Knowles et al. 2008). Other forms of arrays can also be used, e.g. integer, real valued etc., but the bit formulation helps in further processing of other operators used in the algorithm. A population consists of a number of individuals and the population size depends on the overall complexity of the search space. A large population size is useful but it requires considerable computational effort. The search process operates on the encoding of variables rather than decision variables themselves, except where real valued genes are used. Fitness of each solution in terms of objective function in the population is evaluated by decoding of the chromosomes into decision variables. The fitness not only tells about the quality of the solution but also corresponds to closeness of the chromosomes to the optimal solution. Once the fitness value is evaluated for each individual, a selection process can be initiated. The fitness value is then used in the process of selection with a bias towards fit individuals. The individuals with good fitness value have a higher probability of selection than the individuals with a lower fitness value.

To form new solutions for the next generation, genetic operators are applied on the previously selected pool. The consistency of GA strongly depends on the relevant reproduction operators. If the reproduction operators just produce a new solution without any strong link to the previous ones in the last generation, they are essentially performing a random search. The recombination operator normally exchanges genetic information between pairs of individuals. The most commonly used recombination operator is cross over where two chromosomes are cut and the halves thus obtained are spliced to form new chromosomes. This is a very important operator as it assorts the characteristics from two parents into one chromosome. The cross over operator is not necessarily applied to all the individuals in a population and is applied with a probability. The new solution created typically shares characteristics of its parents. Another genetic operator called mutation is then applied to the new population. Mutation changes the individual genetic representation again with some probabilistic rule. In binary string representation, mutation causes the single bit to change its value from 0 to 1 or vice versa. It is a background operator and generally ensures that the probability of searching the search domain never approaches to zero. This has the effect of restraining the algorithm to converge to the local optima. After the application of recombination and mutation operators, the fitness value of each individual is again evaluated. The process continues to form new sets of population that are different from the initial generation. Since only the best particles are selected, this leads to a population of individuals that are better suited for minimizing the objective function. The average performance of the population increases as better individuals are preserved and less fit individuals die. GA is terminated when certain criteria such as the best fitness value, number of generations or mean deviation of population is achieved. Three randomised operators involved in the regeneration namely selection, cross over and mutation are discussed in the following sub-sections.

### *3.3.2.1 Selection*

Selection (Kalyanmoy and Deb 1998) is a process of choosing parents from the initial population that will create the offspring for a subsequent generation. The basic purpose is to emphasise on better fit individuals and basically determine a degree to which better fit individuals are favoured in subsequent generations. Broadly speaking, there are two types of selection schemes: proportional based selection and ordinal based selection. Proportional based selection picks the solutions based on their fitness values relative to fitness values of all other solutions in the generation. Ordinal based selection does not chooses the individuals on their fitness values but based on their rank within the given population, which means that the selection is independent of fitness distribution and takes into account the relative ordering of the population. If the selection only involves the most fit chromosomes, sub-optimal solutions might take over the generation thus reducing the overall diversity of the solution space and result in severely limiting the solution space. Selection pressure is a degree to which better individuals are favoured in the selection. There are different techniques available for the selection.

Roulette wheel selection is one of the traditional selection strategy in GA in which an individual is selected from the population with a probability proportional to the fitness of the objective function. The basic principal consists of a line search on a Roulette wheel. In the most common form, a real valued sum is obtained as the sum of fitness values of all individuals in a population. All individual are mapped into contiguous intervals in the range of 0 to the total sum. The interval size depicts the fitness value of each individual. In Figure 3.2, the circumference of the circle is the sum of fitness of all individuals. Individual 4 is the best fit individual in terms of its fitness value and occupies the largest space whereas individual 1 is the least fit individual and occupies least space in the Roulette wheel. For the selection of an individual, a random number between 0 to sum is generated and the individual

is selected whose segment spans the random number. The process is repeated until the required number of individuals is obtained.

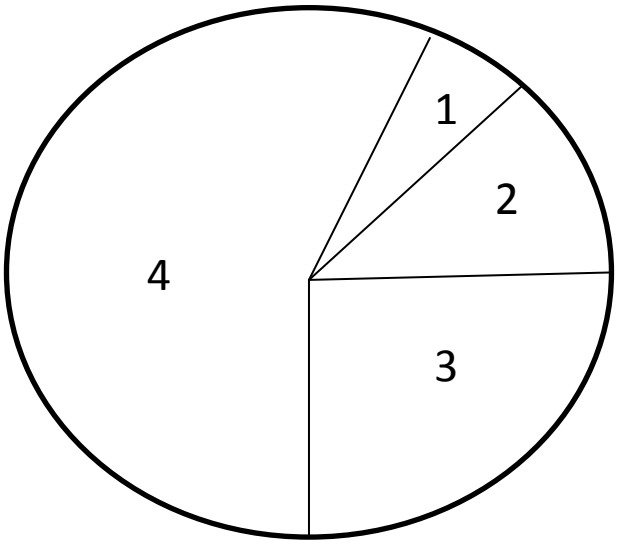


**Figure 3.2 Roulette wheel selection**

There are many other techniques available for the selection. In random selection, a solution from the parent population is randomly selected. However this technique is more disruptive in its nature than Roulette wheel selection. The main drawback of the Roulette wheel selection is that if the best chromosome's fitness value is 80 %, it occupies 80% of Roulette wheel and other chromosomes have scarce chances of being selected. To overcome this drawback, the rank selection ranks the given population from 1 to N; 1 having worst fitness and N having best fitness. Then every chromosome receives its fitness from its ranking value. The benefit of using this technique is that it preserves diversity and prevents too quick a convergence. In tournament selection, selection pressure is selected by holding a tournament between potential solutions and the winner of the tournament is selected with the highest fitness value. Several of such tournaments can be performed and the winners are placed into the mating pool which has a higher average fitness value than the whole population. Increased selection pressure can be applied by having a larger tournament population size as

winner from a larger tournament will have a higher fitness than the winner from a smaller tournament population size.

### *3.3.2.2 Cross over (Recombination)*

The second operator is cross over (Kalyanmoy and Deb 1998) which takes the two parent chromosomes from an enriched population obtained from the selection and exchanges part of the genes to form new chromosome for child generation. The cross over basically inter-mixes the existing population and is a recombination operator. The cross over operator randomly selects a pair of individuals and a cross site is selected in the string. The positions are then swapped between the two individuals on the cross site as shown in the Figure 3.3, where a single point cross over is performed after the third binary.

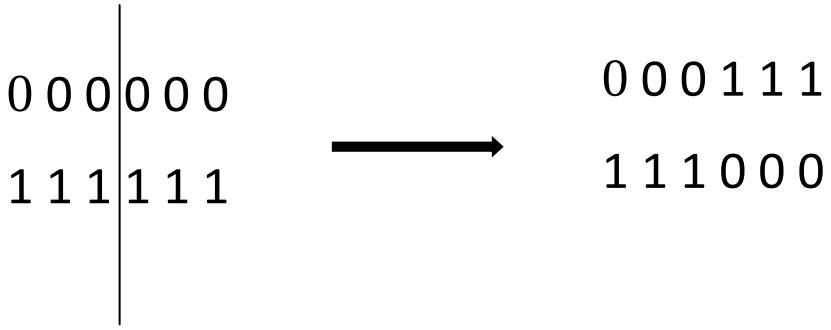


**Figure 3.3 Single point cross over performed after third binary**

The cross over fraction defines the fraction of each population that are made of cross over children. Usual schemes for cross over are based on the point at which cross over is performed on the string and are named as single point, two-point, multipoint, shuffle etc. In single point cross over, the mating chromosomes are cut at a single point and the sections are exchanged between the two. A cross site is selected randomly along the length and bit next to it are crossed. In two point cross over, the chromosomes are cut at two points and the contents of the parent chromosomes are exchanged between these two points. In multi-point cross over, the cross sites are selected randomly at multiple points and information is

exchanged. Adding further points to cross over site leads to better exploration capability but can reduce the overall performance of the algorithm. In uniform cross over, a random binary cross over mask, having the same length as the original chromosomes, is generated. Based on this mask, if the value is 1 then gene is taken from 1$^{st}$ parent and if the value is 0 then the gene is taken from the 2$^{nd}$ parent. Other variants include three point cross over, shuffled cross over, cross over with reduced surrogate etc.

The important parameter is the cross over probability which means that how often cross over will be performed. If the cross over probability is 100%, this means that all the population points will take part in the cross over operation. If the cross over probability is 0%, this means that new generation is the exact copy of the original one. Cross over is applied with a hope of getting good parts of old chromosomes. However, some parts of the old population surviving to the next generation might also help which can be allowed by using cross over probability value less than 100 %.

### *3.3.2.3 Mutation*

The last important randomised operator is mutation (Kalyanmoy and Deb 1998). It is a background operator which maintains diversity in the generation. With the process of selection and cross over, there is an irreversible loss of population. Mutation introduces new genetic solutions which help algorithm to escape local minima and maintain diversity. A simple mutation operator inverts the value of a gene, e.g. mutation of a binary is to change it from 0 to 1 as shown in the Figure 3.4.

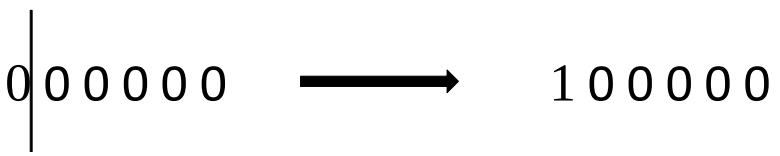


**Figure 3.4 Mutation performed on the first binary**

The mutation fraction defines the fraction of each population that are made of mutated children. The probability of mutation in a regeneration process is usually kept small as it deteriorates the convergence speed of the algorithm. Common types of mutation operators are flipping, interchanging and reversing. In flipping, a masking mutation chromosome is generated and bits in parent chromosome are flipped from 0 to 1 or 1 to 0 at selected locations based on a masking chromosome. In interchanging, random positions of strings are chosen and bits at these positions are interchanged between the two parents. In reversing, a random position is chosen and bits are changed next to that position.

Mutation probability is an important parameter which decides how often the parts of the parent chromosomes be mutated. If mutation probability is 0, offspring after the cross over will be generated immediately without any change. If the mutation probability is 100 %, the whole population is changed. Mutation should not occur frequently as this may lead the algorithm to become a random search.

Some important variants of GA introduced in the literature include elitist selection GA which carries good solutions in successive generations (Knowles et al. 2008), adaptive GAs which control probabilities of cross over and mutation (Srinivas and Patnaik 1994), and gene pool recombination where the whole population is mutated rather than individual members (Abdul-Halim and Abdul-Kader 2006).

### *3.3.3 Simulated annealing*

The main idea of SiA comes from the paper by Metropolis et al. (1953) in which the process of simulation of cooling of metals in a heat bath (also known as annealing) was presented. SiA (Kirkpatrick 1984) used the idea of Metropolis and applied it to solve optimization problems.

SiA is a generalisation of the Monte Carlo method which examines the states of n-body systems. If a solid is heated past its melting point and then allowed to cool down, the properties of the solid thus formed depend on the rate of cooling. The rate of cooling is an essential parameter as too slow cooling results in the formation of large crystals and too quick cooling results in imperfections in the crystalline microstructure. In other words, the atoms can move freely at high temperatures, but with the decrease in temperature the movement of the atoms is reduced. The system is slowly cooled so that the system could remain in thermodynamic equilibrium at any state. The system becomes ordered as cooling proceeds and approaches a frozen state. The atoms finally form crystals with a minimum possible energy. Hence it can be referred as an adiabatic approach to the lowest energy state. However if the cooling is too fast, the lowest energy crystalline state may never be achieved, and the system might end up in an imperfect polycrystalline microstructure.

According to the Metropolis algorithm scheme, for a thermodynamic system an initial state of temperature and energy is chosen (Kalyanmoy and Deb 1998). For a constant temperature, the initial configuration is perturbed and change in energy due to this perturbation is noted. If the energy change is negative, the new configuration is accepted as it is; if the energy change is positive, the new configuration will be accepted based on its Boltzmann probability factor.

In a minimization problem, the SiA technique simulates this process of slow cooling of metals to attain a minimum function value. The current state of the system is analogous to the current solution, the energy equation is analogous to the objective function and frozen state is analogous to the global minimum. A temperature-like parameter is introduced and the concept of Boltzmann probability is used to simulate the cooling phenomenon. SiA is basically a point by point method and the probability of selection of the next point depends on the difference in the objective function value at these two points

$$\Delta E = E(t+1) - E(t) \quad \textbf{3.4}$$

and is calculated by Boltzmann probability (Kirkpatrick 1984) as

$$\mathrm{P}\big(\mathrm{E}(\mathrm{t}+1)\big) = \min\left[1, \exp\left(-\frac{\Delta \mathrm{E}}{\mathrm{kT}}\right)\right] \quad \textbf{3.5}$$

In the above equations, P(E) is the probability of selection, E is the energy of the system, k is the Boltzmann constant, T is the temperature at a specific iteration, and t represents the generation counter.

In a minimization problem, if the energy of the system is decreased between two states, the algorithm accepts it and moves to the new state. But if the energy of the system is increased, the new state is accepted with a probability given by Equation 3.5. This characteristic of the algorithm enables it to explore many states of the system thus escaping local minima during the search process. A certain number of iterations are performed at the same temperature to give good sampling. The re-anneal interval is defined as the number of points which are accepted before the re-annealing process occurs. The temperature is then decreased and the entire process is repeated to the point where a frozen state is achieved. However, to obtain the global minimum, the cooling phenomenon should simulate many possible values of the objective function in order to get a minimum with a higher probability and a frozen crystalline state.

An important parameter of SiA is the cooling schedule which further consists of four components: starting temperature, ending temperature, temperature decrement and iterations at each temperature. Each of these components are explained one by one in the next sub-sections.

### *3.3.3.1 Starting temperature*

A high enough temperature should be allowed at the start of the algorithm so that solutions can be sought at any neighbourhood state. If this is not followed, then the ending solution might be very close to the initial solution or in other words, it simply acts as a hill climbing algorithm. On the other hand, if the temperature is too high at the early stages of the algorithm, the system can move to any state and thus transforms into a random search. The system will behave as random search as long as the temperature is cool enough after which it starts acting as SiA algorithm. Therefore a correct starting temperature might be helpful in exhibiting good convergence properties. There is no known method, at present, which can exactly estimate the correct value of the starting temperature. However, certain methods have been applied to solve this problem. As suggested by Rayward-Smith et al. (1996), the algorithm is started with a high temperature and cooled down rapidly till the point where 60% of the worst solutions are accepted. This can be taken as a good starting temperature and the system can now be cooled slowly. A similar idea was also presented by Dowsland (1993). This method of selection of temperature is analogous to physical heating of the material till it becomes liquid and where further heating of the system does not pose any advantage.

### *3.3.3.2 Ending temperature*

A final temperature equal to zero is sought in ideal conditions but this can increase the time required for computation. In practice, a zero final temperature is not necessary to be sought as a zero temperature decreases the chances of accepting worse moves in the Metropolis algorithm. Therefore, the algorithm can be stopped at a suitably low temperature or when the system attains a frozen state at the current temperature (i.e. no better or worse moves are available).

#### *3.3.3.3 Temperature decrement*

After the setting of initial and final temperatures, next important parameter is the temperature decrement i.e. how to proceed from a high energy state to a lower energy state. This is important in terms of success of the algorithm in reaching the frozen state. A sufficient number of iterations should be allowed at each temperature so that the system is stabilized. On the other hand, the number of iterations required to achieve stabilized condition might be exponential. Therefore, either a small number of iterations are performed at many temperatures or large number of iterations is performed at few temperatures or a balance of the two.

#### *3.3.3.4 Iterations at each temperature*

The last decision is related to the number of iterations to be performed at each temperature level. In the most common form, a constant number of iterations are performed at each temperature. Another method suggested by Lundy and Mees (1986) suggests performing one iteration at a given temperature but the temperature needs to be cooled very slowly. A dynamic system in which a small number of iterations is performed at higher temperatures and a large number of iterations performed at lower temperatures may also be adopted. This can help in fully exploring the local optimal solution in the search space.

It has been proved that SiA algorithm can lead to a best possible solution in the search space but taking more time than an exhaustive search. Although it may not be practical to obtain the best possible solution in a given time for a specific problem with a large search domain, SiA does have this important property which makes it worth exploring.

### *3.3.4 Theoretical comparisons of global optimization algorithms*

#### *3.3.4.1 Theoretical comparisons of GOAs with conventional optimization techniques*

The following are the differences between GOAs and the conventional optimization techniques.

1- The conventional optimization techniques search from a single point whereas GOAs mostly work on a whole population of strings. This also improves the chance of GOAs to reach global minimum.
2- GOAs do not use derivative information and use fitness function values for minimization. Because of this reason, they can be applied to discrete or continuous optimization problems.
3- Conventional optimization techniques use deterministic transition operators where as GOAs use probabilistic rules.
4- GOAs can handle large relatively poorly understood search spaces and therefore suits to multimodal problems, whereas conventional techniques cannot handle multimodal problems well.
5- GOAs require a large number of function evaluations as they work on population of points whereas conventional optimization techniques use a lower number of function evaluations.
6- GOAs cannot incorporate problem specific information such as gradients.

#### *3.3.4.2 Theoretical comparisons of GOAs with each other*

In this section, the operators of each of the three algorithms, i.e. PSO, GA and SiA, are discussed focussing on their effects on search behaviour within the problem domain.

1- The operators used by each of the three algorithms differ from each other. PSO uses a velocity equation, GA uses three operators namely selection, cross over and mutation, and SiA uses the Metropolis algorithm for perturbation of the individuals in search space for minimization / maximization of a particular objective function.
2- PSO and GA work on a number of randomly initialized solutions in parallel whereas SiA works on a point-wise basis.
3- The particles flying in n dimensional space in PSO never die down and explore the search space on their way. In GA and SiA, the particles die down as generation proceeds.
4- In PSO, each particle accelerates in the search space towards its own best previous position pbest and best global position gbest. The cross over in GA exchanges part of the randomly selected gene information in an attempt to produce better off spring. In SiA, the algorithm chooses a random move from its neighbourhood based on Metropolis algorithm.
5- History of a particle is remembered by PSO in the form of pbest during the search process whereas history of a particle is forgotten by GA and SiA.
6- The maximum velocity factor in PSO controls the movement of particles to reach any point in the problem space. In GA, mutation rate is responsible for the algorithm to reach any point and in SiA, temperature parameters controls this factor. Also, PSO can take a directional acceleration using a velocity equation, whereas GA and SiA both can take omnidirectional movement.

It can be seen that in PSO algorithm, the particles never dies down as compared to GA and SiA, and remembers its previous best location. The movement of all particles in a swarm is uni-directional as compared to the two other algorithms. Also the velocity equation is very close to the first gradient information which makes PSO algorithm very close to a gradient

based optimization. Therefore, on the basis of the Free lunch theorem, the suitability of each of these algorithms is worth exploring for model updating problems.

## 3.4 Summary

In this chapter, the basic theory of three different GOAs namely PSO, GA and SiA have been explored. It was found that each of the three algorithms differ from each other and have different parameters responsible for convergence. A number of theoretical differences exist between standard conventional techniques such as SM and GOAs, and within the three GOAs.

# Chapter 4. DYNAMIC TESTING AND MODEL UPDATING OF A LABORATORY STRUCTURE USING GLOBAL OPTIMIZATION ALGORITHMS

## 4.1 Introduction

In this chapter, experimental testing, system identification and model updating of a laboratory structure are carried out. Different GOAs (as detailed in Chapter 3) were applied to this dynamic model updating problem to check their efficacy and accuracy for a relatively simple dynamic system. In the subsequent sections, experimental modal analysis techniques used in this research, such as spectral analysis and subspace state-space system identification methods are explained first. Then, the experimental structure and its modal testing programme are described. Model updating is then performed using the three GOAs ---PSO, GA and SiA--- to compare their accuracy and efficiency in obtaining updated parameters.

## 4.2 Spectral analysis

### *4.2.1 Power spectra*

For system identification in the frequency domain, power spectra and FRF are frequently used. To transform signals from the time domain to the frequency domain, a Fourier transform is performed (Friswell and Mottershead 1995). For a continuous time wave waveform $x(t)$, a Fourier transform is determined as

$$X(f) = \int_{-\infty}^{\infty} x(t) e^{-j2\pi ft} dt \qquad \textbf{4.1}$$

where *f* is the analysis frequency and *X(f)* is the Fourier transform of *x(t).*

The two-sided cross-power spectral density $S_{XY}$ between two signals $X(n)$ and $Y(n)$ is given by

$$S_{XY}(f) = \frac{X(f) \times Y^*(f)}{N^2} \qquad \textbf{4.2}$$

where "*" denotes the complex conjugate.

For a single set of data, a similar spectrum named auto-power spectral density $S_{XX}$ can be obtained as

$$S_{XX}(f) = \frac{X(f) \times X^*(f)}{N^2} \qquad \textbf{4.3}$$

### *4.2.2 Frequency response function*

FRF is a measure of system's spectral response relative to the input signal. FRFs can be calculated from auto-spectral densities and cross-spectral densities of the two signals in the following way

$$H(f) = \frac{S_{XY}(f)}{S_{XX}(f)} \quad \textbf{4.4}$$

where $S_{XY}(f)$ is the cross-power spectrum of the response and excitation signal in the frequency domain, and $S_{XX}(f)$ is the auto-power spectrum of excitation signal in the frequency domain. Normally, the responses are measured in terms of acceleration and $H(f)$ is called inertance.

A Fourier transform is performed on the assumption that the signal is periodic and complete over the length of the observation time. If this assumption is not true, i.e. the signal does not end as a complete cycle, energy leakage occurs in the spectral lines near the true frequencies. The spectral leakage can be alleviated by multiplying the signal with a windowing function as

$$x^w(t) = x(t)w(t) \quad \textbf{4.5}$$

where $x^w(t)$ is the signal obtained after the windowing function is applied, $x(t)$ is the original signal and $w(t)$ is the windowing function.

A window function maintains or magnifies the signals inside a certain interval and tends to zero outside those intervals. The Hanning window (Ljung 1987) is commonly used and is given by

$$w(t) = 0.5\left[1 - \cos\left[\frac{2\pi t}{\kappa}\right]\right] \quad \textbf{4.6}$$

where t is the time step and $\kappa$ is the length of signal.

If both the input signal and output signal are multiplied with the windowing function, rescaling is not required for calculating FRF.

## 4.3 Subspace state-space system identification

The core of most identification algorithms is a least square solution which gives a relationship between input and output of any unknown system. The state space model (Ljung 1987) is one of the most popular models of dynamical systems. The subspace state-space system identification technique is a powerful technique for modal analysis in the time domain to estimate the unknown matrices of the state space model (Overschee and Moor 1996). At any arbitrary step $k$ , a discrete time state space model is given by

$$x_{k+1} = Ax_k + Bu_k + \omega_k \quad \textbf{4.7}$$

$$y_k = Cx_k + Du_k + v_k \quad \textbf{4.8}$$

where $x_k, u_k$ and $y_k$ are state, input and output vectors at time *k*, respectively, *A*, *B*, *C* and $D$ are system matrices to be estimated by the identification algorithm, and $\omega_k$ and $v_k$ are the process and measurement noises respectively. Subspace state-space system identification algorithms determine these matrices to estimate the unknown system characteristics such as natural frequencies, mode shapes and viscous damping ratios.

The subspace algorithm described below follows the development in the book by van Overschee and De Moor (1996) and can be applied to output only or input–output identification problems. A brief generalized procedure of the algorithm is presented here.

The algorithm starts with assembling block Hankel matrices from the input and output sequence. The block Hankel matrix for the input sequence is given by

$$U_{0/2i-1} = \left[\begin{array}{cccc} u_0 & u_1 & \dots & u_{j-1} \\ u_1 & u_2 & \dots & u_j \\ \dots & \dots & \dots & \dots \\ u_{i-1} & u_i & \dots & u_{i+j-2} \\ \hline u_i & u_{i+1} & \dots & u_{i+j-1} \\ \dots & \dots & \dots & \dots \\ u_{2i-1} & u_{2i} & \dots & u_{2i+j-2} \end{array}\right] = \left[\begin{array}{c} U_{0/i-1} \\ \hline U_{0/2i-1} \end{array}\right] = \left[\begin{array}{c} U_p \\ \hline U_f \end{array}\right] \quad \textbf{4.9}$$

The Hankel matrix can be divided into past $U_p$ and future $U_f$ parts. The value of index $i$ separating the past from the future should be greater than the maximum order of the system to be identified. The value of $j$ should be chosen such that $2i+j-2$ does not exceed the input and output sequence length. The block Hankel matrix for output can also be constructed in a similar way.

A combined matrix of input and output sequence is defined as

$$W_p = \left[U_p \,|\, Y_p\right]^{'} \quad \textbf{4.10}$$

The next step is to compute the oblique projection $Ob_i$. An oblique projection of the row space of $Y_f$ along $U_f$ on $W_p$ can be computed as

$$Ob_i = Y_{f/U_f} Wp \quad \textbf{4.11}$$

The oblique projection is the product of extended observability matrix $\Gamma_i$ and state sequence $X_i$

$$Ob_i = \Gamma_i X_i = [C \quad CA \quad \dots \quad CA^{i-1}]^{'}[x_i \quad x_{i+1} \quad \dots \quad x_{i+j-1}] \quad \textbf{4.12}$$

The extended observability matrix $\Gamma_i$ and state sequence $X_i$ can be calculated by singular value decomposition of $Ob_i$ as

$$Ob_i = USV^{*} \quad \textbf{4.13}$$

where *U* and *V* are unitary matrices and *S* is a diagonal matrix of singular values.

The extended observability matrix $\Gamma_i$ can be determined as

$$\Gamma_i = US^{1/2} \quad \textbf{4.14}$$

The state sequence is the remaining half of the decomposition and is given by

$$X_i = S^{1/2}V' \quad \textbf{4.15}$$

System matrices *A* and *C* defined in Equation 4.7 and Equation 4.8 can be determined from the observability matrix $\Gamma_i$. The matrix *A* can be found from the observability matrix by removing rows each from the top and bottom and the system matrix *C* can be determined by taking the first row of the observability matrix. Matrices *A* and *C* can be used to determine the natural frequencies, mode shapes and damping ratios. The system damped properties are calculated from the complex eigen values ($\lambda_i$) and eigen vectors ($\Psi_i$) of matrix *A*. With the assumption of nearly classical and small damping, the modal properties can be calculated as (Alvin and Park 1994; Skolnik et al. 2006)

$$f_i = |\lambda_i| / 2\pi \quad \textbf{4.16}$$
$$\xi_i = \frac{\mathrm{Re}(\lambda_i)}{2\pi f_i}$$
$$\Phi_i = |C\Psi_i| . sign[\mathrm{Re}(C\Psi_i)]$$

where $f_i$ is the modal frequency, $\xi_i$ is the damping ratio, $\Phi_i$ is the mode shape for the ith mode, and Re denotes real part of the complex value. The numerical algorithm for subspace state space system identification (N4SID) (Overschee and Moor 1996), a useful variety of subspace methods, has been used in this study for identification of modal properties.

## 4.4 Description of laboratory structure

The laboratory structure considered in this study has a height of 700 mm and is made up of a steel plate and aluminium angles as shown in Figure 4.1. This structure was initially designed for a previous study by De Lautour (De Lautour 2009). The square steel plate of plan size of 650 mm x 650 mm and a thickness of 4 mm was used for the slab. Equal angles having dimensions of 30 x 30 mm with a thickness of 3 mm were used as columns. The columns were attached to the slab with aluminium brackets having 30 mm width, 4.5 mm thickness and 75 mm length. However, the brackets were connected with bolts at a distance of 20 mm from the corner. The whole structure was fitted on a wooden plywood sheet.

The structure was tested on the shake table situated in the test hall of the Department of Civil and Environmental Engineering, University of Auckland. The shake table uses hydraulic pressure generated by a pump as shown in the Figure 4.2a. A Proportional Integral Derivative controller (PID) (see Figure 4.2b) controls the motion of the shake table. A Direct Current Displacement Transducer is fitted to the shake table to measure the actual displacement and give feedback to the controller.

As the shake table is able to excite the structure in one direction only, the structure was fitted at an angle of 20 degrees to the direction of shaking as shown in Figure 4.1. This was done to excite the structure in both x and y direction, although the excitation level on y-axis would be stronger than that of the x-axis. A mass eccentricity was also present in the system due to eccentric placement of the accelerometers on the slab.


**Figure 4.1 Laboratory structure fitted on the shake table at an angle of 20 degrees to the direction of shaking**

A total of five uni-axial accelerometers were used to measure the response. One uniaxial accelerometer was fitted on the slab for measuring the accelerations in the y direction, whereas three uniaxial accelerometers were used to measure the acceleration in the x and torsional directions, refer Figure 4.3a. One uniaxial accelerometer was fitted on the shake table to measure the input acceleration by the shake table. The data was acquired at a sampling rate of 200 Hz. A separate data acquisition system was used to acquire the data from the accelerometers fitted on the structure during shaking (Figure 4.3b). MATLAB was used to acquire the data from the accelerometers. A total of three frequency sweep tests were conducted on the laboratory structure by exciting the structure within a range between 0 to 15 Hz.


**(a)** **(b)**

**Figure 4.2 Shake table a) Hydraulic pump for shake table b) PID and data acquisition system for shake table**

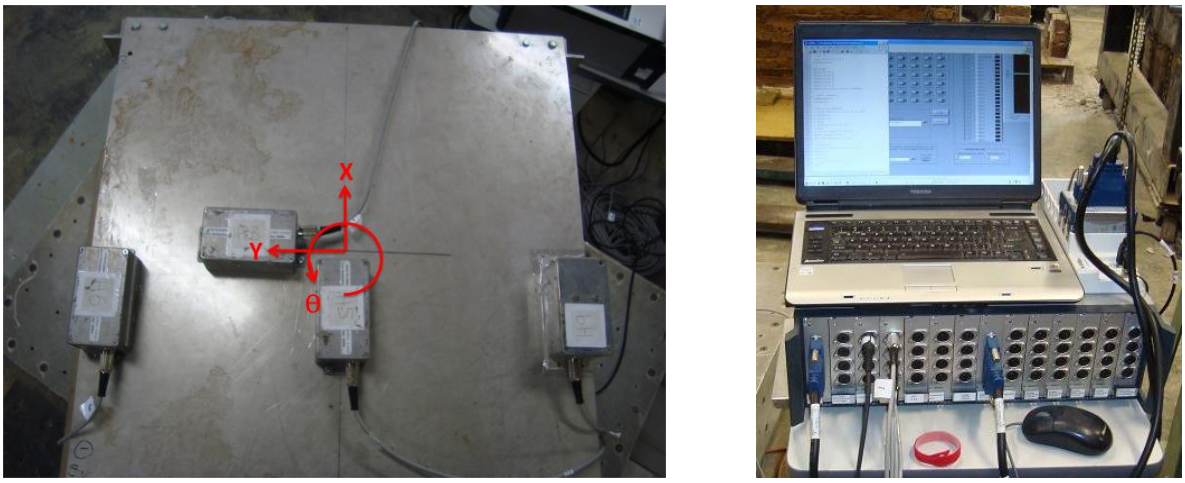


**(a)** **(b)**

**Figure 4.3 Response measurement of the laboratory structure a) three accelerometers in x direction and one accelerometer in y direction b) data acquisition system**

## 4.5 System identification

Spectral analysis was carried out on the data using FRF. The data was first filtered to remove any high frequency content above 50 Hz. Welch's method (Stoica and Moses 1997) has been used for FRF calculations. It is possible to decrease the effects of immeasurable extraneous excitations by performing some averages (Ewins 2000). The data for each test was divided in to 5 segments with 50 % overlap. Hamming window was applied on each segment and a periodogram of each window is estimated. These periodograms were then averaged to estimate the spectrum of input (force) and output (response). FRF is then calculated from the input and output spectrums for each test and an average of the three tests were taken to obtain the FRF curve. The FRF for a single accelerometer in the y direction along with its phase and coherence is shown in Figure 4.4. A significant peak at 3.56 Hz in Figure 4.4 (a) indicates a translational mode in the y direction ($1^{st}$ mode). A phase change of 180 degrees has also been observed at 3.56 Hz in Figure 4.4 (b) (shown by black ellipse) indicating the presence of a mode. Coherence between the force and response at 3.56 Hz in Figure 4.4 (c) (shown by black circle) is higher than 0.85 indicating a good correlation between these two. Another aspect to note in Figure 4.4 (c) is that at the surrounding points of 3.56Hz frequency, the coherence is almost equal to 1 which is due to synchronised movement of the shake table and the laboratory structure. It has also been noted that at higher frequency levels, the excitation force delivered by the shake table decreases.

FRF for the accelerometer in x direction away from the centre of the slab is shown in Figure 4.5. A single peak at 5.02 Hz in Figure 4.5 (a) shows a translational mode in the x direction ($2^{nd}$ mode) along with a small peak for the torsional mode above 7 Hz (3rd mode). The peak corresponding to the torsional mode is smaller in magnitude than other observed translational modes. Possible reasons for this could be that the shaker is only able to excite the structure in one direction and a small unbalanced mass (of the accelerometers) on the structure is

responsible for the torsional motion. A phase change of 180 degrees has been observed at 5.02 Hz in Figure 4.5 (b) as shown by the black ellipse indicating the presence of a translational mode and at 7.3 Hz indicating a torsional mode. Coherence between force and response at 5.02 Hz in Figure 4.5 (c) is higher than 0.85 indicating a good correlation, whereas a coherence of 0.78 is noted around the torsional frequency at 7.3 Hz (which could be attributed to low level of excitation at this frequency) as shown by black circles.

Note that the FRF is plotted in the figures using a linear scale in order to extract the relevant peaks. They are not plotted on logarithmic scale as it results in more noise at the low amplitude data, which can mask the modes of interest. Hence in this thesis, the FRFs as well as the spectra are plotted on linear scale.

To further investigate modes of the structure, two snap back tests were also carried out. The structure was displaced using a string from the top and the string was cut afterwards so that the structure undergoes free vibration. A peak can be seen at 3.56 Hz corresponding to translational mode in the y direction (Figure 4.6). Figure 4.7 shows the auto spectral density of the accelerometer in the x direction away from the centre of the slab. Two significant peaks can be observed wherein the first peak at 5.01 Hz corresponds to the translational mode in the x direction and a second peak at 7.32 Hz corresponds to the torsional mode. It has been observed that these results are in close agreement with the results obtained from frequency sweep tests and validates the previous results.

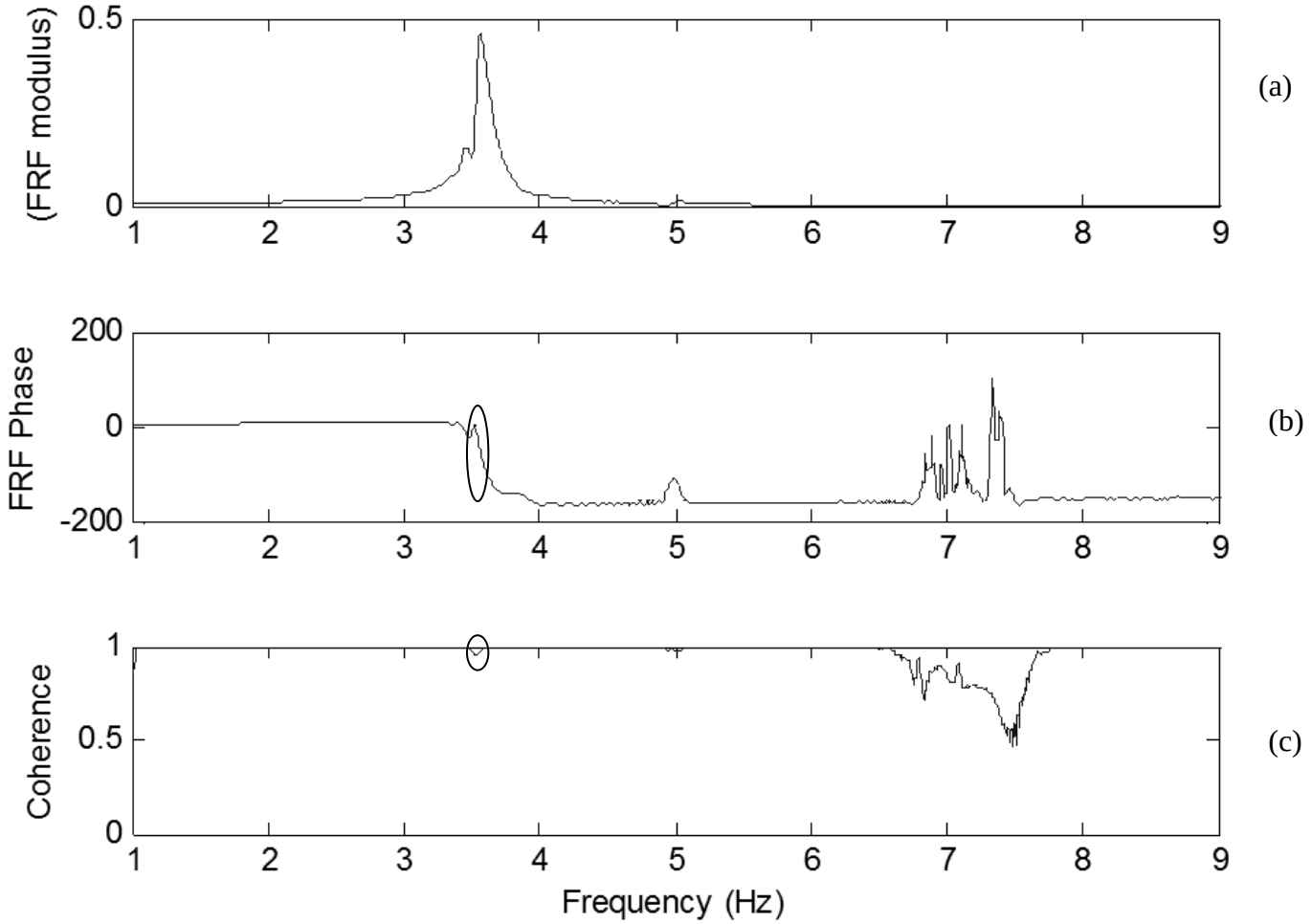


**Figure 4.4 FRF for accelerometer in y direction (a) FRF curve (b) Phase of FRF (c) coherence between force and response**

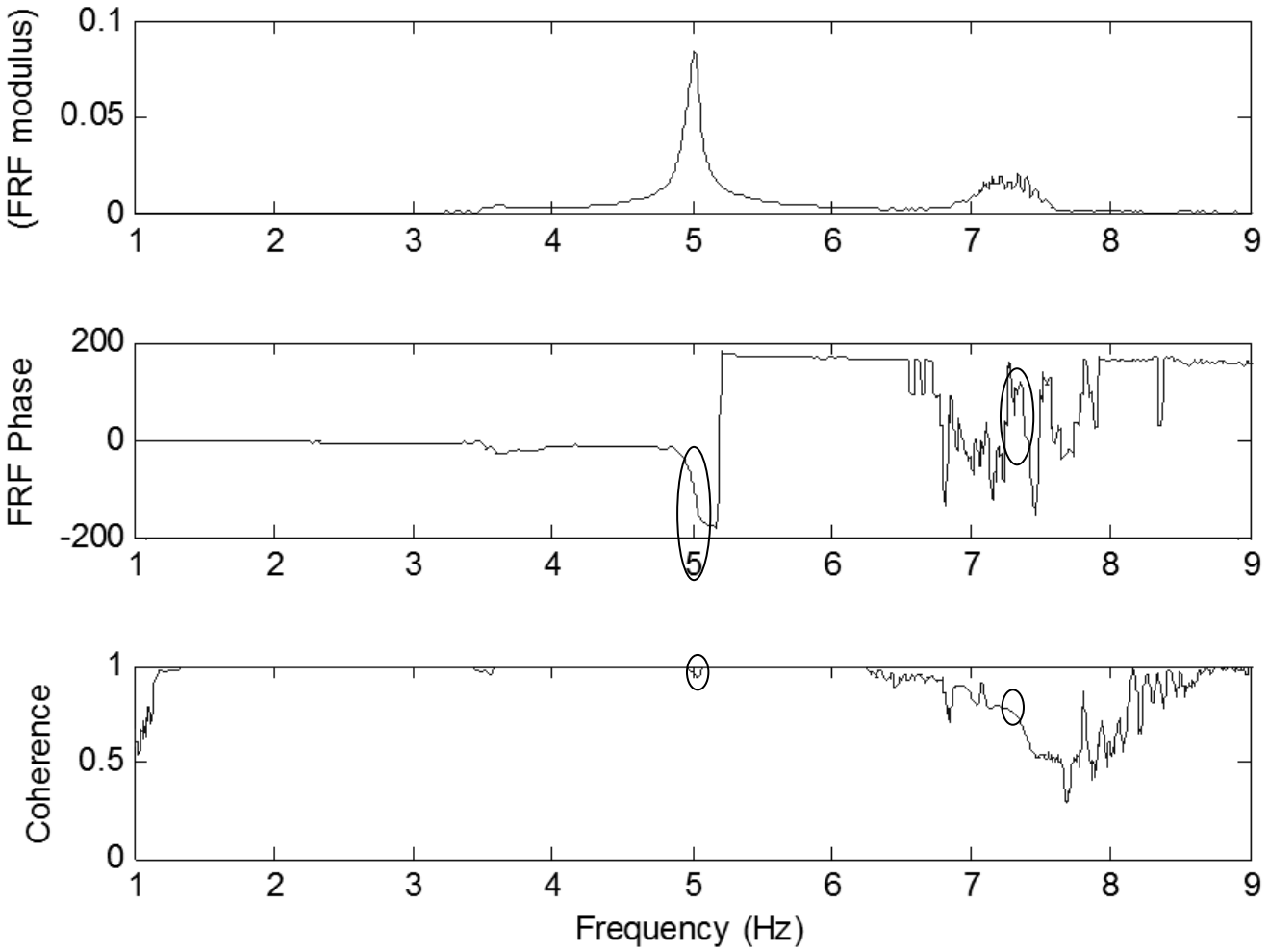


**Figure 4.5 FRF for accelerometer in x direction away from the centre of the slab (a) FRF curve (b) Phase of FRF (c) coherence between force and response**

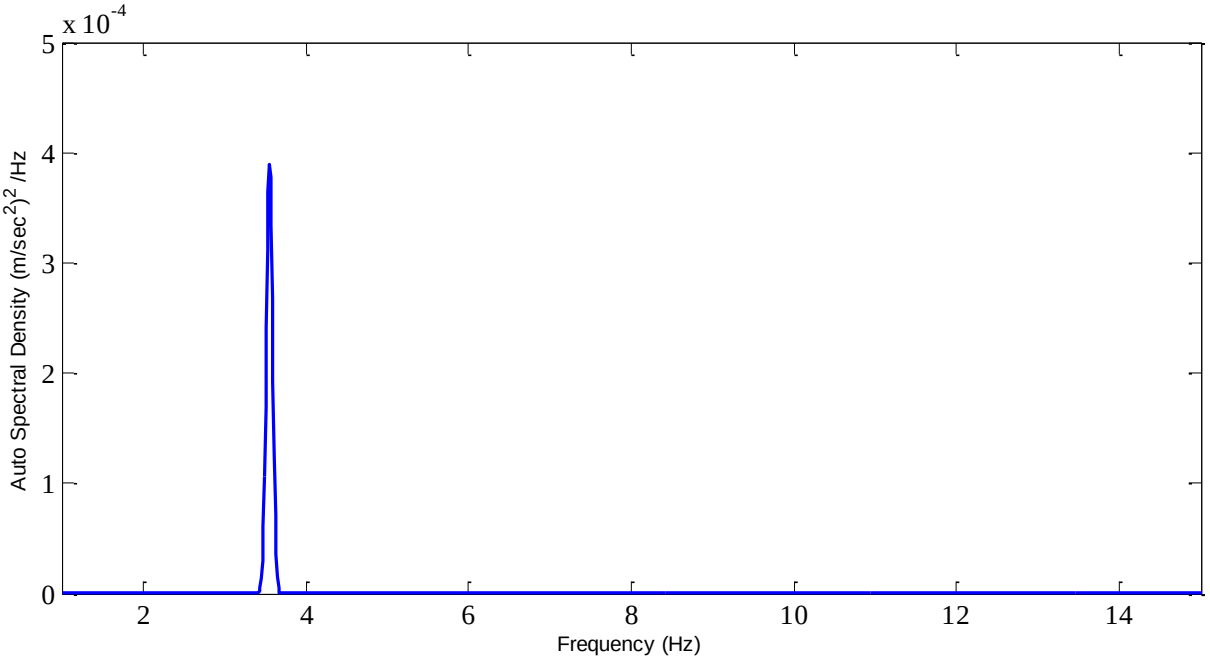


**Figure 4.6 Auto spectral density of accelerometer in y direction by snap back test**

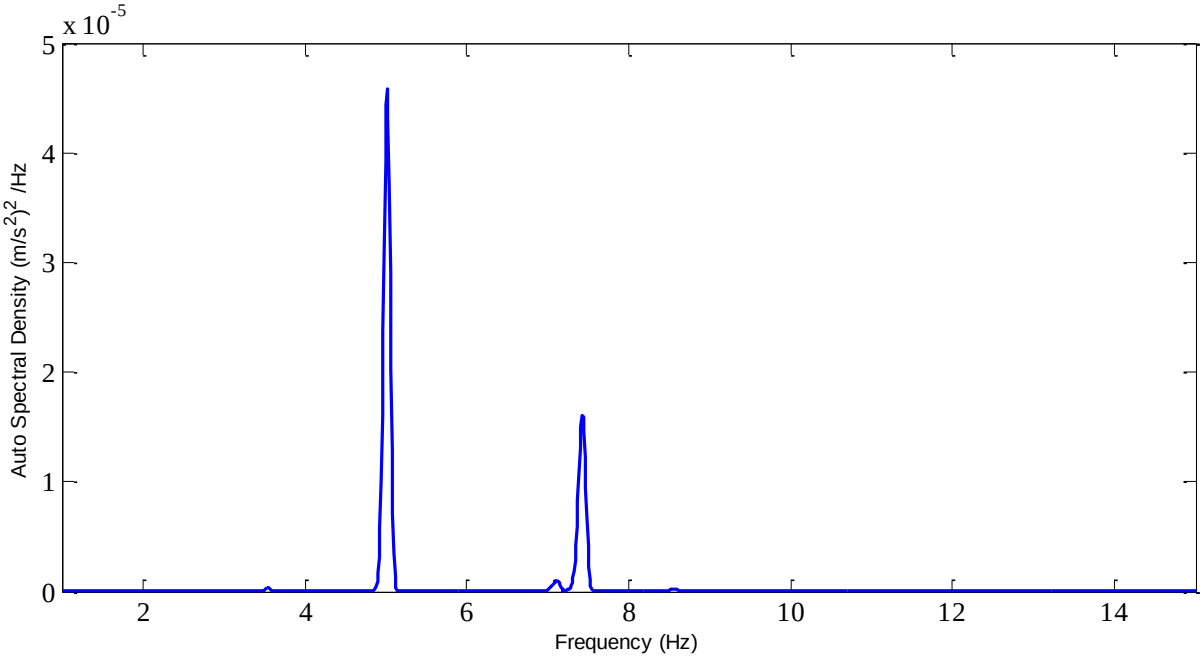


**Figure 4.7 Auto spectral density of accelerometer in x direction away from centre of slab by snap back test**

Modal analysis was also carried out on the time domain data using N4SID. A higher system order is normally chosen to detect all required modes of the system and orders between 6 and 40 were used for this study. The lowest system order of 6 was chosen as it was twice the number of desired modes. A stability diagram (Bodeux and Golinval 2001) is normally utilized to discern the superfluous modes from the structural modes. With the increase in the model order, the identified modal properties should remain stable. A relative change between the identified model properties with the increase in the model order has to be chosen for a given mode. For this research, the relative change in the frequency has been taken as less than 1% and MAC values is assumed to be greater than 0.90. A stable mode is chosen as the one which meets both of these criteria and is shown by black dots in Figure 4.8. It can be noted from Figure 4.8 that there are three frequencies which are stable for the laboratory structure as shown by black dots, when model order has been increased from 6 to 40. Although some superfluous modes were also detected, three frequencies at 3.58, 5.01 and 7.28 Hz remained stable. The frequency at about 14.5 Hz does not satisfy the two stability criteria.

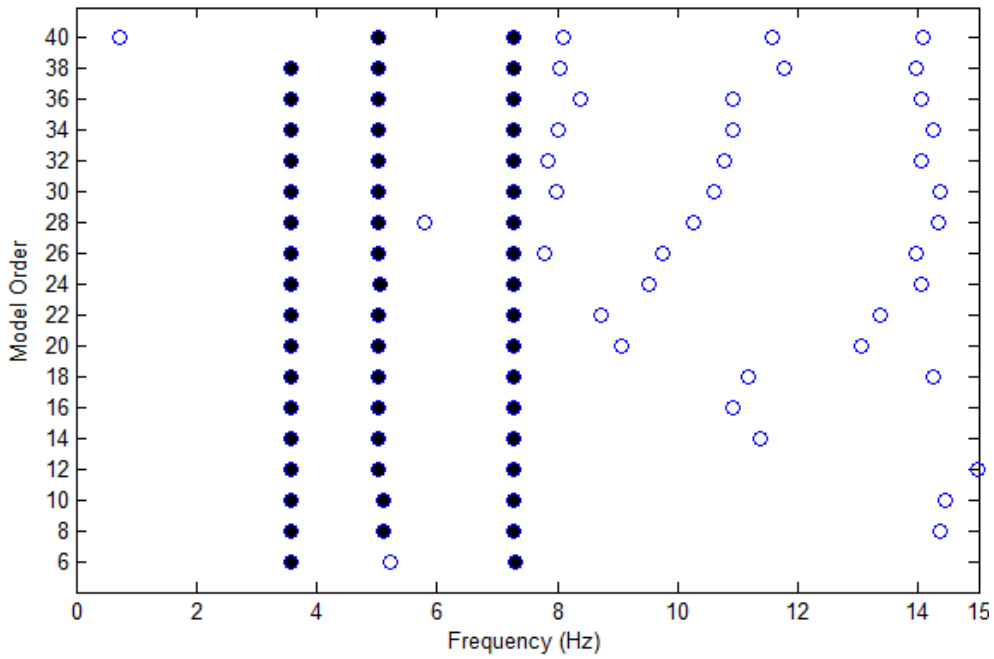


**Figure 4.8 Stability diagram for laboratory structure**

Natural frequencies of the laboratory structure using FRF and N4SID method are shown in Table 4.1. It can be seen that the frequencies identified by both of these methods match quite reasonably. System identification results of natural frequencies obtained from FRF and N4SID have been presented in the form of mean ± standard deviation for three tests. The standard deviation shows that data quality is good and may not significantly affect later updating. Mode shapes identified from the N4SID method are shown in Table 4.2. To have consistent units, mode shape values for the torsional direction are multiplied by (breadth of slab)/2.

**Table 4.1 Natural frequencies of laboratory structure using FRF and N4SID method**

| **Mode** | **Frequency (Hz)** | | **Damping ratio by N4SID method (%age)** |
|---|---|---|---|
| | **FRF** mean ± standard deviation for three tests | **N4SID** mean ± standard deviation for three tests | |
| 1 | 3.56±0.001 | 3.58±0.001 | 1.21±0.004 |
| 2 | 5.02±0.008 | 5.01±0.005 | 0.78±0.13 |
| 3 | 7.37±0.04 | 7.28±0.03 | 0.81±0.24 |

**Table 4.2 Normalized mode shapes of laboratory structure obtained using N4SID**

| **Mode** | **1** | **2** | **3** |
|---|---|---|---|
| y direction | 1.00 | 0.07 | -0.07 |
| x direction | 0.004 | 1.00 | -0.02 |
| Torsion | -0.01 | -0.03 | 1.00 |

Analytical models of structures often differ from the original structures as a result of many uncertainties and simplifications. Model updating is a branch of optimization in which the experimental natural frequencies, mode shapes and damping properties are compared with their analytical counterparts and physical properties of the structure such as stiffness and

mass are modified in the analytical models to reduce the difference between the two. An analytical model of the laboratory structure was derived based on force-displacement and mass-acceleration relationships in the next section.

## 4.6 Mass-spring model for laboratory structure

In this section, stiffness and mass matrices of the system have been determined by the direct equilibrium method. The relationship between the forces and displacements (Chopra 2007) is described as

$$f = Ku \qquad \textbf{4.17}$$

where $f$ is a vector of applied external forces, $K$ is the stiffness matrix and $u$ is the vector of displacements as a result of the applied external forces. For an idealized frame system consisting of a roof diaphragm, which is assumed to be rigid in its own plane, Equation 4.17 can be written for a three DOF system (i.e. translation in the x direction, translation in the y direction and torsional rotation) as

$$\begin{bmatrix} f_{sx} \\ f_{sy} \\ f_{s\theta} \end{bmatrix} = \begin{bmatrix} K_{XX} & K_{XY} & K_{X\theta} \\ K_{YX} & K_{YY} & K_{Y\theta} \\ K_{\theta X} & K_{\theta Y} & K_{\theta\theta} \end{bmatrix} \cdot \begin{bmatrix} u_x \\ u_y \\ u_\theta \end{bmatrix} \qquad \textbf{4.18}$$

The methodology consists of applying unit displacements to each DOF and calculating the stiffness influence coefficients by static equilibrium. We will represent our full structure with an equivalent single column. This stick model was adopted to enable us to locate the centre of stiffness of the whole model as shown in Figure 4.9. The final stiffness matrix of this shear type model is given as

$$\begin{bmatrix} f_{sx} \\ f_{sy} \\ f_{s\theta} \end{bmatrix} = \begin{bmatrix} k_{xx} & k_{xy} & -k_{xx}e_y + k_{xy}e_x \\ k_{yx} & k_{yy} & -k_{yx}e_y + k_{yy}e_x \\ -k_{xx}e_y + k_{yx}e_x & -k_{xy}e_y + k_{yy}e_x & k_{xx}e_y^2 - k_{xy}e_x e_y - k_{yx}e_y e_x + k_{yy}e_x^2 + k_{\rho\rho} \end{bmatrix} \cdot \begin{bmatrix} u_x \\ u_y \\ u_\theta \end{bmatrix} \quad \textbf{4.19}$$

where $k_{xx}$ is the resisting force of the equivalent column in the x direction due to a unit displacement $u_x$, $k_{yy}$ is the resisting force of the equivalent column in the y direction due to a unit displacement $u_y$, $k_{yx}$ is the resisting force of the equivalent column in the y direction due to unit displacement in x direction, $k_{xy}$ is the resisting force of the equivalent column in the x direction due to unit displacement in y direction, $k_{\rho\rho}$ is the rotational stiffness of the system, and $e_x$ and $e_y$ are the stiffness centre eccentricities in the x and y directions, respectively. To ensure symmetry in the stiffness matrix, we set $k_{xy}=k_{yx}$.

Likewise, for a system with three DOF, the inertia forces on the mass component of the structure based on the assumption of rigid diaphragm can be written as

$$\begin{bmatrix} f_{Ix} \\ f_{Iy} \\ f_{I\theta} \end{bmatrix} = \begin{bmatrix} M_{XX} & M_{XY} & M_{X\theta} \\ M_{YX} & M_{YY} & M_{Y\theta} \\ M_{\theta X} & M_{\theta Y} & M_{\theta\theta} \end{bmatrix} \cdot \begin{bmatrix} \ddot{u}_x \\ \ddot{u}_y \\ \ddot{u}_\theta \end{bmatrix} \quad \textbf{4.20}$$

Similar methodology as applied to find out the stiffness coefficients can also be applied to find out mass coefficients by applying unit accelerations instead of unit displacements to each DOF and calculating the mass influence coefficients. The complete mass matrix of the system is represented by

$$\begin{bmatrix} f_{Ix} \\ f_{Iy} \\ f_{I\theta} \end{bmatrix} = \begin{bmatrix} m_t & 0 & -y_{cm}.m_t \\ 0 & m_t & m_t.x_{cm} \\ -y_{cm}.m_t & m_t.x_{cm} & J \end{bmatrix} \cdot \begin{bmatrix} \ddot{u}_x \\ \ddot{u}_y \\ \ddot{u}_\theta \end{bmatrix} \quad \textbf{4.21}$$

where $m_t$ is the translational storey mass of the system (includes mass of the slab, half of column angles, brackets and accelerometers), $y_{cm}$ is the distance to the centre of mass in y axis from the reference point, $x_{cm}$ is the distance to the centre of mass in x axis from the reference point and $J$ represents the moment of inertia (MOI) for different masses.

Using the stiffness and mass matrices, the analytical model of the laboratory structure was implemented in MATLAB (MathWorks 2007). For a system with small damping ratios, the frequencies and mode shape values may be obtained by solving an eigen value problem

$$\left(\begin{bmatrix} k_{xx} & k_{xy} & -k_{xx}e_y + k_{xy}e_x \\ k_{yx} & k_{yy} & -k_{yx}e_y + k_{yy}e_x \\ -k_{xx}e_y + k_{yx}e_x & -k_{xy}e_y + k_{yy}e_x & k_{xx}e_y^2 - k_{xy}e_xe_y - k_{yx}e_ye_x + k_{yy}e_x^2 + k_{\rho\rho} \end{bmatrix} - \omega^2 \begin{bmatrix} m_t & 0 & -y_{cm}.m_t \\ 0 & m_t & m_t.x_{cm} \\ -y_{cm}.m_t & m_t.x_{cm} & J \end{bmatrix}\right)\Phi = 0 \quad \textbf{4.22}$$

where $\omega$ represents a natural frequency, and $\Phi$ represents the associated mode shape.

As the experimentally obtained mode shape values for the torsional direction are multiplied by (breadth of slab)/2, the mass and stiffness matrices are transformed accordingly. For this purpose, a transformation matrix *T=[1 1 b/2]* was applied to both stiffness and mass matrices.

## 4.7 Model updating

Model updating is a branch of optimization in which physical parameters of the structure are changed to decrease the difference between experimental values (such as frequencies and mode shapes) and their analytical counterparts. The experimental frequencies and mode shapes were used to update the lumped mass-spring model.

Estimated starting values of springs $k_{xx}$ ,$k_{yy}$ and $k_{\rho\rho}$ in the mass-spring model are calculated using SA model (using modulus of elasticity of the aluminum angles and their

assumed boundary conditions). To that end, a detailed SA model has been made in SAP2000 using shell elements for a single column. This shell model has been used to estimate the initial stiffness values of bracket-angle-bracket assembly as it enables to connect bracket with the angle and the wooden plywood support at the exact location. To simulate the support conditions, both top and bottom brackets are fixed at the bolt positions. Modulus of elasticity of aluminum angles was assumed as 70 x $10^9$ N/m$^2$. Initial stiffness values i.e. $k_{xx}$ in x and $k_{yy}$ in y direction are estimated by applying unit load method and found to be 20294 N/m and 8904 N/m for four columns, respectively. Although the column angle has the same stiffness in the both directions but the bracket connecting the plate and columns was more flexible. The estimation of rotational stiffness ($k_{\rho\rho}$) of the whole structure using actual eccentricities of columns was obtained by the initial stiffness values $k_{xx}$ and $k_{yy}$, and was found to be 3067.8 N m.

Mass values for the slab, angles, accelerometers, and bolts were determined experimentally to a total of 17.5 kg. The storey MOI of the structure was calculated as 1.26 kg-m$^2$. The actual eccentricity of the mass in x and y directions was calculated to be -0.0103 m and 0.0062 m respectively. The initial values of the parameters of the model are given in Table 4.3.

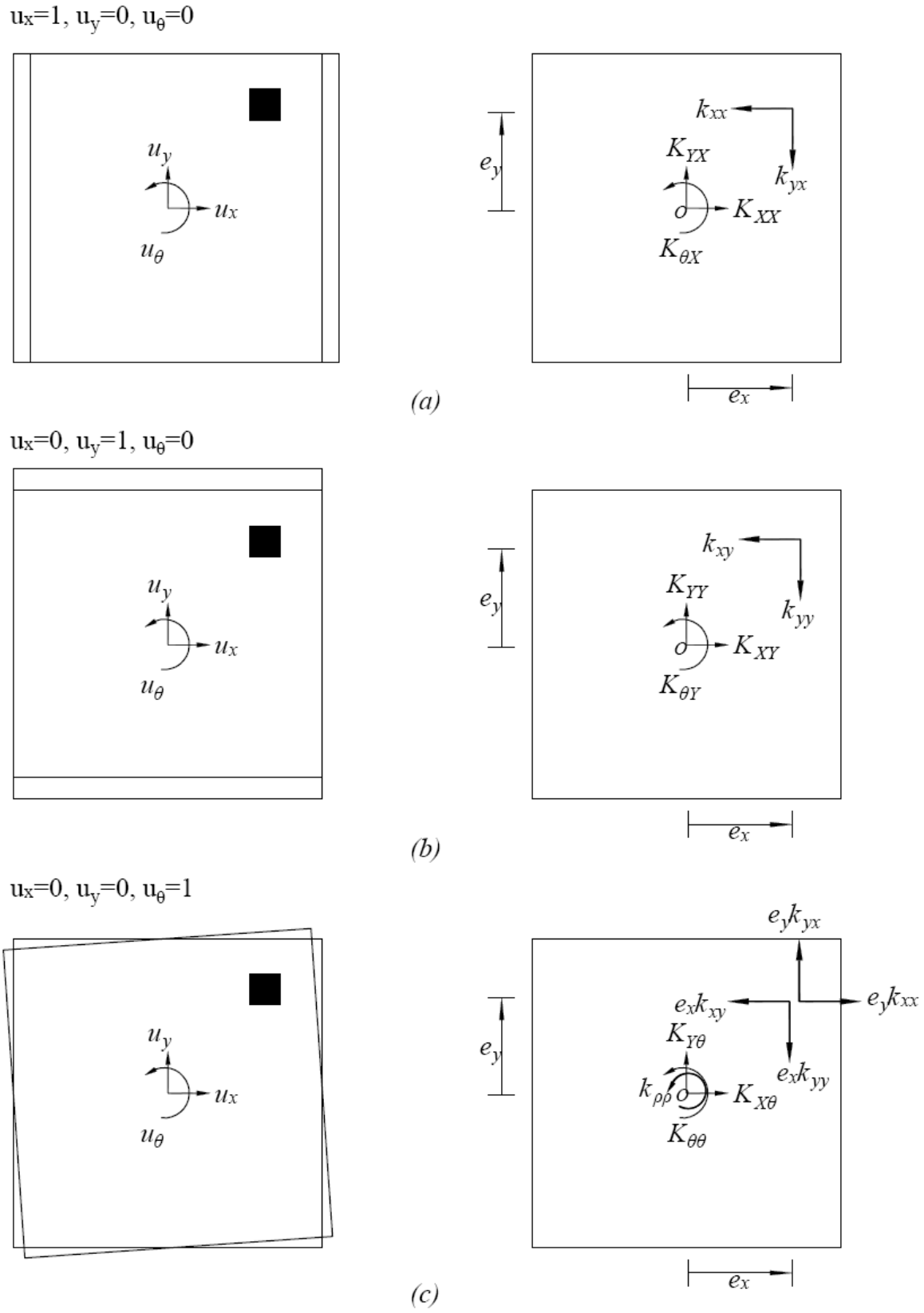


**Figure 4.9 Stiffness coefficients for (a) unit displacement in x direction (b) unit displacement in y direction, and (c) unit displacement in torsional direction (Black square is the equivalent single column)**

**Table 4.3 Initial values of analytical model of laboratory structure**

| Equivalent spring stiffness for four columns in y direction $k_{yy}$ (N/m) | Equivalent spring stiffness for four columns in x direction $k_{xx}$ (N/m) | Mass moment of inertia $J$ (kg-m$^2$) | Total mass $m_t$ (kg) | Mass eccentricity in x direction $x_{cm}$ (m) | Mass eccentricity in y direction $y_{cm}$ (m) |
|---|---|---|---|---|---|
| 8904 | 20294 | 1.2645 | 17.5 | -0.0103 | 0.0062 |

The most common approach to compare the experimental structure with analytical model is by comparing the natural frequencies and the mode shapes (Jaishi and Ren 2005), as was explained in Chapter 2. In this research, a combination of objective functions related to the natural frequencies and mode shapes has been used. The frequency difference between the experimental and analytical frequencies is given as

$$\prod_1 = \sum_{i=1}^{n} [(\omega_{a,i} - \omega_{e,i})/\omega_{e,i}]^2 \quad \textbf{4.23}$$

where ω represents modal frequency, subscripts a and e refer to analytical and experimental values, respectively, and n is the total number of modes to be updated.

The second objective function is related to the difference in mode shapes and can be defined in terms of MAC (Möller and Friberg 1998) as

$$\prod_2 = \sum_{i=1}^{n} \frac{(1 - \sqrt{\mathrm{MAC_i}})^2}{\mathrm{MAC_i}} \quad \textbf{4.24}$$

The combined objective function is given as

$$\prod = \alpha\prod_1 + \beta\prod_2 \quad \textbf{4.25}$$

where α and β are weighting factors and were taken as 1 for this beam tested under laboratory conditions. This objective function has been adopted as it does not require expansion/ reduction techniques (to address the mismatch between the DOF in the SA model and experimental data) which can induce further errors.

From the analytical equations derived in the previous section, it can be observed that possible parameters to be updated in the stiffness matrix are $k_{xx}$, $k_{yy}$, $k_{xy,}$ $k_{\rho\rho,}$ $e_x$ and $e_y$, whereas in the mass matrix possible parameters to be updated are the total mass $m_t$ and distances to the centre of mass $x_{cm}$ and $y_{cm}$. Parameter selection is a crucial step for success of model updating. As we have a total number of six knowns in the experiment (i.e. three frequencies and three MACs), a total of six unknown parameters can be selected for updating to avoid conditioning problems and proliferation of local minima. The total mass of the structure was measured quite precisely in the laboratory so $m_t$ was not taken as an updating parameter. Mass eccentricities $x_{cm}$ and $y_{cm}$ were calculated using actual mass locations and therefore not taken as updating parameters either. The parameter $k_{xy}$ was included in the model updating process as it was considered as an uncertain parameter related to cross-coupling stiffness. Therefore a total of six parameters, namely $k_{xx}$, $k_{yy}$, $k_{xy,}$ $k_{\rho\rho,}$ $e_x$ and $e_y$, were selected for updating against six knowns from the experiment.

Model updating was done using three GOAs, implemented in MATLAB (MathWorks 2007), to check their accuracy and efficiency. For these algorithms, the optimization algorithm was run till the point where the improvement in objective function value between ten subsequent iterations becomes less than $1x\ 10^{-8}$, or a minimum objective function value of $1x\ 10^{-6}$ is achieved, or the maximum number of function evaluations of 50000 was exceeded for PSO/GA/SiA. Ten independent runs were tested for each algorithm with different starting points to check their efficiency in reaching the global minimum.

### *4.7.1 Parameter selection for global optimization algorithms*

Each GOA has some specific parameter values to adjust, as mentioned in Chapter 3. Different trails were carried out by changing population size and other specific parameters for each GOA. All the algorithms were implemented in MATLAB having a working precision of 16 digits.

Upper and lower bounds of the updating parameters were selected based on engineering judgment. Different bounds were assumed in different studies (Jaishi and Ren 2005; Pavic et al. 2007). Upper bounds for the six parameters i.e. $k_{yy}$, $k_{xx}$, $k_{xy}$, $k_{\rho\rho}$, $e_x$ and $e_y$ were taken as 10600 kN/m, 24500 kN/m, 500 kN/m, 3500 N m, 0.1 m and 0.1 m, respectively, whereas the lower bounds for the six parameters were taken as 7000 kN/m, 16000 kN/m, -500 kN/m, 2500 N m, -0.1 m and -0.1 m, respectively.

For PSO, different trials were made and the convergence results are presented in Table 4.4. C1 to C6 are related to change in the population size of 5, 10, 20, 40, 50 and 100, respectively. Other important parameters to adjust were $\gamma$, $c_1$and $c_2$. On the basis of extensive study by Clerc and Kennedy (2002), initial values for PSO parameters were set to $\gamma$ =0.729, $c_1$=1.5 and $c_2$= 1.5 (known as *default contemporary PSO variant*) developed on the basis of an explicit relation between the parameters. The multiplication factors of 0.5, 1, 2 and 5 were multiplied with each of these parameters in a specific run to check their effect on the convergence (Case # C7 to C12).

A total of 10 runs were performed for each of the above cases and convergence has been assumed to be achieved when the average function value in ten runs is less than $1x10^{-5}$. This value has been assumed as the minimum exists at about $1.25x10^{-6}$. Case # C1 to C6 pertains to population size. It can be seen that a population size of 5 (C1) and 10 (C2) does not lead to convergence due to fewer points in the search space. A population size of 20 (C3) requires 34

iterations (total function evaluations required are 34 x 20=680), whereas an increase in population size to 40, 50 and 100 (C4, C5 and C6, respectively) does not result in significant reduction of required iterations. Therefore a population size of 20 was selected for further analysis cases. C7 to C12 pertain to common multiplication factor to PSO parameters $\gamma$, $c_1$and $c_2$. It can be seen that a factor of 0.5 (C7) does not lead to convergence, whereas a factor of 0.75 (C8) requires 17 iterations to converge. Further increase in the factor needs more iterations (C9 and C10) to converge. However, an increase in the factor value to 1.25 (C11) and 1.5 (C12) does not lead to convergence due to high velocity components. As a result, a population size of 20 and factor of 0.75 (C8) was selected as final parameters for PSO. The maximum velocity has been constrained as (maximum bound - minimum bounds)/2.

**Table 4.4 Parameter selection results for PSO**

| CASE # | Population size | Multiplication factor for PSO parameters, $\gamma$, $c_1$and $c_2$ | Iterations required to achieve convergence (average of ten attempts) |
|---|---|---|---|
| C1 | 5 | 1 | Not converged |
| C2 | 10 | 1 | Not converged |
| C3 | 20 | 1 | 34 |
| C4 | 40 | 1 | 30 |
| C5 | 50 | 1 | 28 |
| C6 | 100 | 1 | 27 |
| C7 | 20 | 0.5 | Not converged |
| **C8** | **20** | **0.75** | **17** |
| C9 | 20 | 0.9 | 25 |
| C10 | 20 | 1 | 34 |
| C11 | 20 | 1.25 | Not converged |
| C12 | 20 | 1.5 | Not converged |

For GA, a population size of 20 was used and other parameters i.e. selection and cross over were studied. A convergence criterion similar to that used for PSO was considered. The

results of parameter selection for GA are discussed in Table 4.5. An initial set of parameters were taken following study by Perera and Torres (2006) and is mentioned as D1. Case D2 employed Tournament selection instead of Roulette wheel selection and required a low number of iterations to converge. Cases D2, D3 and D4 compared three crossover functions i.e. single point, two point and scattered. It was found that the two point crossover function needed the least number of iterations to converge. Case D5, D6 and D7 employed a change in the crossover fraction. It was found that Case D5 with a crossover fraction of 0.7 proved to be the best in terms of convergence and needed the least number of iterations, whereas Case D7 with a crossover fraction of 1 with no mutation did not achieve convergence. Therefore, the final parameters selected in this study for GA are related to Case D5.

**Table 4.5 Parameter selection results for GA**

| Case # | Selection function | Crossover function | Crossover fraction | Mutation | Iterations needed to converge |
|---|---|---|---|---|---|
| D1 | Roulette | Single point | 0.8 | 0.01 | 75 |
| D2 | Tournament | Single point | 0.8 | 0.01 | 69 |
| D3 | Tournament | Two point | 0.8 | 0.01 | 56 |
| D4 | Tournament | Scattered | 0.8 | 0.01 | 43-119 |
| D5 | **Tournament** | **Two point** | **0.7** | **0.01** | **47** |
| D6 | Tournament | Two point | 0.25 | 0.01 | 51 |
| D7 | Tournament | Two point | 1 | 0 | No convergence |

A parametric study was also carried out for SiA and the results are presented in Table 4.6. A total of nine cases were studied. To reduce the number of parameters, the initial temperature and re-anneal interval was kept as one parameter. The Boltzmann annealing function was used in all the cases. The temperature function is an important parameter as it determines the rate at which the temperature is decreased as the algorithm proceeds. Two different types of temperature functions are evaluated: Boltzmann and Exponential. The difference between

these two temperature functions is the rate at which the temperature decreases. Cases E1 to E3 employed the Boltzmann temperature function with changes in the initial temperature and re-anneal interval. It was found that solution did not converge because of the Boltzmann temperature function as it implies large changes in temperature in the start of the algorithm and decreases the changes in temperature as the algorithm proceeds. Case E4 to E9 employed the exponential function to decrease the temperature. It can be found from cases E4 and E5 that the algorithm did not converge because of a too low initial value of initial temperature (as it tries to explore a limited area). As the value of initial temperature is increased (cases E6 to E9), the algorithm starts converging to the minimum. This is because of the fact that a larger area is now being explored by the algorithm in the search of a minimum. It has also been found from cases E6 to E9 that too high values of initial temperature and re-anneal interval do not pose any advantage. A value of 200 seems satisfactory in obtaining the convergence in the minimum function evaluations of 1130. To compare with the other two GOAs, the last column of Table 4.6 contains function evaluations divided by population size in GA / PSO. It shows that SiA took more time to converge when compared to PSO and GA.

**Table 4.6 Parameter selection results for SiA**

| CASE # | Initial temperature and re-aneal interval | Annealing Function | Temperature function | Function evaluations | Function evaluations / 20 |
|---|---|---|---|---|---|
| E1 | 25 | Boltzmann | Boltzmann | No convergence | - |
| E2 | 100 | Boltzmann | Boltzmann | No convergence | - |
| E3 | 200 | Boltzmann | Boltzmann | No convergence | - |
| E4 | 25 | Boltzmann | Exponential | No convergence | - |
| E5 | 75 | Boltzmann | Exponential | No convergence | - |
| E6 | 100 | Boltzmann | Exponential | No convergence | - |
| **E7** | **200** | **Boltzmann** | **Exponential** | **1250** | **62.5** |
| E8 | 500 | Boltzmann | Exponential | 2140 | 107 |
| E9 | 1000 | Boltzmann | Exponential | 2310 | 115.5 |

### *4.7.2 Model updating of analytical structure using global optimization algorithms*

Model updating was performed using PSO, GA and SiA independently for ten runs and best updating solutions obtained from each of the three GOAs are reported in Table 4.7 along with their standard deviations for the ten runs. Updated frequencies obtained by each method are shown in Table 4.8 along with experimental and initial analytical model frequencies and the frequency differences. MAC values between experimental and updated model are shown in Table 4.9.

**Table 4.7 Updated best solutions obtained using PSO, GA and SiA, and standard deviation of 10 independent runs**

| Parameters/ Algorithm | Updated parameters | | | | | | Value of objective function |
|---|---|---|---|---|---|---|---|
| | $k_{yy}$ (N/m) | $k_{xx}$ (N/m) | $k_{xy}$ (N/m) | $k_{\rho\rho}$ N m | $e_x$ (m) | $e_y$ (m) | |
| Initial | 8904 | 20294 | 0 | 3067.8 | 0 | 0 | 0.0131 |
| PSO/ | 8872.5 | 17332.6 | 290.6 | 2637.6 | -0.010 | 0.004 | $1.27\text{x}10^{-6}$ |
| Standard | 8.2 | 6.2 | 60.7 | 0.4 | 0.0010 | 0.00005 | |
| GA/ | 8873.6 | 17332.6 | 304.9 | 2637.7 | -0.010 | 0.004 | $1.29\text{x}10^{-6}$ |
| Standard | 5.2 | 5.3 | 90.5 | 0.0 | 0.0001 | 0.00001 | |
| SiA/ | 8876.5 | 17328.8 | 315.6 | 2637.8 | -0.010 | 0.004 | $1.37\text{x}10^{-6}$ |
| Standard | 11.0 | 18.0 | 111.4 | 2.6 | 0.0021 | 0.0002 | |

From the results, it has been found that all algorithms have given improved results as compared to the initial model and have decreased the difference between experimental and analytical values. From Table 4.7, it can be noted that the objective function values obtained for PSO, GA and SiA were $1.27\text{x}10^{-6}$, $1.29\text{x}10^{-6}$ and $1.37\text{x}10^{-6}$, respectively, which shows that all the algorithms gave acceptable results. When comparing PSO with GA, it can be observed that PSO is slightly better than GA in terms of the objective function value. Stiffness values obtained using PSO and GA were close, whereas SiA has shown a difference. From Table 4.7, it can also be noted that the maximum standard deviations of the

updated parameters from PSO, GA and SiA are 60.7, 90.5 and 111.4, respectively. This shows that PSO has the least spread in the obtained results for the ten independent runs.

**Table 4.8 Updated frequencies obtained by PSO, GA and SiA, and frequency differences between updated model and experimental results**

| Mode. No. | Frequencies (Hz) | | | | | Frequency Difference (%) | | |
|---|---|---|---|---|---|---|---|---|
| | Initial model | Experiment | PSO | GA | SiA | PSO | GA | SiA |
| 1 | 3.58 | 3.58 | 3.58 | 3.58 | 3.58 | -0.004 | 0.00 | -0.013 |
| 2 | 5.42 | 5.01 | 5.01 | 5.01 | 5.01 | 0.00 | 0.002 | -0.007 |
| 3 | 7.85 | 7.28 | 7.28 | 7.28 | 7.27 | -0.003 | 0.005 | 0.003 |

**Table 4.9 MAC values between updated model and experimental results for PSO, GA and SiA**

| Mode No. | MAC | | | |
|---|---|---|---|---|
| | Initial Model | PSO | GA | SiA |
| 1 | 0.989 | 1.000 | 0.998 | 0.998 |
| 2 | 0.974 | 0.997 | 0.999 | 0.999 |
| 3 | 0.999 | 0.999 | 0.999 | 0.999 |

Table 4.8 and Table 4.9 show the updated frequencies and MAC values as compared to the initial model. From the updated results, a very good agreement was found between the experimental results and updated analytical model using PSO, with frequency errors not more than 0.004% for all frequencies and MAC values higher than 0.997. Maximum errors in updated frequencies and MAC values were, respectively, 0.005% and 0.998 from GA, and 0.013% and 0.998 from SiA. In comparison to PSO, GA and SiA, SiA produced slightly higher errors in updated frequencies and mode shapes in updated frequencies and mode shapes.

For comparison purposes, the analytical model of the laboratory structure was also updated using a standard SM as explained in Chapter 2. The algorithm gave very similar results to

that of PSO as reported in Table 4.3 with a similar objective function value. This shows that PSO and the standard SM methods both were able to update the laboratory structure satisfactorily. Different starting points for standard SM were also tried in an attempt to see if this method can lead to wrong solution. It has been found that with different starting points, similar results (as obtained earlier) were obtained. This proves that SM is good in finding the minimum solution accurately. The total number of iterations taken by SM was 17 and total function evaluations taken up by the SM was 68.

The average time taken by PSO, GA and SiA to run 50000 function evaluations was 75.3, 76.25 and 111.4 sec, respectively. This shows that PSO and GA took nearly the same time. The convergence speed is shown in Figure 4.10 and indicates that PSO converges faster than GA and SiA. This can be attributed to the fact that PSO updates the parameter values in each generation based on the velocity vector (Equation 3.1) which is basically a secant between the two points if only the *gbest*/*pbest* portion of the equation is considered. This makes PSO closer to the traditional SM, which uses the first order Taylor series expansion for dynamic model updating (Brownjohn et al. 2001). Although the actual situation is a bit more complex than simply the secant in PSO as the equation accounts for the *gbest* position and *pbest* position consecutively. The other two methods, GA and SiA, both work on a point-wise basis and therefore have lower convergence speeds than PSO. However, as compared to SM which has taken 68 function evaluations, PSO has taken a minimum of 335 function evaluations to reach at a function value of $6.3 \times 10^{-6}$. This is because of the reason that PSO is still not a deterministic method and uses non-deterministic rules with a large population size to search the minimum, whereas SM uses deterministic rules to decide on the search direction.

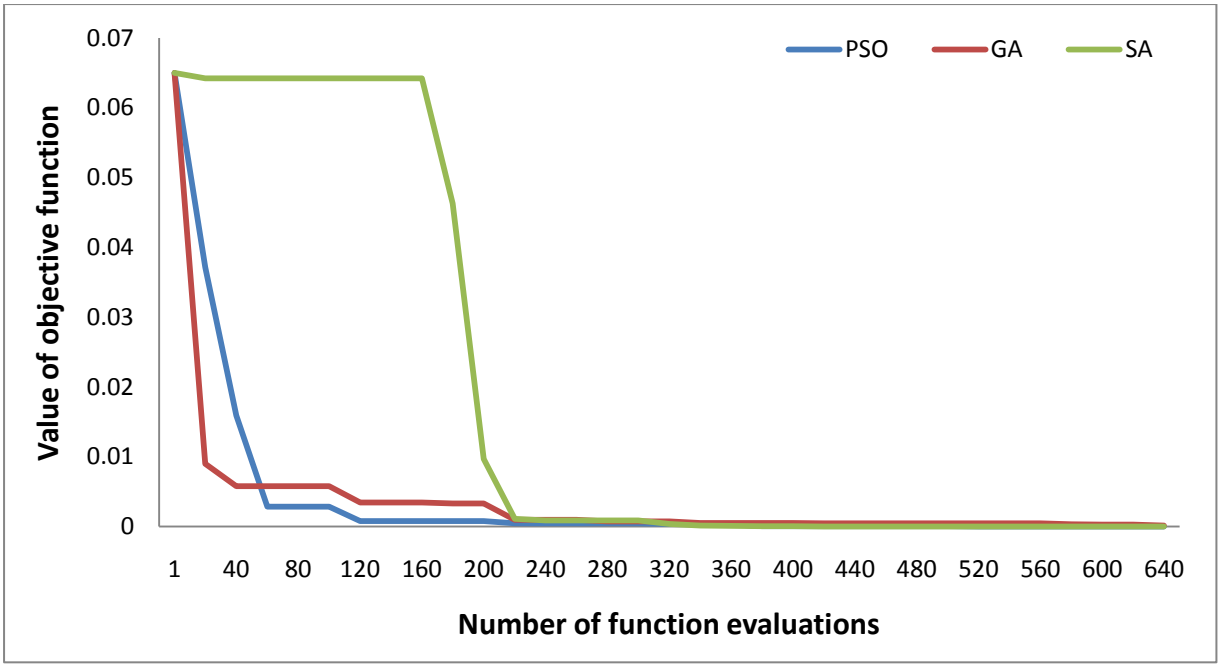


**Figure 4.10 Convergence of PSO, GA and SiA**

The parameters updated by PSO are discussed now. From PSO updated results in Table 4.7, updated stiffness in y direction $k_{yy}$ was found to be 8872 N/m, which is quite close to the initial estimated value of 8904 N/m. However, it has been found that the updated stiffness in x direction $k_{xx}$ was 17332 N/m which was less than the initial estimated stiffness value of 20294 N/m. This might be attributed to the loosening of bolts although every effort was made to tighten the bolts, and to air spaces left between the bracket and the slab. The bolts connect the bracket with the slab at the exact center line in the y direction and the air spaces try to fill up as the structure vibrates. It has also been noted that the values related to stiffness of the column i.e. $k_{xx}$, $k_{yy}$ and $k_{\rho\rho}$ decrease which shows that the initial model has overestimated the stiffness. This is also evident from experimental natural frequencies that initial model have overestimated the stiffness values. Small values for stiffness eccentricities $e_x$ and $e_y$ are also observed which may be attributed to minor structural misalignments. A detailed SA model of the laboratory structure further explains the joint phenomenon of the structure in the section 4.8.

To validate the updated model, two more experiments were performed by changing masses on the slab of the structure. Two masses of 0.654 kg (Mass 1) and 1.379 kg (Mass 2) were placed at the centre of the slab. This known change of mass in the actual experiment was also simulated in the updated analytical model obtained using PSO. Modal analysis was carried out for the analytical model again. Table 4.10 shows the experimental and analytical frequencies, frequency differences and MAC values for the additional mass cases. From the results obtained with the known addition of mass to both the experimental and analytical model, it has been noted that the frequencies and MACs obtained from the experiment and the analytical model still match reasonably. The maximum frequency difference in the first case (Mass 1) was 0.65%, whereas in the second case (Mass 2) it was 2.04%. Also, the lowest MAC value in the first case was 0.986 and in the second case 0.985, indicating a good correlation between the experimental and analytical mode shapes.

**Table 4.10 Experimental and analytical frequencies, frequency differences and MAC values for additional masses**

| Mode No. | Addition of 0.654 kg mass (Mass 1) | | | | Addition of 1.379 kg mass (Mass 2) | | | |
|---|---|---|---|---|---|---|---|---|
| | Experimental Frequency | Analytical Frequency | Frequency Difference (%) | MAC | Experimental Frequency | Analytical Frequency | Frequency Difference (%) | MAC |
| 1 | 3.54 | 3.52 | -0.64 | 0.998 | 3.48 | 3.45 | -0.88 | 0.995 |
| 2 | 4.90 | 4.92 | 0.33 | 0.986 | 4.79 | 4.82 | 0.62 | 0.985 |
| 3 | 7.21 | 7.25 | -0.65 | 0.998 | 7.10 | 7.24 | 2.04 | 0.999 |

## 4.8 Structural modelling of laboratory structure in SAP 2000

In this section, detailed SA modelling of the laboratory structure was carried out in SAP 2000. The SA model was developed using actual measurements of the structure as described in Section 4.4. The aluminium columns were modelled as beam elements having the size of 30 mm x 30 mm x 3mm. second MOI in the x and y direction were set equal to $1.458 \times 10^{-8}$ $m^4$ and the cross-sectional area is $1.71 \times 10^{-4}$ $m^2$. Each column was discretized into six elements. SAP2000 places all the columns in the same configuration. Therefore, orientation of each column was adjusted as per actual structure by rotating it around its local axis. The

steel slab was modelled as a shell structure. The modulus of elasticity of the steel was taken as 200 x $10^9$ N/$m^2$. The steel slab was discretized into 16 elements. Any further discretization was not found to have significant effects on the modal properties of the structure. This was done to reduce the computational cost of the model for further work on its optimization when exported to MATLAB. Actual masses of the accelerometers measured during the experiment were placed at their respective positions on the discretized slab.

Joint modelling is considered as one of the most important tasks in the SA modelling. In this research, joints were modelled as springs. The stiffness of the spring was calculated for a small rectangular beam element having dimensions of 30 mm x 4.5 mm and a length of 20 mm ---the actual dimensions of the connecting aluminium bracket. Second MOI about transverse local axes, $u_2$ and $u_3$, for this small beam element were calculated as 2.278 x $10^{-10}$ $m^4$ and 1.013 x $10^{-8}$ $m^4$, respectively. It is important to mention here that the local longitudinal axis of the connecting beam element is represented by $u_1$. The modulus of elasticity of aluminium was taken as 70 x $10^9$ N/$m^2$ and the shear modulus as 26 x $10^9$ N/$m^2$. The area of the rectangular beam element was calculated as 1.35 x $10^{-4}$ $m^2$. The equivalent stiffnesses of the spring in all six DOFs were calculated (CSI-Analysis-Reference-Manual 2013) and are shown in Table 4-11. The final SA model with spring elements is shown in Figure 4-11.

**Table 4.11 Equivalent stiffness of springs in place of bracket**

| $\mathbf{k_{u1}}$ N/m | $\mathbf{k_{u2}}$ N/m | $\mathbf{k_{u3}}$ N/m | $\mathbf{k_{r1}}$ N-m | $\mathbf{k_{r2}}$ N-m | $\mathbf{k_{r3}}$ N-m |
|---|---|---|---|---|---|
| 4.7x$10^8$ | 1.1 x$10^9$ | 2.4 x$10^7$ | 1128.1 | 797.3 | 35455.0 |

The properties of the aluminium angles and the steel slab can be estimated quite reasonably. Therefore, uncertain parameters in this case could be all six stiffness of the joints. A sensitivity analysis revealed that the four stiffnesses i.e. $k_{u1}$, $k_{u2}$, $k_{u3}$ and $k_{r1}$ are not sensitive to the first three modal frequencies and only $k_{r2}$ and $k_{r3}$ are sensitive. Although it should be

made clear here that any change in $k_{r2}$ and $k_{r3}$ also results in a change in $k_{u2}$ and $k_{u3}$ but that does not influence the first three frequencies.

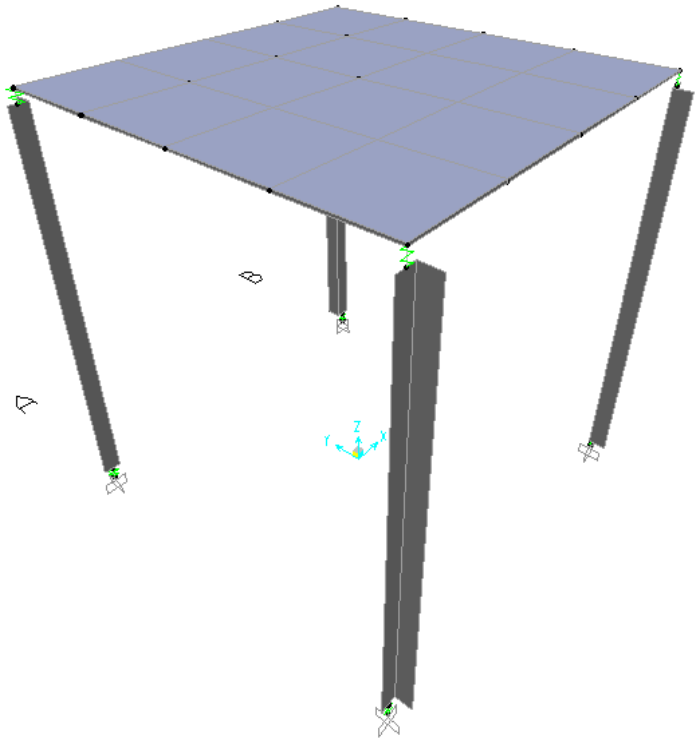

**Figure 4.11 SA model of laboratory structure in SAP 2000**

This is due to the fact that the aluminium angle and bracket springs are placed in series and their stiffnesses are added in an inverse relationship. Higher spring stiffness $k_{u2}$ and $k_{u3}$ of the bracket will not greatly affect the combined overall stiffness of the assembly. The modal frequencies of the initial SA model are reported in Table 4.13. It has been found from the modal results of the initial SA model that the frequency of Mode # 1 resembles well the experimental results. However, the frequencies of Mode # 2 and Mode # 3 are much higher than the experimental results. This is mainly attributed to factor $k_{r3}$ as the pure bending stiffness of the spring element is expected to be much less.

Only two parameters i.e. $k_{r2}$ and $k_{r3}$ were updated to match the modal data obtained from the experiment with the SA model predictions. The stiffness and mass matrices of the SA model of the laboratory structure were exported to MATLAB for subsequent model updating. PSO

was applied on the laboratory structure for updating two unknown parameters and the updated parameters after model updating are presented in Table 4.12. Updated frequencies and MACs obtained after model updating and corresponding frequency differences between updated model and experimental results are shown in Table 4.13.

**Table 4.12 Updated best parameters obtained using PSO**

| | Updated parameters | |
|---|---|---|
| **Algorithm** | **$k_{r2}$ (N m)** | **$k_{r3}$ (N m)** |
| PSO | 799 | 2205 |

**Table 4.13 Updated frequencies and MAC obtained by PSO, and frequency differences between updated model and experimental results**

| | Frequencies (Hz) | | | Frequency difference (%) | MAC | |
|---|---|---|---|---|---|---|
| **Mode. No.** | **Initial model** | **Experiment** | **PSO** | | **Initial model** | **PSO** |
| 1 | 3.58 | 3.58 | 3.58 | 0.11 | 0.996 | 0.998 |
| 2 | 7.97 | 5.01 | 5.03 | 0.30 | 0.988 | 0.980 |
| 3 | 10.29 | 7.28 | 7.23 | -0.65 | 0.985 | 0.986 |

It has been found that PSO has improved the correlation between the SA model predictions and the experimental results. The overall frequency difference has been reduced to 0.65%. The value of the updated parameter $k_{r2}$ shows that the initial model has a good estimate of its value. However, the value of the updated parameter $k_{r3}$ shows that the initial model has overestimated the value of the pure bending stiffness in the x direction. This is mainly attributed to the fact that the bracket is fastened with the bolts which are exactly at the centre line of the bracket in the y direction. Also, the wooden base provides a lesser resistance to bending in the x direction. As a result the joints exhibit less pure bending stiffness in this direction.

This updated model by PSO was also validated against the two experiments, involving mass additions on the slab, as reported in the previous section. Two masses of 0.654 kg (Mass 1)

and 1.379 kg (Mass 2) were placed at the centre of the slab. This known change of mass in the actual experiment was again simulated in the updated analytical model obtained using PSO. Modal analysis was carried out for analytical model again. Table 4.14 shows the experimental and analytical frequencies, frequency differences and MAC values for the additional mass cases. It can be seen that these values, both from the experiment and the SA model, match reasonably. The maximum frequency difference in the first case (Mass 1) was 0.61%, whereas in the second case (Mass 2) it was 1.04%. Also, the lowest MAC value in the first case was 0.982 and in the second case 0.971, indicating a good correlation between the experimental and analytical mode shapes.

**Table 4.14 Experimental and analytical frequencies, frequency differences and MAC values for additional masses for SAP 2000 model**

| Mode No. | Addition of 0.654 kg mass (Mass 1) | | | | Addition of 1.379 kg mass (Mass 2) | | | |
|---|---|---|---|---|---|---|---|---|
| | Experimental Frequency | SA model Frequency | Frequency Difference (%) | MAC | Experimental Frequency | SA model Frequency | Frequency Difference (%) | MAC |
| 1 | 3.54 | 3.52 | -0.56 | 0.997 | 3.48 | 3.45 | -0.86 | 0.994 |
| 2 | 4.90 | 4.93 | 0.61 | 0.991 | 4.79 | 4.84 | 1.04 | 0.977 |
| 3 | 7.21 | 7.20 | -0.14 | 0.982 | 7.10 | 7.16 | 0.85 | 0.971 |

## 4.9 Summary

In this chapter, a three-dimensional laboratory structure has been tested and updated, and later validated using an SA model. The findings are summarized below:

1- A laboratory structure was tested using a shake table and three natural frequencies in x, y and torsional direction were identified from system identification techniques.

2- Six parameters related to the stiffnesses and eccentricities were selected for model updating of the analytical model.

3- Three different GOAs, namely PSO, GA and SiA, were used for model updating and the results were compared in terms of accuracy and computational efficiency of the updated model. A total of ten independent runs were performed for each algorithm. It

was found that PSO has given the least error between experimental and analytical frequencies, followed by GA and then SiA. Similar results were obtained for the standard deviation in the parameter values in which PSO was found to have a lower deviation than the other two algorithms.

4- Stiffness values obtained using PSO and GA matched well. The SiA values have shown more divergence than the other two algorithms.

5- PSO was found to have faster convergence than GA and SiA. This is because of the use of particle velocity which makes PSO closer to the gradient based methods.

6- Two cases of mass addition were also studied to validate the updated analytical model. It was found that a reasonable updated model of the laboratory structure was obtained by PSO.

7- SA model of the structure was also analysed using SAP 2000 and its joint stiffnesses were updated. It was found that the pure bending stiffness of the joint in one of the direction is considerably less than the assumed starting value. The model was also validated with the two additional mass cases.

# Chapter 5. APPLICATION OF PARTICLE SWARM OPTIMIZATION WITH SEQUENTIAL NICHE TECHNIQUE FOR DYNAMIC MODEL UPDATING OF A FULL SCALE BRIDGE

## 5.1 Introduction

SA modeling is nowadays routinely used for the determination of responses of full-scale structures to a variety of actions, but the formation of a model which replicates the behavior of the original structure with high accuracy is not easy due to inherent simplifying assumptions in model building (Friswell and Mottershead 1995). Full-scale dynamic testing of structures often reveals important and considerable differences between the original structure and its SA model. These differences can be attributed to modeling errors associated with simplifications of complicated structural systems, inadequate discretization and parametric errors in the estimation of materials properties, geometry and boundary and connectivity conditions.

The number of model responses, such as natural frequencies and mode shapes, that can be determined experimentally of full scale structures with adequate confidence, is always

limited. This can be attributed to two main reasons, namely, difficulties in identifying higher modes because of poorer signal-to-noise ratios, and difficulties arising from coarse mode shape mapping due to the limited numbers of sensors used. A relatively small number of experimental responses compared to the number of uncertain parameters in the SA model may lead to wrong solutions in the solution space for the updating problem (Jaishi and Ren 2007). Adding to that, the assumptions made in the development of the SA model and uncertainties associated with material properties, boundary conditions and geometry may result in significant differences in the natural frequencies and mode shapes between the initial SA model and their experimental counterparts (Mottershead and Friswell 1993). The algorithm searching for the global minimum of the error function may then be lured into local minima in problems that Goldberg et al. (1992) call ‘deceptive’. This undesirable behavior is well known in the context of model updating. For example, the widely used SM, which is essentially an iterative steepest-gradient approach sometimes combined with regularization (Titurus and Friswell 2008), has a tendency to converge to a local minimum (Deb 1998). Accordingly, many previous model updating studies report a single solution (Brownjohn et al. 2001; Jaishi and Ren 2005; Zivanovic et al. 2007) but acknowledge that there might be other solutions as well. A popular countermeasure is to run the updating algorithm several times with perturbed initial parameter values, however, such an approach is not a systematic search over the solution domain. Only limited studies have reported multiple model updating solutions and consequently the problem and its remedies have not been sufficiently explored (Zárate and Caicedo 2008).

GOAs are numerical techniques that explore the search space systematically and widely in an attempt to increase the chance of discovering the global minimum (Pintér 1996; Storn and Price 1997; Price et al. 2005). While there has been some documented history of their

applications to model updating (Levin and Lieven 1998; Perera and Ruiz 2008; Tu and Lu 2008), such studies still remain relatively limited.

One of the efficient GAOs, which is used in this study, is PSO (Konstantinos and Vrahatis 2010). PSO is based on a biologically inspired mathematical metaphor of how a swarm of bees, school of fish or similar animal grouping collectively move in search of the most fertile feeding location.

While, as explained earlier, GAOs in their basic form attempt to locate the global solution to an optimization problem, they cannot fully guarantee a search will always be successful. These shortcomings of GOAs in general and their previous applications to model updating motivated the approach proposed and explored in this study which is based on a systematic search over the solution domain. The SNT (Beasley et al. 1993) is combined with PSO to that end. SNT is simple and does not require modifications in the search algorithm itself. It only modifies the objective function after any local (or global) solution has been reached is such a way that subsequent searches avoid the vicinity of the previously found solutions and are forced to search for new, yet undiscovered, ones.

The outline of the chapter is as follows. In the first section, the theory of SNT is explained. Then forced vibration testing of a full-scale, cable-stayed pedestrian bridge and modal system identification are described. Next a detailed study of updating of a SA model of the bridge is presented. Firstly, the development of an initial SA model is explained and sensitivity and uncertainty study carried out to determine the most suitable parameters for updating. Then, sensitivity based model updating is applied with different initial values. SNT with PSO is applied to SA model updating. The main contributions of this study comprise a novel approach to model updating that combines PSO and SNT, and a systematic, detailed exploration of the new method's performance using data from a full-scale structure.

## 5.2 Theory

For the problems involving complex optimizations, GOAs try to find the global minimum among many possible local minima in the search space. In model updating, the topology of the search space can be complex due to the large number of updating parameters and their influence on the objective function via numerically evaluated responses. A methodology based on combining the stochastic search algorithm SNT with PSO is proposed and investigated in this chapter to improve the performance of GOA-based model updating in finding the global minimum. In the subsequent section, the theory of SNT is explained.

### *5.2.1 Sequential niche technique*

The principle of SNT is to carry over knowledge gained during subsequent iterations of an optimization algorithm (Beasley et al. 1993) so that different minima are discovered in turn. The basic approach is that when a minimum is found in the search domain, the surrounding area, referred to as niche, is ‘filled in’ and no longer attracts the particles in subsequent iterations. This forces the optimization algorithm to converge to another, yet unvisited, niche. The process continues until the criteria such as the maximum number of iterations, maximum number of discovered minima and the upper threshold value of the objective function at a minimum have been met.

Initial iterations in search of the first minimum are made with the basic search algorithm, PSO in this case, without SNT by using the raw objective function. Once the first minimum has been found, the objective function values of the particles in the vicinity of the minimum are modified, and the search for the next minimum commences. The modifications to the objective function are introduced by multiplying it by a derating function using the following recursive formula

$$\prod_{n+1}(\mathrm{x}) = \prod_{n}(\mathrm{x}) \times G(\mathrm{x}, \mathrm{s}_n) \tag{5.1}$$

where $\prod_{n+1}(\mathrm{x})$ is the modified objective function to be used for searching for the *n*+1-th minimum, $\prod_{n}(\mathrm{x})$ is the previous objective function used for searching for the *n*-th minimum, $G(\mathrm{x}, \mathrm{s}_n)$ is the derating function, and $\mathrm{s}_n$ is the *n*-th found minimum.

The following exponential derating function is used in this study (Beasley et al. 1993)

$$G(\mathrm{x}, \mathrm{s}_n) = \begin{cases} \exp\left(log\ m \times \dfrac{r - d(\mathrm{x}, \mathrm{s}_n)}{r}\right) & if\ d(\mathrm{x}, \mathrm{s}_n) < r \\ 1 & otherwise \end{cases} \tag{5.2}$$

where *m* is the derating value used to control concavity of the derating function, *r* is the niche radius, and $d(\mathrm{x}, \mathrm{s}_n)$ defines the distance between the current point x and best individual $\mathrm{s}_n$.

The niche radius *r* is an important parameter as it is used to define the size of the part of the search domain in the neighborhood of a minimum where the objective function is modified. Smaller values of niche radii produce more concavity, while larger niche radii can affect the other minima in the search space. Furthermore, too small a radius will enable detection of very close solutions and too large a radius can lead to wrong results as it has a harmful effect on the surrounding search space. The niche radius has been determined in this study by the method proposed by Deb (1989) who suggested using a value calculated as

$$r = \frac{\sqrt{k}}{2 \times \sqrt[k]{p}} \tag{5.3}$$

where *k* represents the dimension of the problem (the number of parameters) and *p* is the expected number of minima. Each parameter has to be normalized between 0 and 1 for the use of SNT. This approach assumes that all minima are fairly equally distributed throughout the search domain.

## 5.3 Bridge description

The full-scale structure under study is a 59,500 mm long cable-stayed footbridge with two symmetrical spans supported on abutments, a central A-shaped pylon and six pairs of stays as shown in Figure 5.1. Figure 5.2 shows the deck cross-section, which comprises a trapezoidal steel girder with overhangs of a total width of 2,500 mm and depth of 470 mm, made of 16 mm thick plates, and a non-composite concrete slab of thickness 130 mm. Closed steel rectangular pipes having a cross-section of 250 x 150 x 9 mm also run on both sides of the bridge deck and enclose two 100 mm ducts for service pipes with the surrounding void spaces filled with grout. Railing was provided on both sides of the bridge and it has a total height of 1,400 mm. The sections of railings were disconnected from each other at every 8,000 mm.

**Figure 5.1. Full-scale cable-stayed footbridge.**

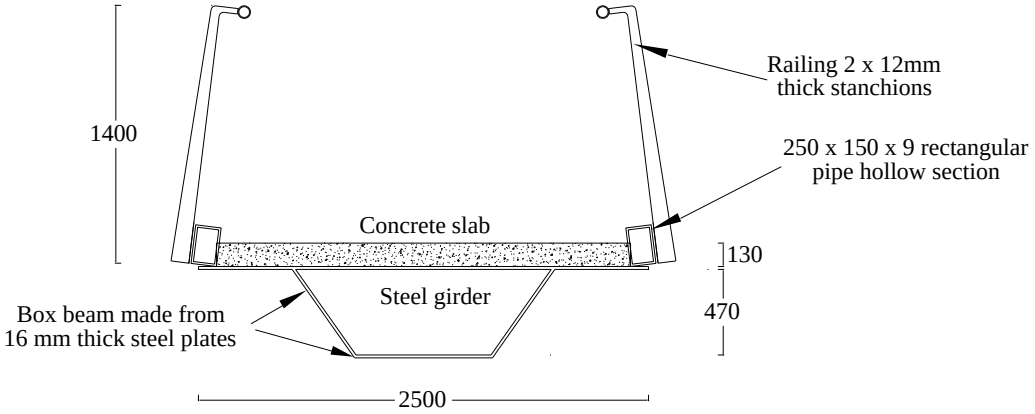


**Figure 5.2. Cross-section of bridge deck (all dimensions in mm).**

The deck is continuous over the entire span. It is supported on two pivot type steel bearings at the central pylon and two sliding steel-concrete bearings at each abutment. The sliding bearings were provided to accommodate creep, shrinkage and temperature deformations, and to allow the bridge to move longitudinally in the event of a strong seismic excitation. The distance between bearing axes is only 450 mm and they do not provide a strong torsional restraint. The abutments are supported by two concrete piles, and 10 concrete piles and a pile cap are used at the central pylon.

The six pairs of stay cables are fixed to the deck at distances of about 8,000 mm center to center as shown in Figure 5.3. All the cables have a diameter of 32 mm. Different post-tension forces, ranging from 55 kN to 95 kN in each cable, were specified in design. The cables were connected to the top of the 22,400 mm high center pylon, which is composed of two steel I-sections joined with cross bracing that supports the deck. The size of the pylon I-sections is 400WC328 (AS/NZS 1996). The bridge has been considered as an appropriate candidate for mode updating as it has a number of potential uncertain parameters.

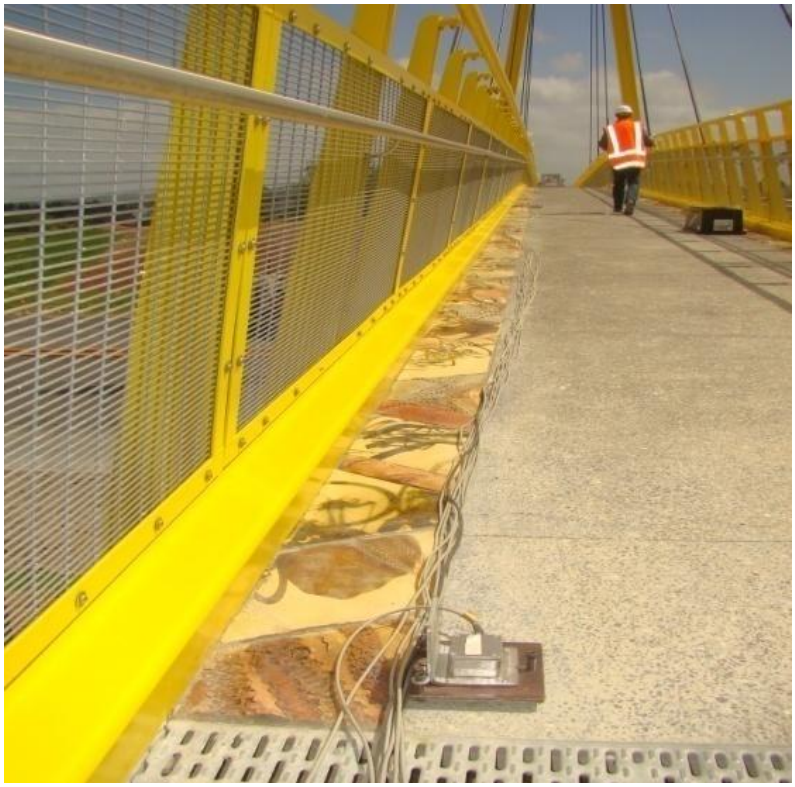

**Figure 5.3 Accelerometers (in the center) and shakers (at the back) placed on the bridge.**

## 5.4 Experimental program and system identification

Experimental work has been carried out using uni-axial Honeywell QA 750 accelerometers to measure structural response, uni-axial Crossbow CXL series MEMS accelerometers to measure shaker input force and a desktop computer fitted with an NI DAQ 9203 data acquisition card. Data was collected at a sampling rate of 200 Hz. Three APS ElectroSeis Model 400 shakers (APSDynamics 2012), capable of providing a combined dynamic force of up to 1.2 kN, were used in a synchronized mode to impart excitation to the structure.

Full scale tests can be conducted by output only (no measured force) or input-output (measured force) methods. The cable stayed bridge under study has been tested using both of these methods. The output only test was conducted using jumping to establish the initial

estimation of the natural frequencies of the bridge. Two people jumped on the bridge in unison to excite the structure and thereafter the bridge was allowed to freely vibrate for two minutes. This was done to establish the range of excitation frequencies for subsequent forced vibration tests. References such as (Brownjohn et al. 2003; Pavic et al. 2007) demonstrates that frequency sweep tests are a standard and successful approach to such full scale testing. Different sweep rates have been used by various researchers to excite full scale structures. Pioneer bridge (Brownjohn et al. 2003) was excited using a frequency sweep ranging from 5 to 32 Hz in a frame of 20.48 s, whereas a full scale open plan floor (Pavic et al. 2007) was excited using a frequency sweep ranging from 3-19 Hz in a frame of approximately 15 s. Following that, a sweep sine excitation ranging from 1 to 15 Hz with a total duration of 391 seconds was adopted to excite the structure. The shakers were located away from the center line of the deck to excite both the vertical and torsional modes. To excite the horizontal modes, the shakers were tilted at 90 degrees. Figure 5.4 shows the locations of the shakers and accelerometers on the bridge during testing. Accelerometers were placed on both sides of the deck to capture vertical and torsional responses. One of the accelerometers was also placed on the bridge abutment to measure its response. Figure 5.5 shows the time history of force delivered by a shaker, and Figure 5.6 shows the time history of bridge response recorded by one of the accelerometers during the vertical testing. It can be seen in Figure 5.6 how subsequent modes are excited as the shakers sweep through their corresponding resonant frequencies. The vertical and horizontal tests were repeated twice to ensure good quality data.

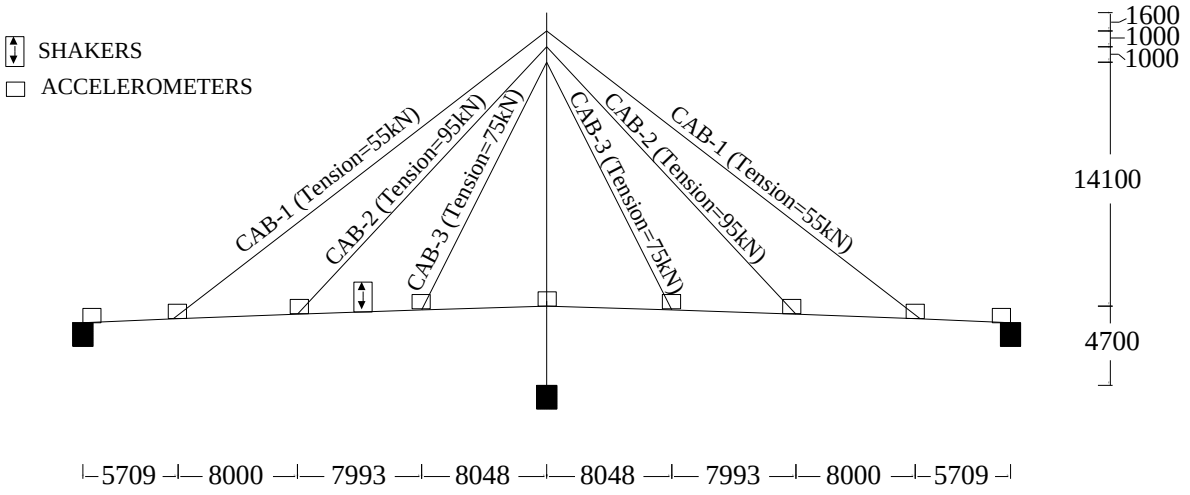


**Figure 5.4. Basic bridge dimensions, cable post-tension forces and location of shakers and accelerometers in the experiment (all dimensions in mm).**

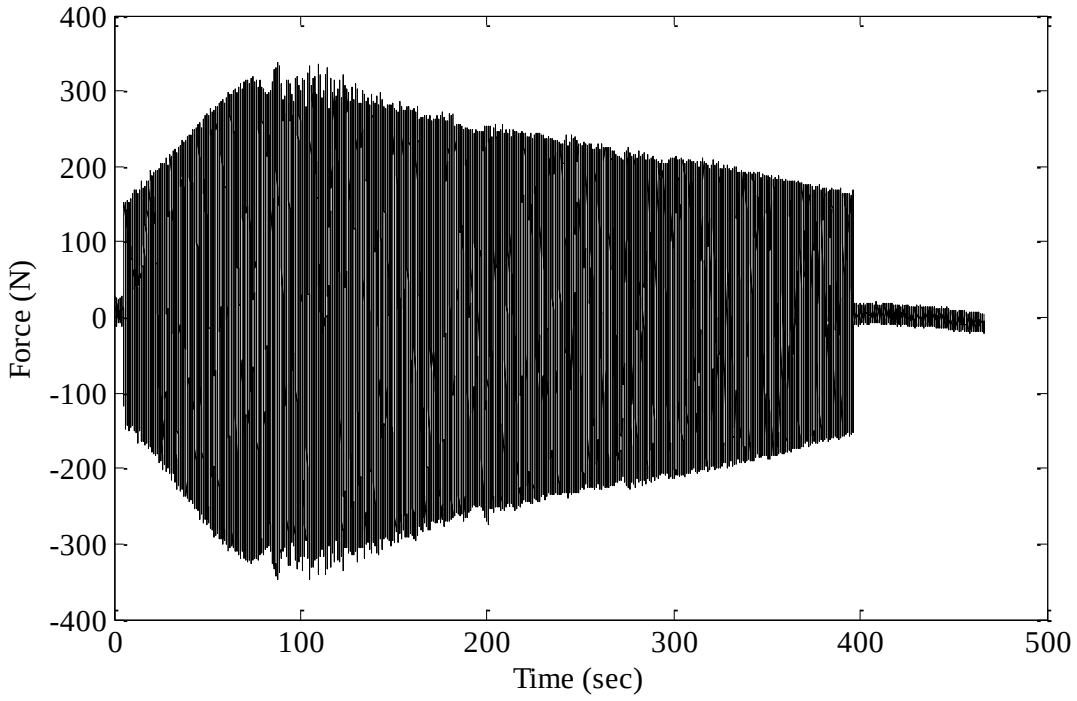


**Figure 5.5 Time history of force applied by a shaker.**

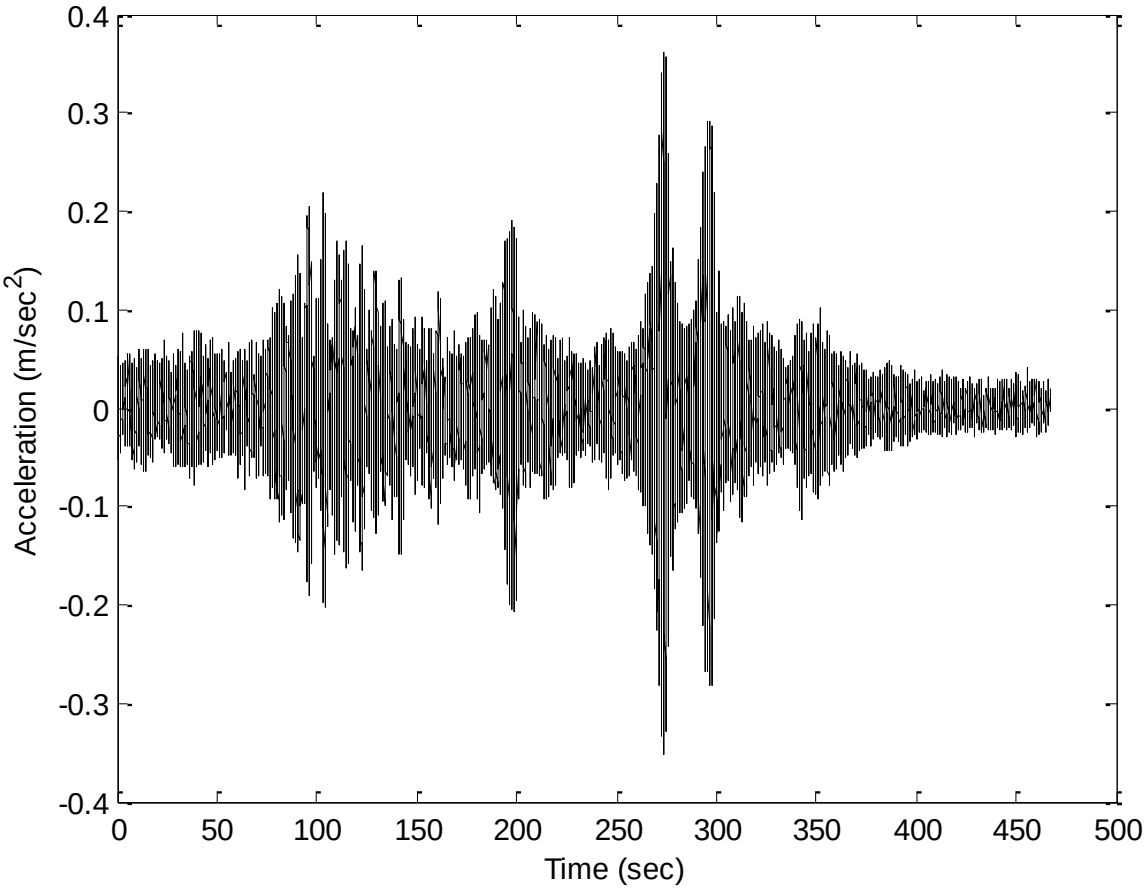


**Figure 5.6 Time history of bridge response recorded during vertical shaker excitation.**

For system identification in the frequency domain, peak picking using FRF is a commonly used, simple method (Ewins 2000). FRF is a measure of system response to the input signal at each frequency and can be calculated from the auto-spectrum of excitation and cross-spectrum between response and excitation (Friswell and Mottershead 1995). For calculating the spectra, the Welch averaging method was used (Proakis and Manolakis 1996) with each time history is divided into five segments with 50% overlap and Hamming windowing. Finally, FRFs from three available experiments were averaged. To assess the quality of an FRF and distinguish between real and spurious peaks, coherence can be used (Ewins 2000). Coherence can be calculated using the two aforementioned spectra and the auto-spectrum of response. High coherence values, close to one, indicate that response at a given frequency is caused by the measured input rather than other sources of excitation or is a false result

introduced by noise. An example of an FRF obtained during a vertical shaker test is shown in Figure 5.7 a, where FRF magnitude, phase and coherence are shown. It can be noted that the magnitude has peaks at 1.64 Hz, 1.90 Hz, 3.66 Hz, 6.32 Hz, 7.42 Hz and 8.33 Hz. All but the last peak at 8.33 Hz, which is a torsional mode, correspond to vertical modes. Higher peaks are observed at modes corresponding to 6.32 Hz and 7.42 Hz, which shows that these modes are responding more strongly than the others. Also, the torsional mode peak at 8.33 Hz is less clearly visible possibly due to low levels of excitation torque delivered by the shakers. The phase of the FRF shows a change of 180° close to 1.64 Hz, 1.90 Hz, 3.66 Hz, 6.32 Hz, 7.42 Hz and 8.33 Hz further confirming that these are modal frequencies. The phase change is again much clearer at 6.32 Hz and 7.42 Hz as they are better excited than the other modes. The coherence between excitation and response have values of more than 0.8 at 1.64 Hz, 1.90Hz, 3.66 Hz, 6.32 Hz, 7.42 Hz and 8.33 Hz, indicating that a reasonably good correlation exists between the force and response signals. Much better coherence values, very close to one, were observed at 6.32 Hz and 7.42 Hz. Some other peaks, e.g. just above 10 Hz, can be also be seen but the corresponding coherence values are low. Also, the auto power spectral density from the jump test was shown in Figure 5.7 b. Two peaks at 6.31 Hz and 7.39 Hz can be clearly seen along with smaller peak at 1.66 Hz. These frequencies match well with the already identified frequencies from FRF. The well-known challenges of in-situ testing of full-scale large systems, like bridges, must be kept in mind while assessing the FRF. These include, but are not limited to, poorer signal-to-noise ratios because of the limited capacity of the exciters, very limited control of several ambient sources of excitation and noise (wind, construction works, vehicles, occupants, machinery, etc. – some of which are always present), and limited data as, unlike in the laboratory, tests cannot typically be repeated tens or hundreds of times for averaging. Given those challenges, it can be concluded that data of

sufficient quality has successfully been acquired. Similarly, two resonance frequencies were identified using horizontal shaker excitation at 4.85 Hz and 5.36 Hz, respectively.

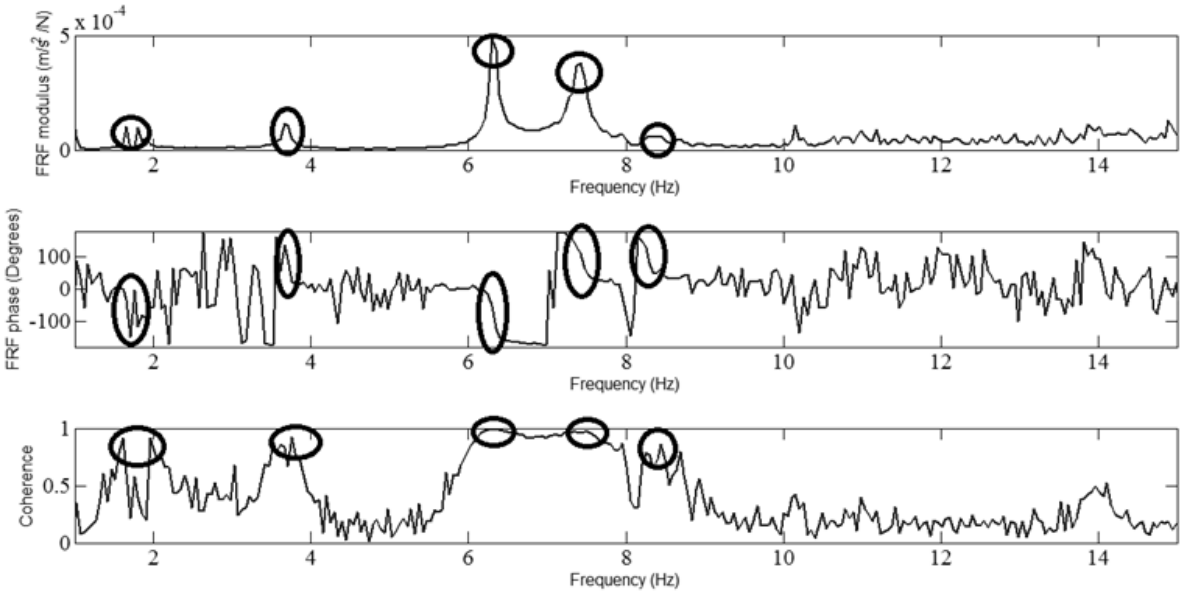


(a)

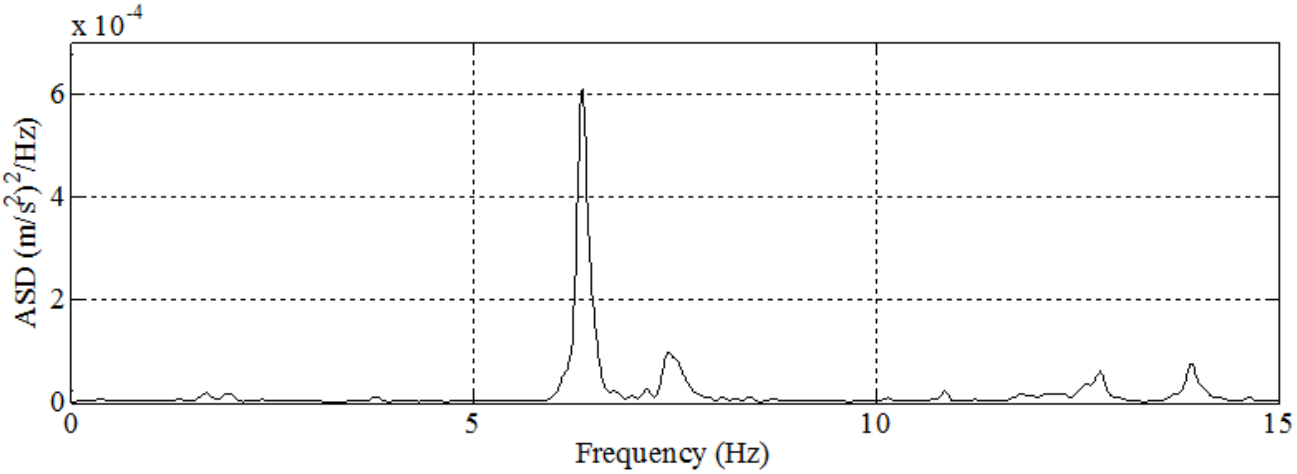


(b)

**Figure 5.7 a) FRF measured during vertical shaker test b) ASD of a response signal during jump test**

For cross-checking the results of pick peaking and also to identify damping ratios and mode shapes the N4SID technique (Van Overschee and De Moor 1994), operating in the time domain and utilizing a subspace identification algorithm, was used. The general subspace algorithm (Overschee and Moor 1996) can be applied to both input-only and input-output identification. In these approaches, state space system matrices are first obtained from the measurements, and then natural frequencies, damping ratios, and mode shapes can then be derived from these system matrices.

The adequate order of the state space model needs to be carefully determined. Theoretically, the system order should be twice the number of the DOFs, i.e. modes, of interest. However, due to measurement noise a higher model order is normally required to extract the modes of interest with higher confidence and discard spurious, artificial results. To that end, stability diagrams are employed. As the system order increases, the structural modes identified by the algorithm should remain consistent and stable (Bodeux and Golinval 2001). The model order selected for this study ranged from 10 to 80 for the vertical shaker configuration. Stability thresholds were selected based on previous experience and data quality. A threshold of 1% for frequency variation and a value above 0.8 for MAC (Allemang and Brown 1982) between two subsequent model orders were used. MAC for two modes shapes $\emptyset_i$ and $\emptyset_j$ is defined as

$$\boldsymbol{MAC} = \frac{|\emptyset'_i \emptyset_j|^2}{(\emptyset'_i \emptyset_i)(\emptyset'_j \emptyset_j)} \qquad \textbf{(5.4)}$$

where the apostrophe denotes vector transposition. MAC takes a value of one for perfectly correlated modes and zero for two orthogonal modes.

The stability diagram for a vertical shaking test is shown in Figure 5.8. It can be seen from the stability diagram that the six previously observed modes, five vertical and one torsional, are stable and can be identified from the vertical tests as shown by the black dots in the Figure 5.8. Some spurious modes, that did not meet the stipulated stability criteria, were also

detected as shown by the white dots in the Figure 5.8. In a similar way, two modes previously seen in the FRFs were identified from the horizontal tests.

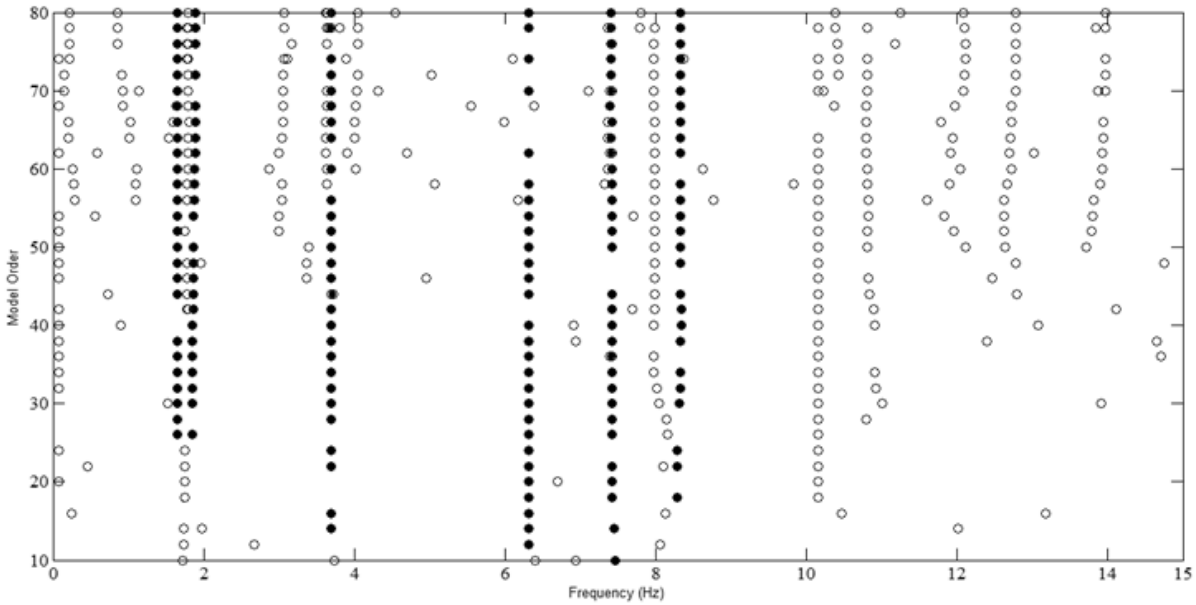


**Figure 5.8 Stability diagram for a vertical shaker test (black dots indicate stable modes).**

Table 5.1 summarizes the natural frequencies identified from the peak picking and N4SID methods. It can be seen from the results that the frequencies identified by both methods match very well. The damping ratios identified by the N4SID method are also shown in Table 5.1. It is observed that damping in the bridge is small, ranging between 0.22% and 1.43% that tends to clearly separate modes in the modal analysis. Generally, higher damping coefficients lead to lower response values and may be a source of concern in large structures such as buildings and bridges. Due to the size of these structures, ambient excitation is the usual choice and other excitation mechanism may not be a practical choice. As the level of excitation is usually very low, resulting low response values may hamper the quality of natural frequencies and mode shapes.

**Table 5.1 Experimentally identified natural frequencies and damping ratios.**

| Mode No. | Mode type | Experimental frequencies (Hz) | | Damping ratios (%) |
|---|---|---|---|---|
| | | Peak picking | N4SID | N4SID |
| 1 | 1st vertical | 1.64 | 1.64 | 0.22 |
| 2 | 2nd vertical | 1.90 | 1.90 | 0.87 |
| 3 | 3rd vertical | 3.66 | 3.69 | 0.52 |
| 4 | 1st horizontal | 4.85 | 4.86 | 0.81 |
| 5 | 2nd horizontal | 5.36 | 5.33 | 0.61 |
| 6 | 4th vertical | 6.32 | 6.31 | 0.49 |
| 7 | 5th vertical | 7.42 | 7.42 | 0.96 |
| 8 | 1st torsional | 8.33 | 8.32 | 1.43 |

Five vertical, two horizontal and one torsional mode shape identified from modal tests using the N4SID method are shown in Figure 5.9. It has been observed from the system identification results that the first two vertical modes have nearly identical sinusoidal shapes over the deck. An additional accelerometer was attached to one of the cables closest to the abutments during the vertical shaker tests and it has been found that the cable also vibrates laterally at the frequency of the second mode, i.e. at 1.89 Hz. SA simulations conducted later confirmed that the pattern of cable vibration sets the two modes apart. Figure 5.10 (b & c) shows the pattern of cable vibrations for the two modes.

The first two vertical frequencies are critical when designing for vibration serviceability under frequency tuning approach (Pimentel et al. 2001), wherein the fundamental frequency of the bridge should not coincide with the pedestrian walking frequency of 1.6-2.5 Hz or the second harmonic of walking frequency of 3.5-4.5Hz. The first three vertical frequencies identified at 1.64 Hz, 1.89 Hz and 3.69 lies within the range of pedestrian walking frequency. This indicates that the bridge might have some undesirable vibrations during its service life. However, the first horizontal mode is at 4.86 Hz which is well above the specified criteria i.e. 1.5Hz.

Only one torsional mode of the system was identified by the forced vibration tests at 8.32 Hz. Typically, one would expect a torsional mode of a shape similar to a full sinusoid where the deck twists in the opposite directions in each span (Ren and Peng 2005). However, in the observed torsional mode the whole deck twists in the same direction. The reason behind this is that the main girder is a closed trapezoidal cross-section (Figure 5.2) thus having a large torsional stiffness, which makes it difficult to twist the bridge deck in a full-sine pattern. Also, the closed rectangular pipes with service ducts and railing that run near the edges throughout the length of the bridge further increase the torsional stiffness of the deck. It is thus easier to deform the pylon resulting in the torsional mode shape as indicated in Figure 5.9.

## 5.5 Bridge initial model

There are many ways to model cable-stayed bridges to obtain a realistic representation of their dynamic behavior. The main elements to be modeled are the deck, pylon, cables, and connections of cables and deck. A good representation of bridge deck for box girder sections can be achieved by using beam elements with rigid links joining the cable elements with the deck elements (Chang et al. 2001; Ren and Peng 2005). In this research, the bridge was modeled in SAP2000 (2009) and the SA model is shown in Figure 5.10 (a). The deck and pylon were modeled using beam type FEs. The deck was discretized into 48 elements, whereas the pylon was discretized into 40 elements. These numbers of elements were selected as further discretization did not appreciably affect the results of numerical modal analysis and only resulted in an increased computational cost. The cables were modeled using catenary elements provided in SAP2000 and were discretized into four elements for each cable.

Mode 1 (1st vertical): Frequency 1.64 Hz

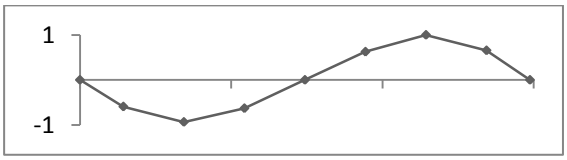


Mode 2 (2nd vertical): Frequency 1.89 Hz

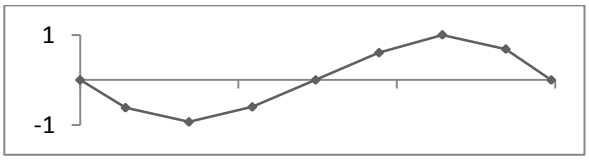


Mode 3 (3rd vertical): Frequency 3.69 Hz

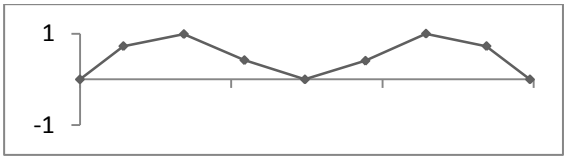


Mode 4 (1st horizontal): Frequency 4.86 Hz

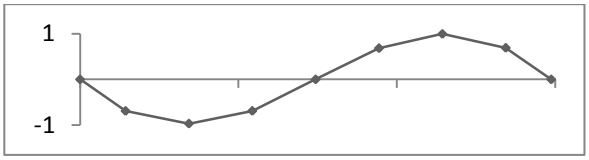


Mode 5 (1st horizontal): Frequency 5.33 Hz

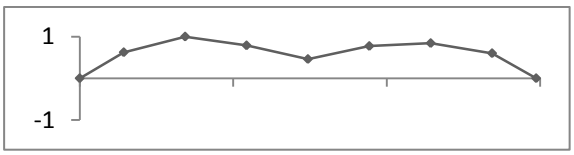


Mode 6 (4th vertical): Frequency 6.31 Hz

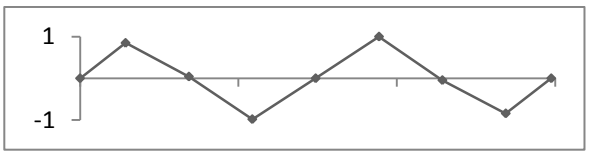


Mode 7 (5th vertical): Frequency 7.42 Hz

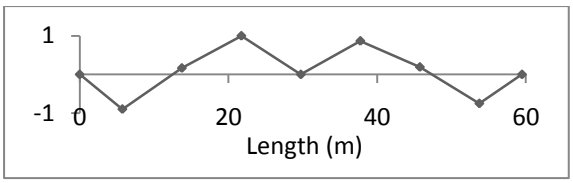


Mode 8 (1st torsional): Frequency 8.32 Hz

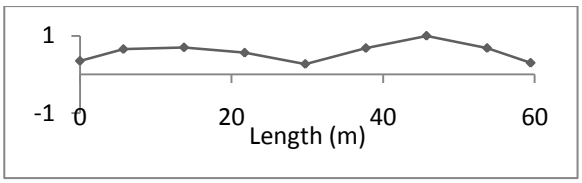


**Figure 5.9 Normalized vertical, horizontal and torsional modes identified using N4SID method.**

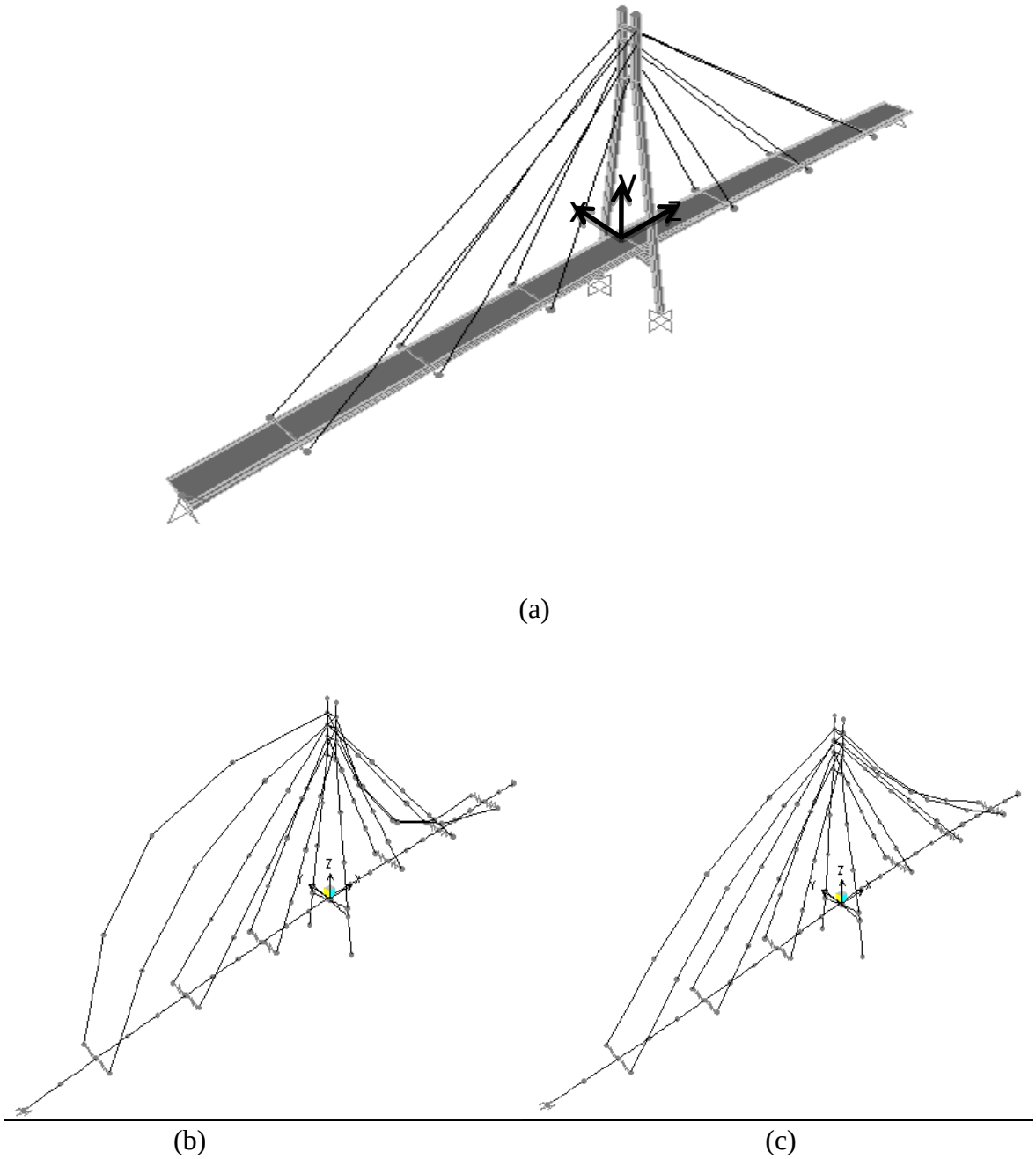


**Figure 5.10 (a) SA model of the bridge. (b) 3D picture of Mode 1 showing cable vibrations (c) 3D picture of Mode 2 showing cable vibrations**

As indicated earlier, the first two experimentally identified vertical modes (Figure 5.9) have very similar shapes of girder vibrations and an initial SA model with no discretization of the cables did not show the second of the two modes. After discretization of the cables into four elements all the experimentally observed modes were correctly replicated in the SA model.

The modulus of elasticity for steel was taken as 200 GPa, for cables as 165 GPa and for concrete as 28 GPa. The cast is situ concrete slab was assumed to be fully composite with the steel girder resulting in a combined cross-sectional second MOI of 0.06140 $m^4$ for horizontal bending, 0.00439 $m^4$ for vertical bending and torsional constant of 0.00810 $m^4$. (Note that this contradicts the assumption made in design that there is no composite action. However, it was anticipated that partial composite action did exist, as is often the case in real structures, and its actual extent will be quantified via model updating later.) An initial non-linear static analysis was performed to account for the geometric non-linearity caused by the cable sag and this was followed by a linear dynamic analysis to obtain natural frequencies and mode shapes. A linear analysis that uses stiffness from the end of non-linear static analysis for cable-stayed structures has been demonstrated to provide good results (Abdel-Ghaffar and Khalifa 1991).

The response of the bridge was also measured with sensors on the bridge abutment beneath the deck. The abutment did not show any appreciable response in the vertical or horizontal direction and so both abutments were ignored in the SA model. However, the stiffness of the bearings for shear and compression has been calculated in terms of geometry and modulus (Gent 2012). The two bearings at each abutment have dimensions of 150 mm x 150 mm x 12 mm and the two bearings at the pylon have dimensions of 90 mm x 180 mm x 12 mm. The shear stiffness $K_s$ and vertical stiffness $K_v$ of the bearings have been calculated using the formula (Gent 2012)

$$\boldsymbol{K_s = \frac{AG}{t}} \qquad \textbf{(5.5)}$$

$$K_v = \frac{AE_c}{t} \qquad \textbf{(5.6)}$$

where A is the effective load area, G is the shear modulus, $E_c$ is the compression modulus and t is the thickness of bearing. The effective compression modulus has been calculated using the formula

$$E_c = E_0(1 + 2\Phi S^2) \quad \textbf{(5.7)}$$

where $E_0$ is Young's modulus, $\Phi$ is compression coefficient of the elastomer and S is the shape factor for a rectangular block determined as

$$\boldsymbol{S = \frac{\text{Load Area}}{\text{Bulge area}} = \frac{(\text{Length})(\text{Width})}{2t(\text{Length}+\text{Width})}} \quad \textbf{(5.8)}$$

Furthermore, as explained before the distance between bearing axes is 450 mm and the torsional restraint provided by the bearings is calculated by the formula (Jaishi and Ren 2007)

$$\boldsymbol{K_{rot} = \frac{M}{\theta} = \frac{K_v L^2}{2}} \quad \textbf{(5.9)}$$

The shear, vertical and torsion stiffness values for the abutment bearings were found to be $2.58\text{x}10^6$ N/m, $1.60\text{x}10^8$ N/m and $8.86\text{x}10^8$ Nm/rad respectively. Likewise shear, vertical and torsion stiffness values for the pylon bearings were found to be $1.86\text{x}10^6$ N/m, $7.70\text{x}10^7$ N/m and $3.90\text{x}10^6$ Nm/rad respectively. The freedom of the abutment bearings to slide was ignored; this was not expected to have any strong effects on the model accuracy as neither was the bridge excited in the longitudinal direction during the dynamic tests, nor were the corresponding modes identified or considered in the analysis.

Table 5.2 summarizes the errors between experimental frequencies and mode shapes and those identified by the initial SA model. To compare experimental and numerical mode shapes, MAC (Equation (6)) was used. It has been found that the frequencies obtained from the initial SA model differ from the experimental frequencies by up to 8.64% and MAC values are between 0.98 and 0.999. The systematic attempts to improve the agreement

between the experimental and numerical predictions via sensitivity and PSO and SNT-based model updating are discussed in the next section.

**Table 5.2. Initial SA model and experimental frequencies and MACs.**

| Mode No. | Frequency | | | MAC |
|---|---|---|---|---|
| | Experiment by N4SID (Hz) | Initial SA model (Hz) | Error (%) | |
| 1 | 1.64 | 1.66 | 1.22 | 0.999 |
| 2 | 1.90 | 1.88 | -1.05 | 0.995 |
| 3 | 3.69 | 3.88 | 5.15 | 0.999 |
| 4 | 4.86 | 5.28 | 8.64 | 0.999 |
| 5 | 5.33 | 5.45 | 2.25 | 0.993 |
| 6 | 6.31 | 6.79 | 7.61 | 0.990 |
| 7 | 7.42 | 7.76 | 4.58 | 0.980 |
| 8 | 8.32 | 8.66 | 4.09 | 0.993 |

## 5.6 Bridge model updating

In model updating, dynamic measurements such as the natural frequencies and mode shapes are correlated with their SA model counterparts to calibrate the SA model. There is a degree of uncertainty in the assessment of the actual properties of the materials used in the full-scale structure as well as the most realistic representation of the element stiffness, supports and connections between structural parts in the initial SA model. The challenge of finding a set of suitable parameters having physical justification necessitates the need for use of physically significant updating parameters and suitable optimization tools.

### *5.6.1 Objective function for model updating*

An objective function quantifies the deviation of the analytical predictions of modal parameters from those obtained experimentally. Two error measures, related to frequencies and mode shapes, respectively, have been used in this study. The total relative frequency difference between the experimental and analytical frequencies is represented as

$$\prod_f = \sum_{i=1}^{n} \left( \frac{f_{a,i} - f_{e,i}}{f_{e,i}} \right)^2 \quad \textbf{(5.10)}$$

where $f$ represents the frequency, subscripts $a$ and $e$ refer to analytical and experimental, respectively, and $n$ is the total number of frequencies considered.

The second error measure is related to difference in mode shapes and can be defined in terms of MAC (Möller and Friberg 1998) as

$$\prod_\theta = \sum_{i=1}^{m} \frac{(1 - \sqrt{MAC_i})^2}{MAC_i} \quad \textbf{(5.11)}$$

where $m$ is the total number of modes considered.

The combined objective function is given as

$$\prod = \boldsymbol{\alpha} \prod_f + \boldsymbol{\beta} \prod_\theta \quad \textbf{(5.12)}$$

where $\alpha$ and $\beta$ are weighting factors. These factors are used to differentiate between frequencies and mode shape deviations, as these are measured with different accuracies in the experiment.

### *5.6.2 Selection of updating parameters*

The selection of parameters in model updating is critical for the success of any such exercise. An excessive number of parameters compared to the number of available responses, or overparametrization, will lead to a non-unique solution, whereas an insufficient number of parameters will prevent reaching a good agreement between the experiment and numerical model (Titurus and Friswell 2008). Updating parameters are selected with the aim of correcting the uncertainties in the SA model. Only those parameters should, therefore, be selected to which the numerical responses are sensitive and whose values are uncertain in the initial model. Otherwise, the parameters of SA model may deviate far from the initial SA model and thus lose their physical significance while achieving acceptable correlations. One

way to deal with ill-conditioning is to test the structures in different configurations (Zapico et al. 2003). The problem related to ill-conditioning is central to SA model updating and is dealt with many researchers (Mottershead and Foster 1991; Friswell and Mottershead 1995; Ahmadian et al. 1998; Hua et al. 2009). The main focus of these studies is in the use of conventional regularization techniques such as the technique developed by Tikhonov (Tikhonov 1963). However, another efficient approach is to reduce the number of updating parameters to a minimum to avoid ill-conditioning.

The discrepancies between the different parameters of the initial SA model and the full-scale structure can be attributed to many inherent uncertainties and modeling assumptions, such as material density and stiffness and boundary and connectivity conditions. Parameter selection therefore requires a considerable insight into the structure and its model. In this study, only a small number of parameters were selected based on a prior knowledge of their potential variability and a sensitivity analysis was carried out to confirm they influence the responses. The various inertia parameters of the structure were not included as these are typically less uncertain than the stiffness parameters. The bridge was also supported at clearly defined points using specialized bearings that permitted making good judgment about the appropriate modeling of the boundary conditions. Thus, the candidate parameters considered for calibration in this study were cable tensions, cable axial stiffness, bending and torsional stiffness of the deck and stiffness of the bearings.

The likely uncertainty of the parameters characterizing cable stiffness, i.e. cable axial stiffness and tension force, can be attributed to many factors such as application of different tensioning forces than those specified in design, relaxation of steel stresses with time, and slippage in anchorages and between cable strands. Stiffness of the deck depends on Young's modulus of both steel and concrete; especially as the latter shows considerable variability. The connection between the steel girder and the concrete slab will typically be designed to

allow for either composite action or a lack thereof. However, real bridges will always exhibit a certain degree of composite action (less than full because of connector flexibility, and more than none because of, for example, steel-concrete friction) eluding the analyst. Furthermore, non-structural elements, such as the pavement, railings, services, also make a contribution to the stiffness that is difficult to quantify and model precisely. A change in one or more of the above mentioned parameters related to deck may influence the modal data in a similar way. Therefore, the whole deck is considered as a unit and, the bending and torsional stiffness of the deck are taken as updating parameters in this study. Also, the stiffness of the bearings is difficult to quantify as there is more uncertainty as to the initial value of this parameter.

There are three pairs of stay cables on each side of the central pylon. The four identical cables closest to the abutments are referred to as Cab-1, the four cables in the middle as Cab-2, and the four cables nearest to the pylon as Cab-3 (Figure 5.3). The cables were post-tensioned, as per design documentation, with forces $T_{Cab-1}$=55kN for the four cables closest to the abutments, $T_{Cab-2}$=95kN for the middle cables, and $T_{Cab-3}$=75kN for the cables nearest to the central pylon (Figure 5.3). The effective axial stiffness of a cable depends on its projected length, self-weight, axial stiffness *EA* (where *E* is Young's modulus and *A* is cross-sectional area) and tension force in the cable (Nazmy and Abdel-Ghaffar 1990). For taut cables with small sag, the influence of axial stiffness *EA* on the effective stiffness is more pronounced than that of the tension force (Nazmy and Abdel-Ghaffar 1990). A simple hand calculation using the Ernst formula (Ernst and Der 1965) for cable stiffness showed that the effect of the tension force on the stiffness is much more important in cables Cab-1 compared to the remaining cables. This was later confirmed by the sensitivity analysis on the SA model, and therefore only tension $T_{Cab-1}$ was included in the updating parameters.

Sensitivity analysis using the SA model was also conducted for all remaining potential parameters to select the most influential ones for subsequent model updating. Relative

sensitivity is the ratio of the relative change in the response value caused by a relative change in the parameter value. In this study, sensitivities were calculated using a finite difference method by changing the parameters by 0.1% with respect to their initial values. The final selected parameters based on sensitivity analysis and engineering insight were deck flexural stiffness for vertical ($K_{y,deck}$) and horizontal ($K_{x,deck}$) bending, deck torsional stiffness ($K_{t,deck}$), axial stiffness of all cables ($K_{cable}$), cable tension for Cab-1 ($T_{Cab-1}$), stiffness of bearings at abutments ($K_{,abut\ bearing}$) and stiffness of bearings at pylon ($K_{,pylon\ bearing}$) . The sensitivities of modal frequencies and MACs to the updating parameters are shown in Figure 5.11 and Figure 5.12, respectively.

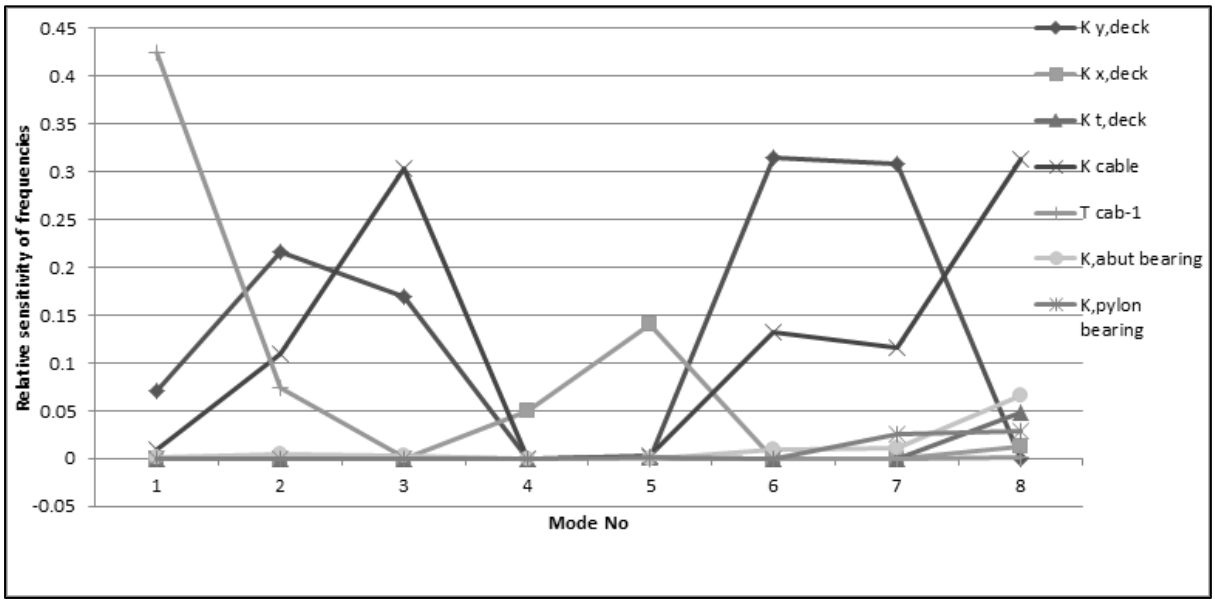


**Figure 5.11 Sensitivity of modal frequencies to selected updating parameters.**

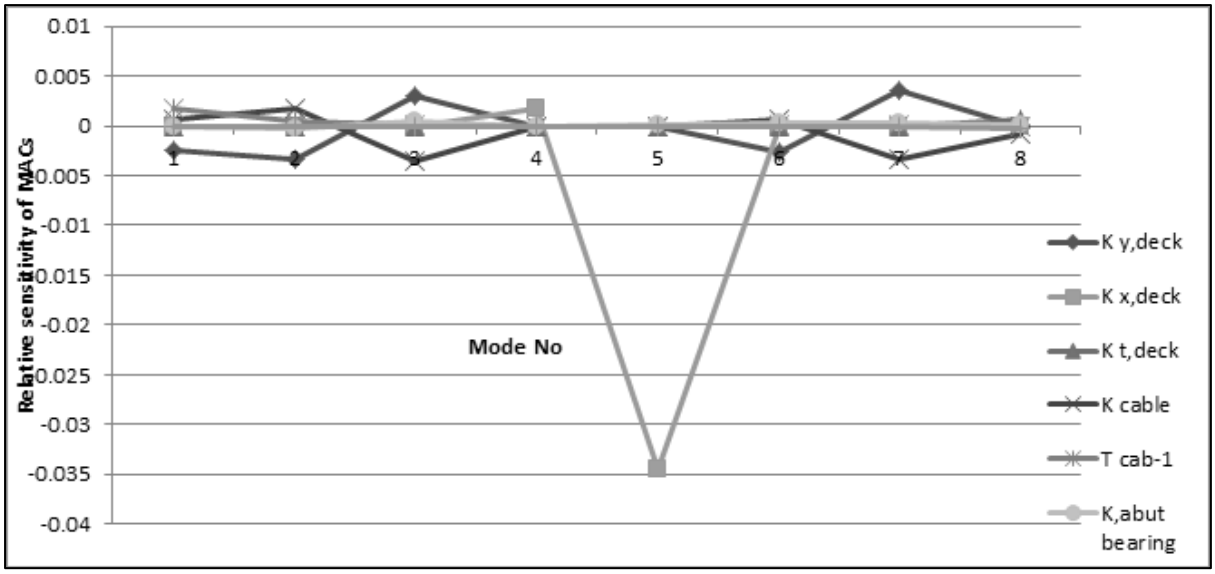


**Figure 5.12 Sensitivity of MACs to selected updating parameters.**

It can be seen that the frequencies are more sensitive to the parameters than MACs. It can be noted from Figure 5.11 that the parameters $K_{cable}$ , $K_{y,deck}$, $T_{Cab-1}$ and $K_{v,abutment}$ are more influential to the vertical modes (i.e. Mode No. 1, 2, 3, 6 and 7) and torsional mode (Mode No. 8), whereas the parameter $K_{x,deck}$ is influential to the horizontal modes (i.e. Mode No. 4 and 5). Also the parameter $K_{t,deck}$ influences the torsional mode (Mode No. 8). $K_{,abut\ bearing}$ and $K_{,pylon\ bearing}$ were lumped into one parameter $K_{bearing}$ for subsequent model updating. This essentially means that all bearing stiffness parameters are linked (horizontal, vertical and torsional) so that during updating, they all change by the same amount. It has also been found that sensitivity of $K_{bearing}$ and $K_{t,deck}$ is similar for the torsional mode (Mode No.8), and updating the parameters might result in a non-unique answer. Therefore, a soft constraint is applied to keep the ratio of $K_{t,deck}$ / $K_{bearing}$ constant by adding a penalty functional. Therefore, the objective function of Equation 5.14 must be augmented with the following term:

$$\prod \quad = \left(\alpha \prod \quad_{f} + \beta \prod \quad_{\theta}\right) + \alpha \text{ x norm} \left(\frac{\text{Kt,deck}_i}{\text{Kbearing}_i} + \frac{\text{Kt,deck}_0}{\text{Kbearing}_0}\right) \qquad \textbf{(5.13)}$$

where α is a arbitrary parameter; norm is Euclidian norm; subscript '*i*' represents current values of these parameters and subscript'*0*' represents initial values of these parameters. The

value of α determines the compromise between the two and essentially penalizes large deviations of these two parameters with respect to each other. Based on trial and error, a value of 0.0002 has been selected as an appropriate value; a higher value tends to fix the two parameters $K_{t,deck}$ and $K_{bearing}$ to change together and a lower value tends to move them away from each other during updating.

Selecting appropriate bounds on the allowable parameter variations during model updating is challenging and is normally done using engineering judgment. Different bounds have been used in previous research (Jaishi and Ren 2005; Zivanovic et al. 2007). From the frequency errors in Table 5.2, it can be concluded that the initial SA model generally overestimates the stiffness, therefore the lower bound has been selected as -40% and the upper bound was selected as +30% for all the parameters. A value of 1 was used as the weighting factor for $\alpha$ and $\beta$ in Equation (9) for this research work.

### *5.6.3 Assessment of the performance of the model updating methodology*

This section applies the proposed combination of SNT with PSO to the pedestrian bridge SA model updating in order to explore the performance of the approach. In the first phase, uncertain parameters were updated using available experimental information measured from physical testing using the traditional sensitivity based model updating. The effect of different starting points on results of the sensitivity based model updating was explored. In the second phase, uncertain parameters were updated using the proposed approach of PSO and SNT.

#### *5.6.3.1 Phase 1: Updating of parameters using sensitivity based model updating technique*

In this Phase, experimentally identified modal data from the field tests were updated considering the stiffness parameters as listed earlier in section 5.6.2. A sensitivity based

iterative model updating method is applied to the full scale bridge to decrease the difference between the modal properties of the SA model and those identified from measurements. The vector of analytical eigen values and eigen vectors is a non-linear function of the uncertain parameters. It is the goal of optimization to determine the set of parameters which decrease the error residual. As explained in Chapter 2, one way to solve this problem is to expand the eigen properties into a Taylor series, which is truncated to include only the linear term (Friswell and Mottershead 1995). Consequently, the non-linear minimization problem becomes a linear minimization problem. The sensitivity matrix *S* is used in the iterative updating algorithm. At the ith iteration, the sensitivity matrix can be written as

$$S_i = \frac{\partial d_i}{\partial p_i} \tag{5.14}$$

where $\partial p_i$ represents the perturbation in the parameters and $\partial d_i$ represents the differences in the eigen properties of the SA model and the experimental data. The sensitivity matrix *S* can be computed via analytical methods or by perturbation techniques. The direct derivation involves the differentiation of the eigen value problem with respect to the parameters. On the other hand, perturbation techniques can be used by multiple SA runs to numerically evaluate the sensitivity matrix. In this research, the perturbation technique is used and the sensitivity matrix is computed using a forward difference method in lieu of each parameter. For *n* uncertain parameters, a total of *n + 1* function evaluations are required to calculate the matrix in each iteration. One column of the sensitivity matrix is represented by the vector $\frac{\Delta d}{\Delta p}$. The sensitivity matrix needs to be computed in each iteration until convergence is obtained. The algorithm is implemented in MATLAB. The initial SA model of the bridge was updated and the initial values of the parameters of the initial SA model were taken as the starting point for the sensitivity analysis. A factor of 1 was multiplied with parameters and is taken as Run # 1.

The updated solution obtained in the form of the ratios of updated to initial stiffness values is shown in Table 5.3.

The initial and updated frequencies, their errors compared to the experimental results, and initial and updated MACs are shown in Table 5.4. All frequency errors are generally less than 2% after updating. The largest error dropped from 8.62% to 2.8%, and in fact corresponds to a small error increase for the first vertical mode. This indicates that it is possible of improve the SA model considerably via adjusting the particular set of updating parameters considered, but some trade-off is inevitable. On the other hand, MAC values did not change appreciably, with some small positive and negative changes in different modes and the minimum value remaining at 0.987.

The updated parameters should be physically meaningful; otherwise it is difficult to justify the updating results. The vertical bending stiffness of the bridge deck has decreased by 15.5%, horizontal stiffness by 16.3% and torsional stiffness by 6.5%, respectively. This could be mainly attributed to the fact that the initial model takes the cast in-situ concrete slab as fully composite with the steel girder. The updated results reveal that there is only partial composite action between the slab and the steel girder resulting in a lower stiffness of the whole deck. The consistent decrease in all the parameters related to the deck stiffness supports this conclusion. The increase in cable tension $T_{Cab-1}$ by 12%, shows that these post-tension forces are more than the designed value of 55 kN, indicating possible overstressing of the cables. On the other hand, the cable axial stiffness shows a 7 % decrease. The latter result can be attributed to many factors. The SA model uses a rather coarse parameterization. As a result, potential localized stiffness changes may be lumped into those parameters. For example, the identified drop in the cable axial stiffness may be because of slippage in the cable anchorages, i.e. uncertainty in the modeling of structural connectivity.

As mentioned in Chapter 2, there are a number of uncertainties associated with realization and subsequent SA modeling of the full scale structure. Therefore, an attempt has been made to update the SA model but with different starting points. A factor of 0.92 and 1.11 was used to multiply the starting values of all six parameters and is named as Runs # 2 and 3 respectively. The corresponding model updating results are presented in Table 5.3. The factors were so selected that the initial values still remain within the search bounds. The corresponding frequency differences and MAC values for these runs are shown in Table 5.4. It can be seen that the sensitivity based algorithm has failed to converge to the values of parameters found in Run # 1. The SM is a deterministic algorithm and uses deterministic rules to find the optimal solution. By looking at the condition number of the sensitivity matrix for Runs # 2 and 3, it has been found that the value has been increased as compared to Run # 1. The problem can be addressed by incorporating regularization techniques but not normally exercised in model updating of constructed systems (Jaishi and Ren 2005; Zárate and Caicedo 2008). This agrees with the model updating attempts of full scale structures presented by other researchers, that sensitivity based methods might lead to different solutions in the search space (Jaishi and Ren 2005; Zárate and Caicedo 2008). The authors in those papers have tried to update at different starting points within the search bounds and the answer that satisfied the judgment of the analyst was taken as the final updated solution. This is a limitation of the method as any wrong conceptualization in the a priori model can make the updating exercise meaningless.

**Table 5.3. Solution obtained by sensitivity based model updating for Phase 1.**

| Run # | Factors for starting values of parameters | Ratio of updated to initial stiffness | | | | | | Final value of objective function |
|---|---|---|---|---|---|---|---|---|
| | | $K_{y,deck}$ | $K_{x,deck}$ | $K_{t,deck}$ | $K_{cable}$ | $T_{Cab-1}$ | $K_{v,bearing}$ | |
| 1 | 1 | 0.845 | 0.837 | 0.935 | 0.930 | 1.120 | 0.981 | 0.0022 |
| 2 | 0.92 | 0.812 | 0.822 | 0.901 | 0.917 | 0.928 | 0.901 | 0.0072 |
| 3 | 1.11 | 0.967 | 0.803 | 1.056 | 0.661 | 1.279 | 1.065 | 0.0139 |

**Table 5.4. Updated SA model and experimental frequencies and MACs using SM for Phase 1.**

| Mode No. | Experimental frequencies by N4SID | Run #1 | | | Run #2 | | | Run #3 | | |
|---|---|---|---|---|---|---|---|---|---|---|
| | | Updated SA model frequencies | Error in frequencies | | Updated SA model frequencies | Error in frequencies | | Updated SA model frequencies | Error in frequencies | |
| | (Hz) | (Hz) | (%) | MAC | (Hz) | (%) | MAC | (Hz) | (%) | MAC |
| 1 | 1.64 | 1.69 | 2.84 | 0.999 | 1.59 | -3.27 | 0.999 | 1.72 | 4.94 | 0.999 |
| 2 | 1.9 | 1.86 | -2.05 | 0.996 | 1.78 | -6.49 | 0.996 | 1.94 | 2.15 | 0.995 |
| 3 | 3.69 | 3.70 | 0.22 | 0.999 | 3.66 | -0.91 | 0.999 | 3.42 | -7.20 | 1.000 |
| 4 | 4.86 | 4.97 | 2.16 | 0.990 | 4.92 | 1.24 | 0.990 | 4.86 | 0.07 | 0.990 |
| 5 | 5.33 | 5.28 | -1.03 | 0.987 | 5.27 | -1.21 | 0.987 | 5.25 | -1.58 | 0.988 |
| 6 | 6.31 | 6.39 | 1.23 | 1.000 | 6.30 | -0.21 | 1.000 | 6.40 | 1.38 | 0.999 |
| 7 | 7.42 | 7.30 | -1.61 | 0.992 | 7.18 | -3.27 | 0.992 | 7.38 | -0.51 | 0.993 |
| 8 | 8.32 | 8.41 | 1.05 | 0.993 | 8.29 | -0.41 | 0.993 | 7.70 | -7.40 | 0.991 |

As can be noted that the analyst normally has little knowledge of the parameter interaction in many dimensional solution spaces and trial and error solutions were normally sought. Another important point is that the initial model has to be a very good realization of the actual structure (Friswell and Mottershead 1995) otherwise the updating results can move far away from the actual structure. This is also the reason why manual model updating has been required in most previous model updating studies (Brownjohn and Xia 2000; Brownjohn et al. 2001) so that the initial SA model closely matches the as built structure. Regularization techniques also require that the initial SA model is a good representation as these mathematical techniques try to decrease the change in the values of the parameters. GOAs can be applied with the aim of finding the best solution within the search bounds. In the next section, PSO was applied to this problem. An extension of GOA is also presented in the next section i.e. SNT which searches the space sequentially thus gives more information about the search space rather than running blind independent runs with different starting points.

#### *5.6.3.2 Stage 2: Updating of uncertain parameters using PSO*

In this Phase, the experimentally identified modal data from field tests were updated using GOAs. A population of 20 points was used and the maximum number of generations was set to 200. PSO parameters were set according to the study in Chapter 4. The maximum velocity has been constrained as half of the allowable parameter variation range (-40% - +30%). The niche radius for SNT was assumed according to Equation (5.5) for four solutions and was found to be 0.97.

Model updating by PSO, i.e. without SNT, was attempted initially. Ten independent runs were tested with different, randomly selected starting points to check the efficiency in detecting the best solution. The best solution in the form of the ratios of updated to initial stiffness values and their standard deviations from the 10 runs are shown in Table 5.5. It can

be seen that the maximum standard deviation of the updated parameter ratios is 0.0058, giving confidence that all the solutions correspond to the same point in the search space. The results obtained are in close agreement with the ones obtained using the SM.

**Table 5.5. Ratios of updated to initial stiffness and final objective function values for SNT with PSO for Phase 2.**

| Ratio of updated to initial stiffness (standard deviation) | | | | | | Final value of objective |
|---|---|---|---|---|---|---|
| $K_{y,deck}$ | $K_{x,deck}$ | $K_{t,deck}$ | $K_{cable}$ | $T_{Cab-1}$ | $K_{v,bearing}$ | |
| 0.845 (0.0006) | 0.837 (0.0003) | 0.935 (0.0001) | 0.925 (0.002) | 1.160 (0.0011) | 0.932 (0.0058) | 0.0021 |

**Table 5.6. Ratios of updated to initial stiffness and final objective function values for SNT with PSO for Phase 2.**

| Minimum No. | Ratio of updated to initial stiffness | | | | | | Final value of objective function |
|---|---|---|---|---|---|---|---|
| | $K_{y,deck}$ | $K_{x,deck}$ | $K_{t,deck}$ | $K_{cable}$ | $T_{Cab-1}$ | $K_{v,bearing}$ | |
| **1** | **0.845** | **0.837** | **0.935** | **0.925** | **1.160** | **0.932** | **0.0021** |
| 2 | 0.662 | 0.798 | 0.600 | 1.300 | 1.044 | 0.600 | 0.0060 |
| 3 | 0.880 | 0.801 | 0.600 | 0.600 | 1.300 | 0.600 | 0.0049 |
| 4 | 0.600 | 0.802 | 0.657 | 1.300 | 1.219 | 0.950 | 0.0079 |

SNT with PSO was then applied to confirm that there is no better solution less than the solution found earlier by PSO alone. SNT with PSO was iterated four times and the results are shown in Table 5.6 It can be seen that the first solution found (shown in bold) is the same solution as the one found earlier by PSO alone. In further iterations, different solutions with increased objective function values were found. The second minimum has the objective function greater than the first minimum. Also, the updated parameter values for those

solutions were in many cases quite different than for the first minimum. This is because SNT does not let the search algorithm to converge again to the same niche. This also confirms that the basic PSO algorithm, i.e. without SNT, has converged to the global minimum in all 10 independent runs in this stage.

For checking the effect of the niche radius, the raw objective function values were compared with the modified function values obtained after the derating function was applied. It has been found that the niche radius used in this study has not affected the other solutions in the search space. It is recommended that all the 'modified' objective function values obtained using SNT should be compared with raw function values to check if the results are similar and does not have effects due to niche radius.

The technique proposed in this research is based on combination of SNT with PSO for dynamic model updating. This technique increases the confidence in the obtained results as most of the solution space has been searched sequentially and the user can select the best solution from a list of different available solutions. The traditional SM cannot ensure that a thorough investigation of the search space has been carried out in most cases (Deb 1998; Jaishi and Ren 2005). Therefore, SNT with PSO gives the analysts more confidence about the behaviour of the search space and has its superiority over most of the current techniques used for model updating. The results of Phase 2 demonstrate how combining SNT with PSO overcomes some of the shortcomings of the SM and extends its applicability for more challenging updating problems.

The following steps (Figure 5.13) are recommended for setting up the model updating method proposed in this research:

1. Initial modelling based on idealised drawings and/or actual measurements to extract stiffness and mass matrices.
2. Dynamic testing to detect natural frequencies and mode shapes of the actual structure.
3. Error residual between experimental results and their initial model counterparts.
4. Select most significant uncertain parameters to the experimental responses.
5. Use the proposed SNT with PSO for dynamic model updating to decrease the difference between experimental and analytical results.

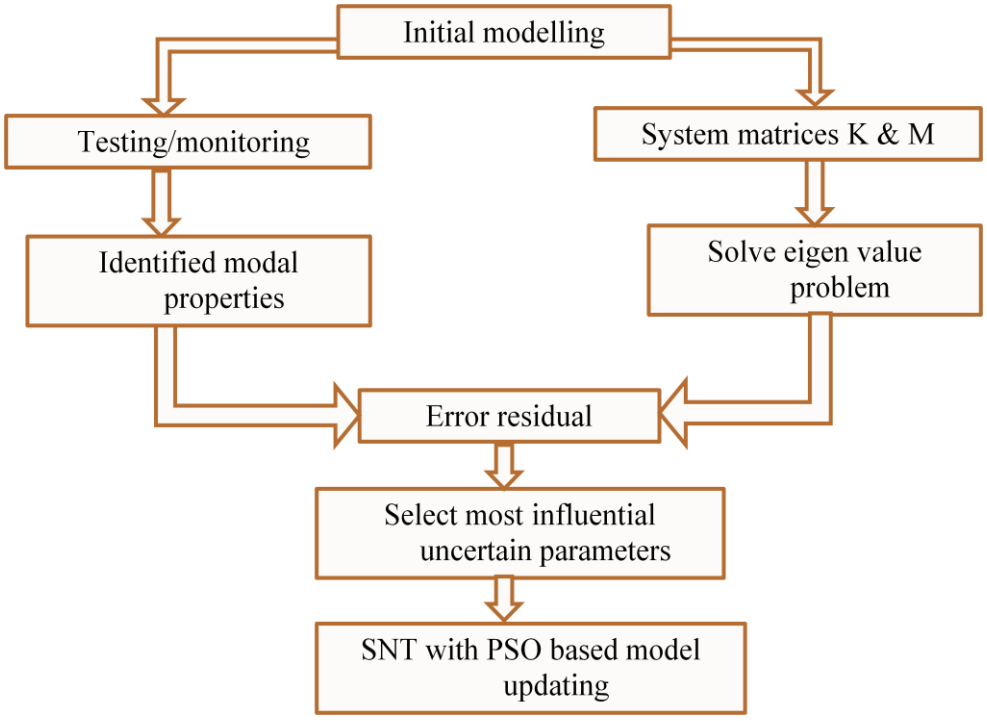


**Figure 5.13 Flow chart for model updating**

Specific guidelines from the current research are:

1. In cable stayed pedestrian bridges, the natural frequencies of bridges may coincide with pedestrian walking frequency, thereby leading to serviceability issues.
2. Even if the concrete slab on steel girder deck of some pedestrian bridges is assumed to be non-composite in the initial design, there may be some, albeit at best only

partial, composite action between the slab and the steel girder contributing to the stiffness of the whole deck. This aspect should be taken into account in the initial design of these types of bridges.

## 5.7 Summary

A combination of PSO and SNT has been proposed in this study to enhance the performance of model updating using GOA. SNT works by ‘filling in’ the objective function niches, corresponding to the already known solutions, and forces PSO to expend its region of search, thereby increasing the chance of exploring the full search space. The performance of PSO augmented with SNT has been explored using experimental modal analysis results from a full-scale cable-stayed pedestrian bridge, and improved performance over PSO alone demonstrated. The results show that the methodology proposed herein gives the analyst more confidence in the model updating results and that it can successfully be applied to full-scale structures.

# Chapter 6. DAMAGE ESTIMATION USING GLOBAL OPTIMIZATION ALGORITHMS

## 6.1 Introduction

This chapter presents a novel damage estimation method which simultaneously updates the damaged and the undamaged structure models in a MOO process. The main aim of this chapter is the application of a MOO technique to damage estimation problems, to effectively use the experimental data of both undamaged and damaged structures concurrently. Contemporary damage detection and estimation methods which are based on model updating typically requires an updated baseline SA model of the undamaged structure. The updated undamaged model is then compared with an updated damaged model for assessment of the damage severity. There might be many errors associated with this model updating technique, e.g. experimental errors, updating procedure errors or parametric errors. These errors may be aggregated in the subsequent model updating runs.

A damage estimation algorithm is being proposed in this chapter which simultaneously updates undamaged as well as damaged structures in a MOO process for improving performance of the damage estimation procedure. In order to evaluate the performance of the

proposed approach, it is applied to a simulated beam model. Different noise levels are added to the identified mode shapes to assess the performance of the proposed procedure for accurate damage estimation in noisy conditions. Multi-objective GA, which is well implemented, has been used in this study (Knowles et al. 2008). The contribution and novelty of this study is in the application of the MOO for damage estimation which utilizes the data of the undamaged and damaged structures concurrently to improve the performance of the damage estimation procedure. Compared to the single objective optimization (SOO), which gives one optimal solution, MOO formulation gives a set of alternative solutions. A desirable solution can then be selected based on acceptable trade-off between the two objective functions (in this case related to the undamaged and damaged structure). However, due to the wrong detections of damage in many elements, a simple regularization using PSO is proposed.

This chapter is structured as follows: Section 6.2 describes the MOO. This is followed by model updating of a simulated beam using SOO and MOO, in Section 6.3 and 6.4, respectively. The results of simple regularization using PSO are detailed in Section 6.5 and summary of the study is reported in Section 6.6.

## 6.2 Multi-objective optimization

An optimal solution for a physical system modelled using one objective function can be found using SOO. However, when a system is modelled using two or more objective functions, the task of finding one or more optimal solutions is referred to as MOO. Many real-world optimization problems involve multiple objectives. The extremist principle which prioritizes one objective over the others may lead to erroneous results especially in cases where the rest of the objectives are also important or interdependent. Selecting a solution which is optimal for only one objective may compromise the other objectives.

EAs are a popular approach to solve MOO problems using the concept of domination (Kalyanmoy 2001). According to this concept, one solution dominates the other solution if the following two conditions are satisfied:

1. The first solution is not worse than the second solution in all objectives
2. The first solution is strictly better than the second solution in at least one objective.

Violation of any of the above conditions indicates that the first solution does not dominate the second solution. It is intuitive that, if any solution dominates the other solution, then it is also better in the context of MOO. This concept of domination is used to find 'non-dominated' solutions. When all pair-wise comparisons have been made for a given finite set of solutions, we expect to have a set comprising a number of solutions which do not dominate one another. An important property of this set is that each of its solutions dominates all other solutions outside of this set. Simply speaking, the solutions in this set are better when compared to the rest of the solutions. This leads to the definition of *Pareto optimality* which states that, among all solutions, a non-dominated set of solution are those which are not dominated by rest of the solutions. This concept of Pareto optimality leads to a set of solutions known as the *Pareto Optimal set* and a rank is assigned to such a set (Deb et al. 2002; Deb 2004). A plot of objective function values corresponding to Pareto optimal set gives the *Pareto Front*. Two basic approaches have been mentioned in the literature to obtain Pareto optimal set; namely *preference* and *multi-objective evolutionary optimization* (MOEO). While a large number of optimization runs is required to construct a Pareto front following a preference-based approach, a single run is required using EAs.

### *6.2.1 Preference based multi-objective optimization*

The conventional method of solving multi-objective problems is by transforming the problem into a single objective one. This is attained by using different preference indices to each of

the objectives and combining the end results by adding or multiplying the weighting criteria into a single value 'Q' (Kahraman et al. 2008). The value Q of a candidate solution can be written in one of the following two forms:

$$Q = w_1 \times q_1 + w_2 \times q_2 + \cdots + w_n \times q_n \quad \textbf{6.1}$$

$$Q = q_1^{w_1} \times q_2^{w_2} \ldots\ldots \times q_n^{w_n} \quad \textbf{6.2}$$

where $w_1$ to $w_n$ are the preference indices given to the objective functions $q_1$ to $q_n$, respectively. The particular advantage of this approach is that it is relatively simple to apply. The main disadvantage is the ad-hoc selection of different weights to different objective functions (Coello and Lamont 2004). The selections are normally based on user judgment or on trial and error approaches. Such selections do not have a logical basis and are subjective in nature.

### *6.2.2 Multi-objective evolutionary optimization*

The fundamental difference of this approach from the preference-based approach is that all the objectives are evaluated concurrently instead of converting them into a single objective function. As discussed in Chapter 3, EAs such as GA concurrently work on a population and use genetic operators such as selection, crossover and mutation to obtain globally optimal solutions. This evolution mechanism helps to explore the trade off between solutions with different blends and grades of objectives. Also, they do not require gradients of the objective function; their chance to reach global optimal solutions is increased. Detailed reviews of multi-objective techniques can be found in (Coello and Lamont 2004; Deb 2004).

Many variants of MOEO, based on Pareto front approach and using multi-objective evolutionary algorithms (MOEA), have been proposed (Coello and Lamont 2004). These include NPGA (niched Pareto genetic algorithm), NSGA (non dominated sorting genetic algorithm), MOMGA (multi-objective messy genetic algorithm) and SPEA (strength Pareto

genetic algorithm). NSGA-II is one of the most popular and efficient MOEA and has been used in many studies in the last decade (Deb et al. 2002; Koppen and Yoshida 2007; Li and Zhang 2009; Chan and Sudhoff 2010). Therefore NSGA-II has been adopted for this study to investigate its effectiveness for damage detection and estimation via dynamic model updating. The general steps involved in NSGA-II are as follows:

1. A termination criterion based on the accuracy required and total number of generations is selected
2. A random population of chromosomes (solutions) is initialised
3. Values of objective functions for each of the chromosome is obtained
4. Different ranks are assigned to each of the solution based on non-dominated sorting algorithm to classify the population into fronts.
5. An offspring of the parent population, by randomly arranging a duplicate copy of the parent solutions, is created.
6. A tournament selection to select best solutions obtained from the previous step is performed. Cross-over is performed on the parent solutions to form new offspring with cross-over probability.
7. The new off springs are mutated with a mutation probability.
8. A non-dominated sorting is performed on the new offspring and, once again, all the solutions are classified into fronts using a non-dominated sorting algorithm.
9. If the termination criteria or maximum number of generations are achieved, stop or else go to step 6.

After some trial and error, the following parameters of NSGA-II have been used in the present research for MOO:

Population size =500

Maximum number of generations =200

Stopping criterion (Tolerance of objective function value) = $1x\ 10^{-10}$

Cross-over probability =0.8

Mutation probability =0.01

Pareto fraction (fraction of solutions to be kept in the first front) =0.35

## 6.3 Structural model updating in a multi-objective context

In the previous decade, numerous studies have been performed to establish the health of the structure under in-situ conditions (Hu et al. 2001; Begambre and Laier 2009). In the context of dynamic SA model updating, assessment of the physical characteristics of the structure is done by comparing basic modal properties (such as natural frequencies and mode shapes) with their SA model counterparts.

A simulated simply-supported beam has been studied to demonstrate the effectiveness of the damage estimation method which simultaneously updates the undamaged as well as the damaged structure model in a MOO process. The simulated beam has a total length of 5 m and was discretized into 10 elements, as shown in Figure 6.1. The beam has a total depth of 0.2 m and width of 0.25 m. The density of the beam was assumed as 2500 kg / $m^3$ and the modulus of elasticity as $3.2 \times 10^4$ MPa. The area of the cross section was 0.05 $m^2$ and the MOI was $1.66 \times 10^{-4}$ $m^4$. The preliminary model of the beam was assumed as the one which has the above mentioned section properties with 20 discretized elements and is referred to as *initial SA model* (Figure 6.1(a)). For further model updating, the *a priori SA model* was assumed with only 10 discretizations (Figure 6.1(b)). This introduces a discretization error in the model, and thus formulates the initial and a priori model differently to make the updating exercise more challenging. In the simulated 'experimental' model for the *damaged structure 1*, the half of MOI of element No.6 of the initial SA model has been reduced by 20%, which resulted in an overall 10% decrease in the MOI of element No.6 in as shown in Figure 6.1(c).

For obtaining simulated 'experimental' modal parameters for the *damaged structure 2*, half of the MOI of element No. 6 have been further reduced from 20% to 30 % and half of the MOI of element No.3 has been reduced to 20 %. This has resulted in an overall decrease of 15% in Element No.6 and 10% in Element No.3 (Figure 6.1(d)). This methodology is advantageous in checking the effectiveness of the proposed approach in updating both damaged models simultaneously.

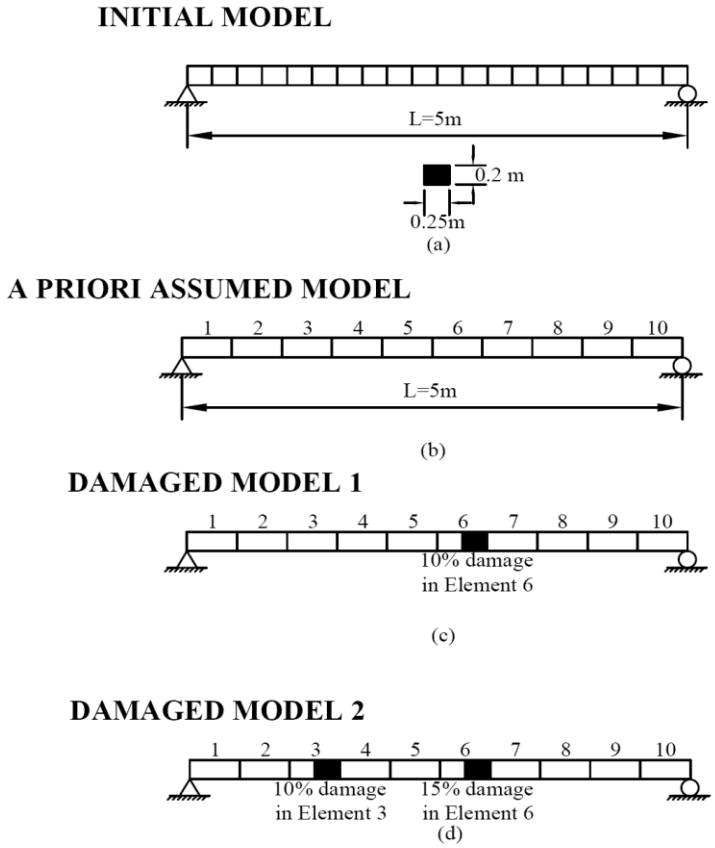


**Figure 6.1 (a) Initial SA model without any reduction in MOI and with no discretization errors (b) A priori assumed model with discretization error (only 10 updating parameters) (c) Damaged model 1 with 10 % reduction in MOI of Element No. 6 (d) Damaged model 2 with 15 % reduction in MOI of element No. 6 and 10 % in Elements No. 3**

The modal analysis was carried out on both the damaged beams to obtain the first five natural frequencies and mode shapes. The values of the first five natural frequencies for the initial SA model, a priori assumed model, damaged model 1 and damaged model 2 are shown in Table 6.1. It can be seen that maximum difference between the frequencies from the initial

SA model to the undamaged beam is 1.16 % and to the damaged beam is 2.62 %. Only 10 vertical DOFs are assumed to be known (Figure 6.1(b)), as it is a usual practice to have fewer measurements in the actual experiments.

**Table 6.1 Frequencies of the simulated beam before model updating**

| Sr. No. | Frequencies of initial SA model (Hz) | Frequencies of a priori assumed beam (Hz) | Frequencies of damaged beam 1 (Hz) | Frequencies of damaged beam 2 (Hz) | Difference between initial SA and undamaged model (%) | Difference between initial SA and damaged model (%) |
|---|---|---|---|---|---|---|
| 1 | 12.98 | 12.98 | 12.83 | 12.64 | -1.16 | -2.62 |
| 2 | 51.91 | 51.91 | 51.78 | 51.07 | -0.25 | -1.62 |
| 3 | 116.80 | 116.73 | 115.99 | 115.04 | -0.69 | -1.51 |
| 4 | 207.63 | 207.14 | 206.04 | 204.71 | -0.77 | -1.41 |
| 5 | 324.36 | 322.11 | 323.64 | 320.15 | -0.22 | -1.29 |

It can be assumed that the modal frequencies are accurately determined in modal testing and experimental errors are usually present in the amplitude of the mode shapes (Udwadia 2005). Consequently some random noise has been added to each of the 'k'th component of the 'j'th modal amplitude and the 'measured' component of the mode shape is given as

$$\Phi_{jk} = \Phi_{jk}(1 + \alpha_{noise}\varepsilon) \qquad \textbf{6.3}$$

where ε is a random number between -1 and +1 and $\alpha_{noise}$ is the degree of noise. A 3% noise level was added in the mode shapes (Perera and Torres 2006) for checking effectiveness of the proposed approach.

A combined objective function related to the frequencies and MACs (Equation 4.25) is used in this study. Two separate objective functions were defined for the damaged structure 1 ( $\prod_{dam1}$) and damaged structure 2 ( $\prod_{dam}$) as

$$\prod_{dam1} = \alpha\prod_{1.dam1} + \beta\prod_{2.dam1} \quad \textbf{6.4}$$

$$\prod_{dam2} = \alpha\prod_{1.dam2} + \beta\prod_{2.dam2} \quad \textbf{6.5}$$

where weighting factors α and β were taken as 1.

## 6.4 Model updating of a simulated simply supported beam using single and multi objective optimization

Model updating of the two damaged beams has been performed in this section. The first five frequencies and mode shapes were selected to have a similar number of unknowns (MOI for each FE) as the number of knowns (frequencies and MACs). All the twenty parameters related to MOIs of the damaged beam 1 and damaged beam 2 were updated.

As a conventional approach, an updated *baseline model* was obtained for the damaged structure 1 using Equation 6.4 and SOO. A total of ten parameters were updated with ten knowns (i.e. 5 frequencies and 5 MACs of the undamaged beam). After obtaining the baseline model, the next step is to update the damaged model 2 using Equation 6.5.

For MOO, a total of twenty parameters need to be concurrently updated in which case ten parameters belong to the damaged beam 1 and ten parameter belongs to the damaged beam 2. Both Equation 6.4 and 6.5 were concurrently used as two separate objective functions. The optimum solution is selected from the Pareto optimal set. A typical Pareto front is shown in Figure 6.2 which considers both the objective functions equally important and identifies the non-dominated solutions. The front consists of those Pareto solutions for which there does not exist any solution which is better in both the objective functions simultaneously. Thus, the trade-off between both the objective functions can be explicitly decided by observing the Pareto front. The two straight lines parallel to x and y axis were drawn as shown in Figure 6.2

and the final solution is selected which is at the shortest distance from the intersection point of these two lines.

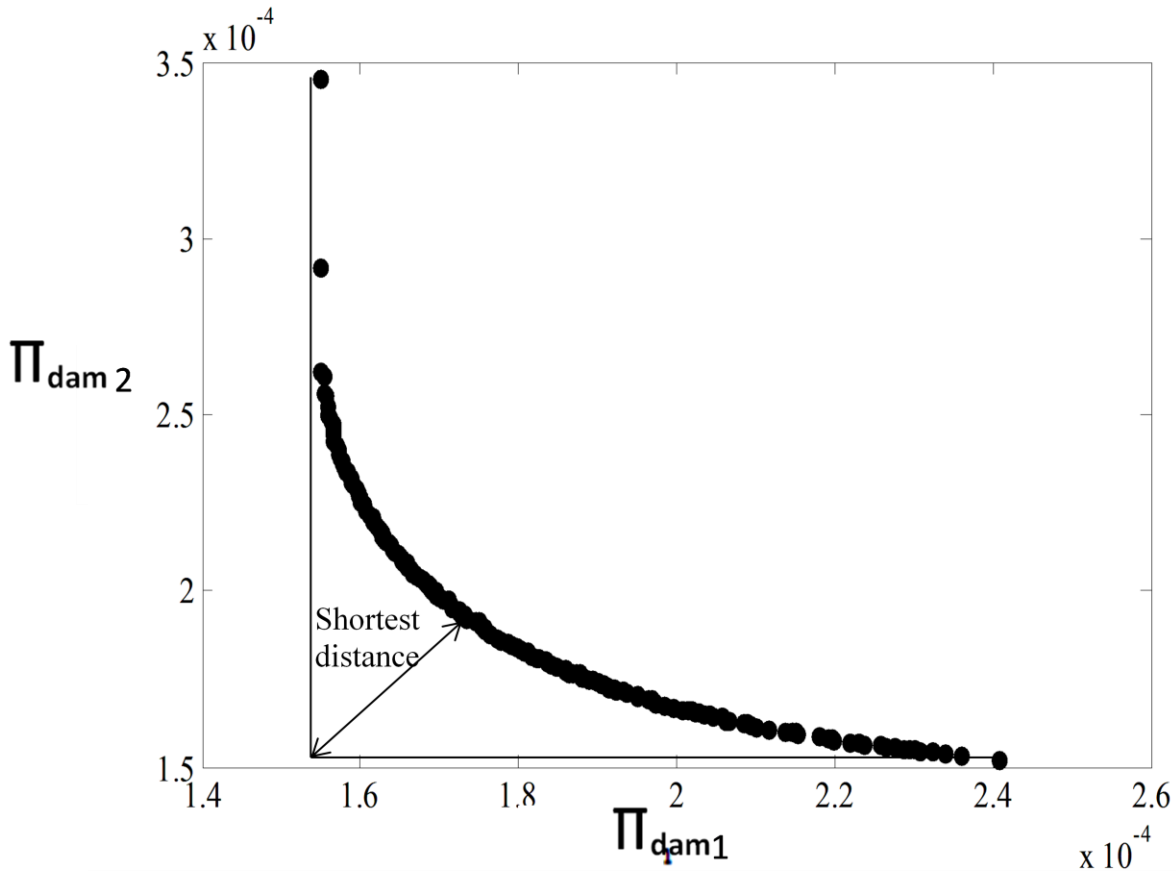


**Figure 6.2 Typical Pareto front between two objective functions related to damaged beam 1 and damaged beam 2**

Both SOO and MOO were performed to obtain the updated parameters. Figure 6.3 shows the mean errors in the stiffness ratio of the updated damaged model 1 and damaged model 2 to the true values of stiffness for 3% of added noise.

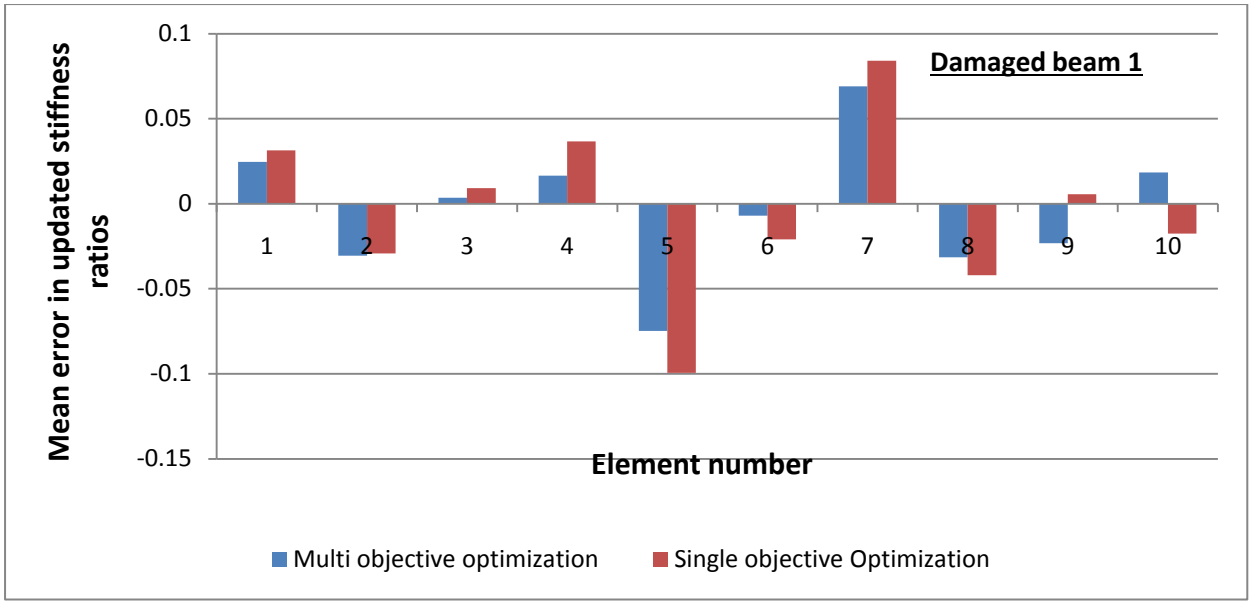


(a)

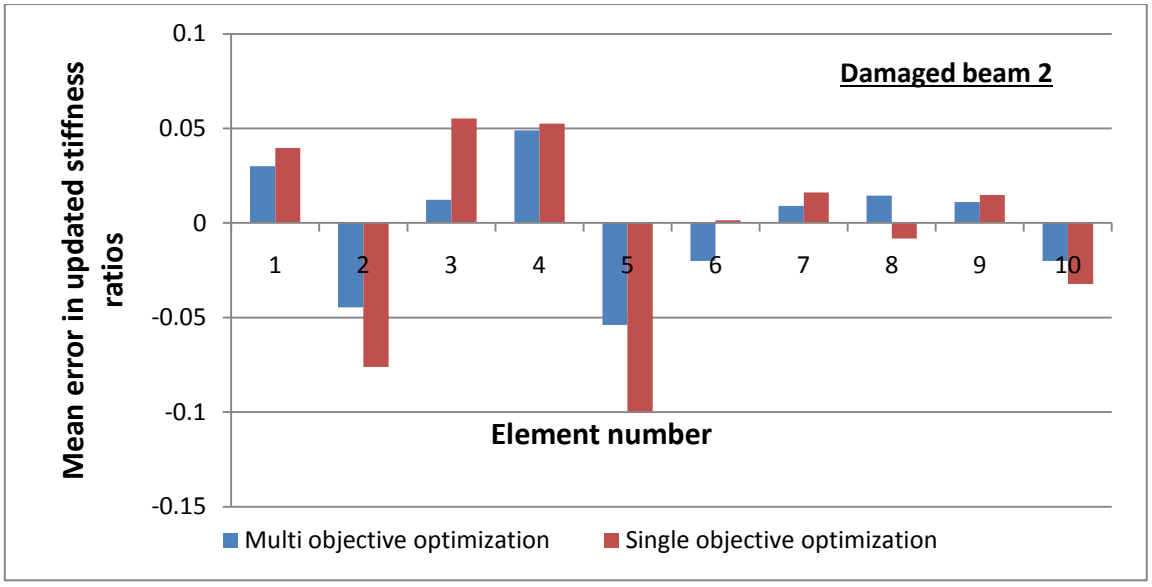


(b)

**Figure 6.3 Results for model updating with 3% noise level (a) error in updated stiffness ratios in damaged beam 1 (b) error in updated stiffness ratios in damaged beam 2**

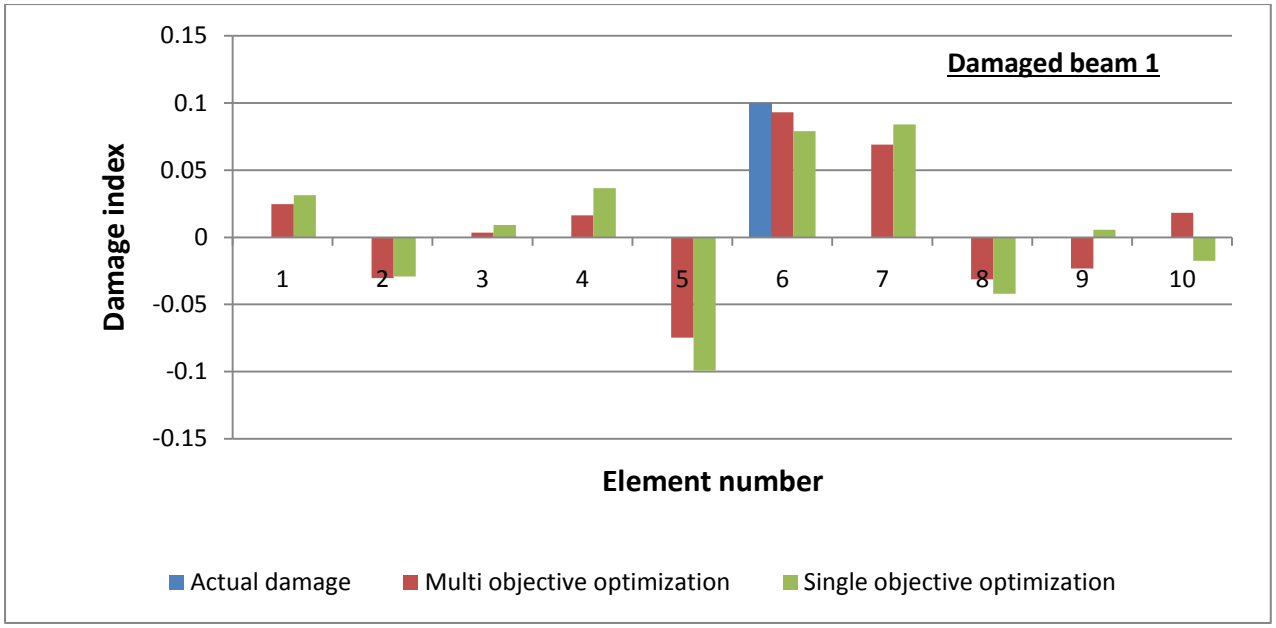


(a)

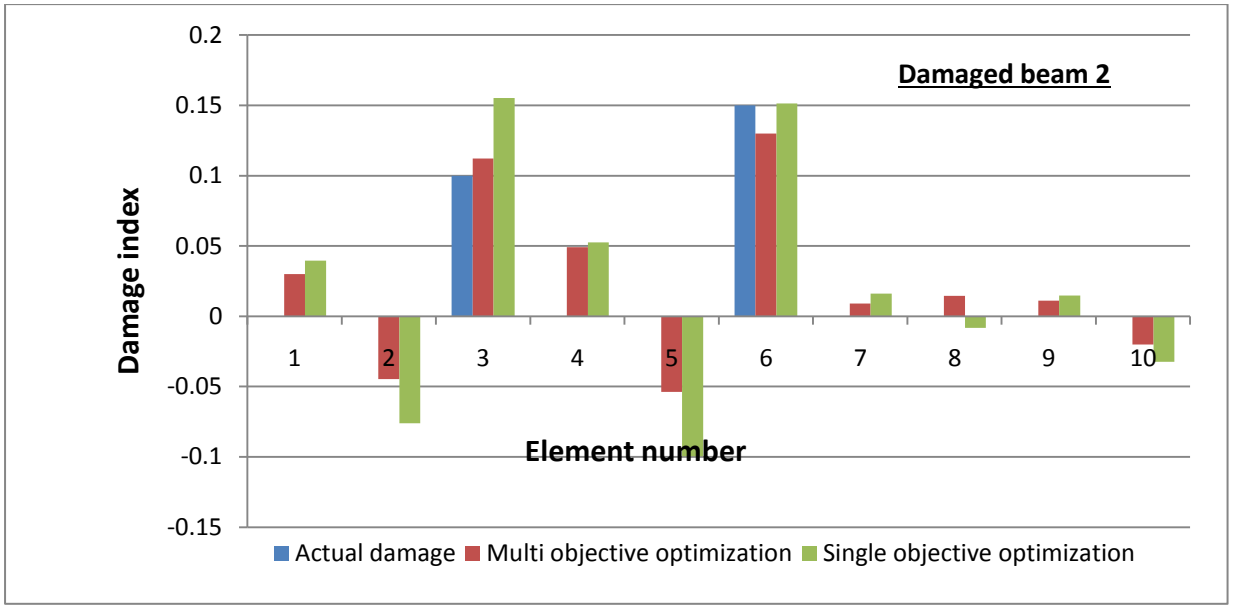


(b)

**Figure 6.4 Damage estimation (a) for damaged beam 1 (b) for damaged beam 2**

For damaged beam 1, the maximum mean error for single objective updating is found to be 0.084 and maximum mean error for multi-objective case is 0.069. For damaged beam 2, the maximum mean error for single objective updating is found to be 0.055 and maximum mean error for multi-objective case is 0.049. It can be seen from the errors in the updated stiffness ratios from Figure 6.3 that MOO has less error in the updated parameters than SOO. This proves that the proposed approach is better in updating both the models and is less sensitive to experimental errors than SOO. This is because of a trade off solution that was reached in MOO for the objectives related to the undamaged and the damaged beams, whereas SOO tries to minimize each of the objectives separately. More information is essentially available to the optimization algorithm in the multi-objective case as it considers both the models consecutively.

For assessment of damage severity, the updated damaged model 1 is compared with the updated damaged model 2 for both single objective and multi-objective model updating results. The damage severity is estimated by subtracting the updated stiffness ratios of the damaged model 1 and damaged model 2 obtained for different elements. The actual damage index has been calculated as 0.9 for element No. 6 in this study for damage model 1 (as evident from Figure 6.1), which indicates a reduction of MOI of element No. 6 from factor of 1 to a factor of 0.9. Also the actual damage index has been calculated as 0.85 for element No. 6 in this study for damage model 2 and 0.9 for element No. 3. As the damage location was unknown, the damage severity index was calculated for all of the elements and is shown in Figure 6.4.

From the results, it can be seen in all the cases that the damage estimation from MOO is relatively more accurate than from SOO. The damage index for element No. 6 (actual damage index = 0.9) was found to be 0.92 and 0.91 for the single and multi-objective cases, respectively, for damage case 1. For damage case 2, the damage index for element No. 6

(actual damage index = 0.85) was found to be 0.85 and 0.87 for the single and multi-objective cases, respectively. Likewise, the damage index for the element No.3 (actual damage index = 0.9) is found to be 0.84 and 0.89 for the single and multi-objective case, respectively. Generally speaking, SOO overestimated the damage severity to a higher degree than MOO. The SM was also applied to the problem and similar results to that of SOO were obtained.

However, it has been noticed that both the SOO and MOO has wrongly detected damage in other elements too. This leads to the fact that either only those parameters should be selected that have uncertainties in their correct estimation and which have strong influence on the modal data. In the earlier studies carried out (Chapter 4 and 5) in this thesis, this technique has been applied. However in this case of damaged beam, stiffnesses of all the elements have to be found so a suitable technique needs to be explored.

A sensitivity analysis of all the elements was performed. It has been revealed that elements closer to the supports have very low sensitivities. Such elements cause ill-conditioning of the problem and a small change in the value results in a large change in the modal data. Also elements at equal distance from the centre of the beam have equal sensitivities e.g. element No. 5 and 6 influence the modal data in a similar manner. Such elements can also lead to similar modal values. Furthermore, due to the discretization error and the experimental error assumed in the initial model, the situation is further complicated and has led to erroneous detection of damage in other elements of the beam close to the damaged elements. To mitigate the above mentioned influences, a suitable regularization technique needs to be exploited for this problem.

## 6.5 Model updating of a simulated simply supported beam using regularization

Regularization techniques in the context of model updating have been applied by various researchers using the SM as explained in Chapter 2. However, in the context of this thesis, a regularization technique was applied using GOA. The regularization expressions usually concern the parameter variations during iterations. Most frequently used conditions are: 1) parameter values will be small, 2) parameter changes with respect to a reference model will be small and 3) parameter steps between subsequent model updating iterations will be small (Titurus and Friswell 2008). In this work, the second condition which mainly concerns the physical assumption of the initial model is used. In order to give preference to a particular solution, the regularization term is included in the minimization as

$$\prod_{\text{damaged.reg}} = \prod_{\text{damaged 1}} + \tau \|x - x_o\|^2 \qquad \textbf{6.6}$$

where x refers to the parameter values in the current iteration and $x_0$ refer to the initial parameter values. $\tau$ is the regularization parameter. For a small regularization parameter, the updated parameters are almost unrestricted and the solution resembles the original ill posed problem. For a large regularization parameter, the updating parameters remain limited in size and may have larger errors in the fitting of the data.

A L curve has been utilized in this study to find out optimal regularization parameter. A typical L curve for damaged beam 1 is shown in Figure 6.5. It has been found that a value of $1.5 \times 10^{-7}$ gives a suitable trade off between the two axes. Likewise a regularization parameter of $0.8 \times 10^{-7}$ has been selected for damaged case 2 based on its corresponding L curve.

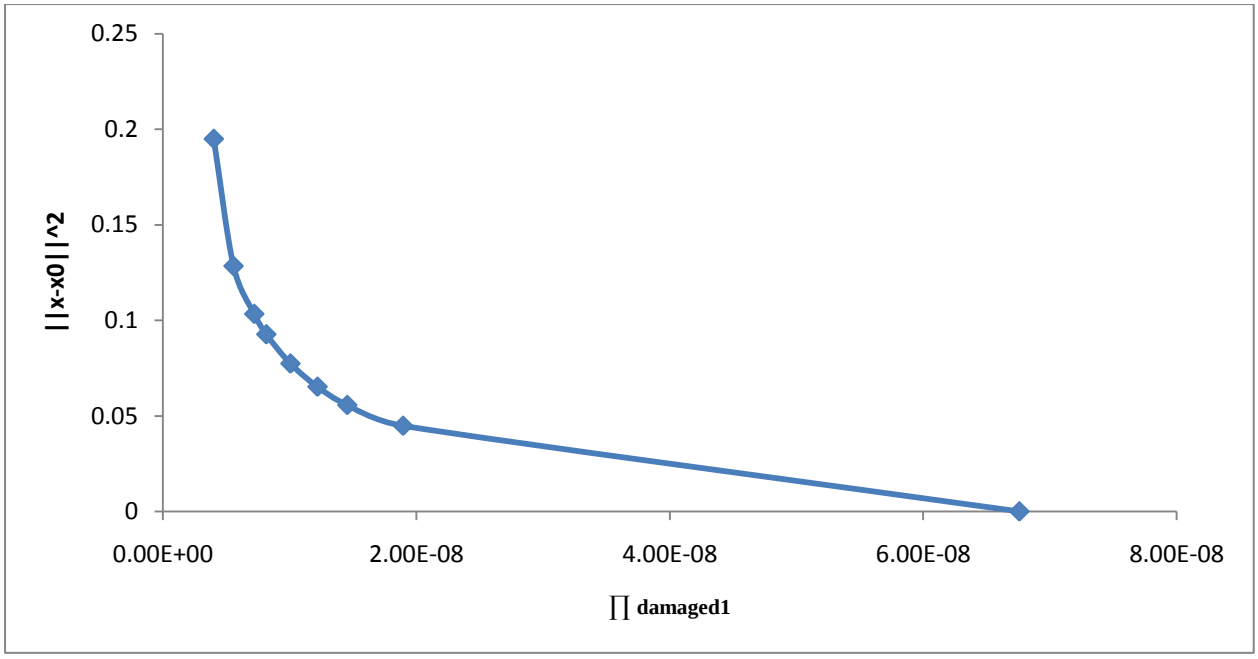


**Figure 6.5 L curve for damaged beam 1**

PSO was applied using Equation 6.6 for the damage case 1. Likewise, Equation 6.6 was modified for the damage case 2 accordingly. Figure 6.6 shows the mean errors in the stiffness ratio of the updated damaged model 1 and damaged model 2 to the true values of stiffness for 3% of added noise.

For damaged beam 1, the maximum mean error for regularised model updating was found to be 0.033 and for damaged beam 2, the maximum mean error was found to be 0.021. It can be noted from the errors in the updated stiffness ratios from Figure 6.6 that regularised model updating has shown promising results.

A similar technique as used earlier for SOO and MOO was used for assessment of the damage severity, where the updated damaged model 1 is subtracted from the updated damaged model 2. The damage severity index was calculated for all of the elements and is shown in Figure 6.7.

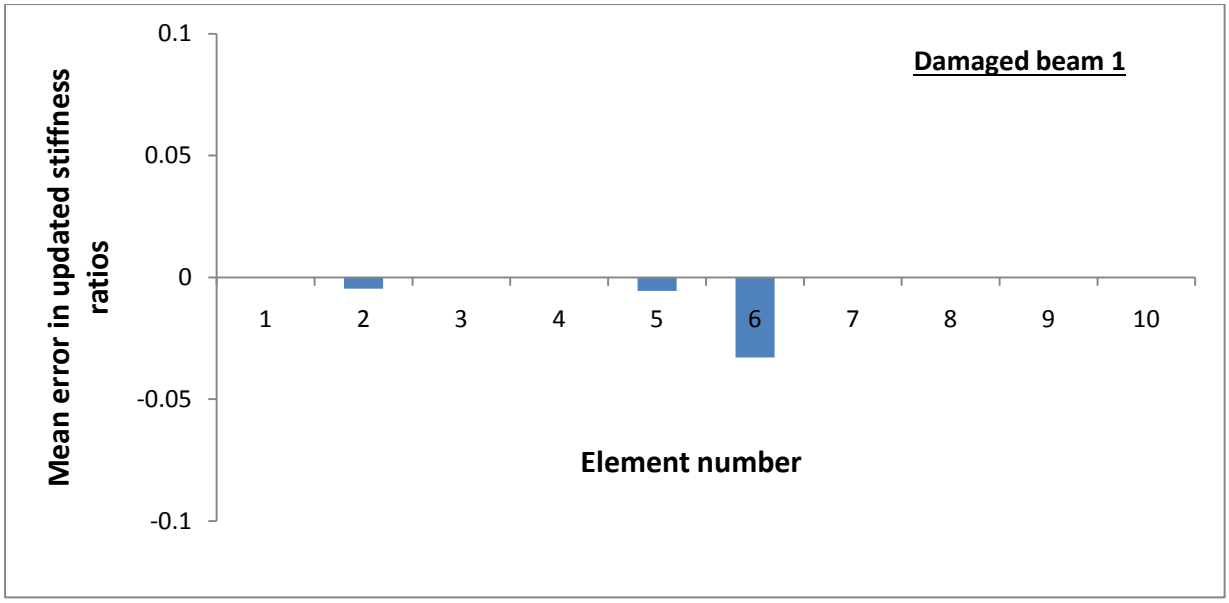


(a)

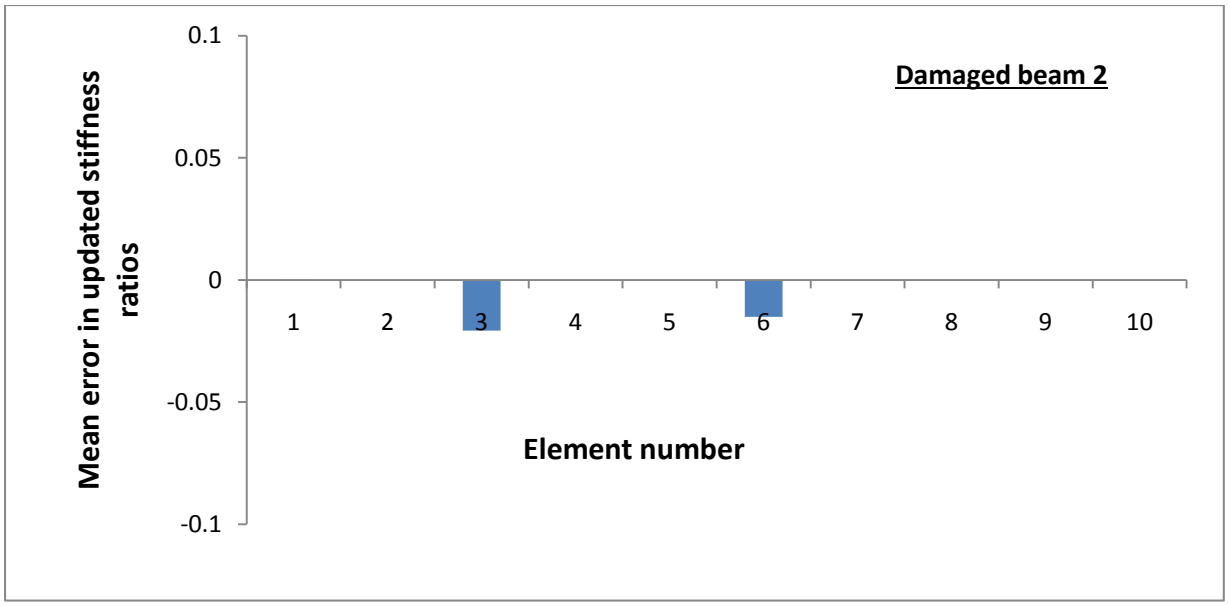


(b)

**Figure 6.6 Results of model updating with 3% noise level for regularised case (a) Error in updated stiffness ratios in damaged beam 1 (b) Error in updated stiffness ratios in damaged beam 2**

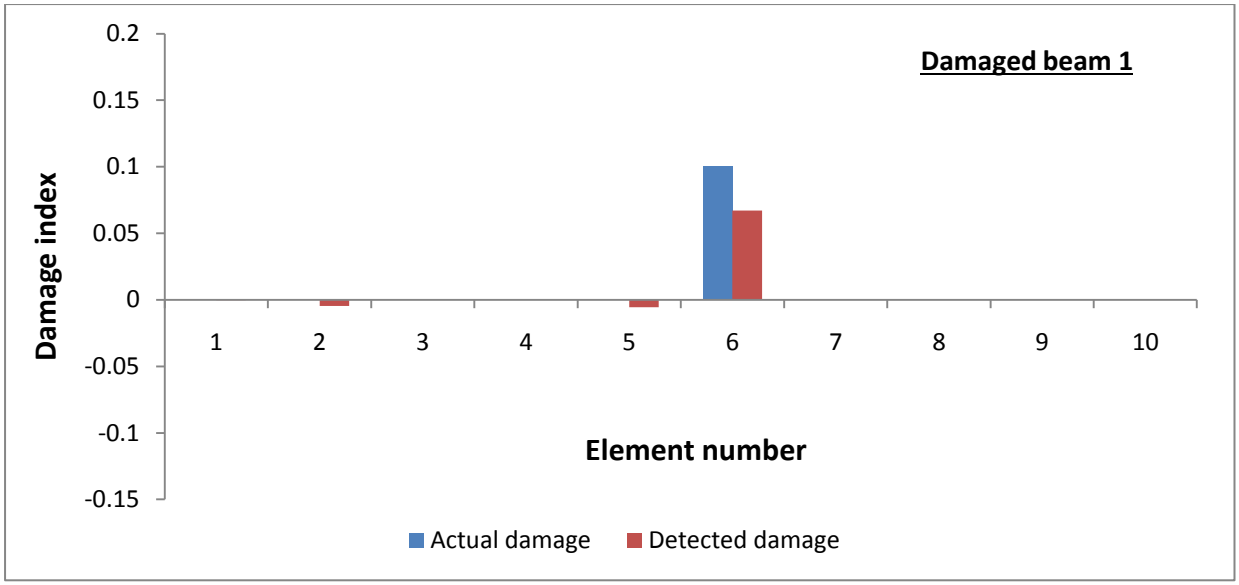


(a)

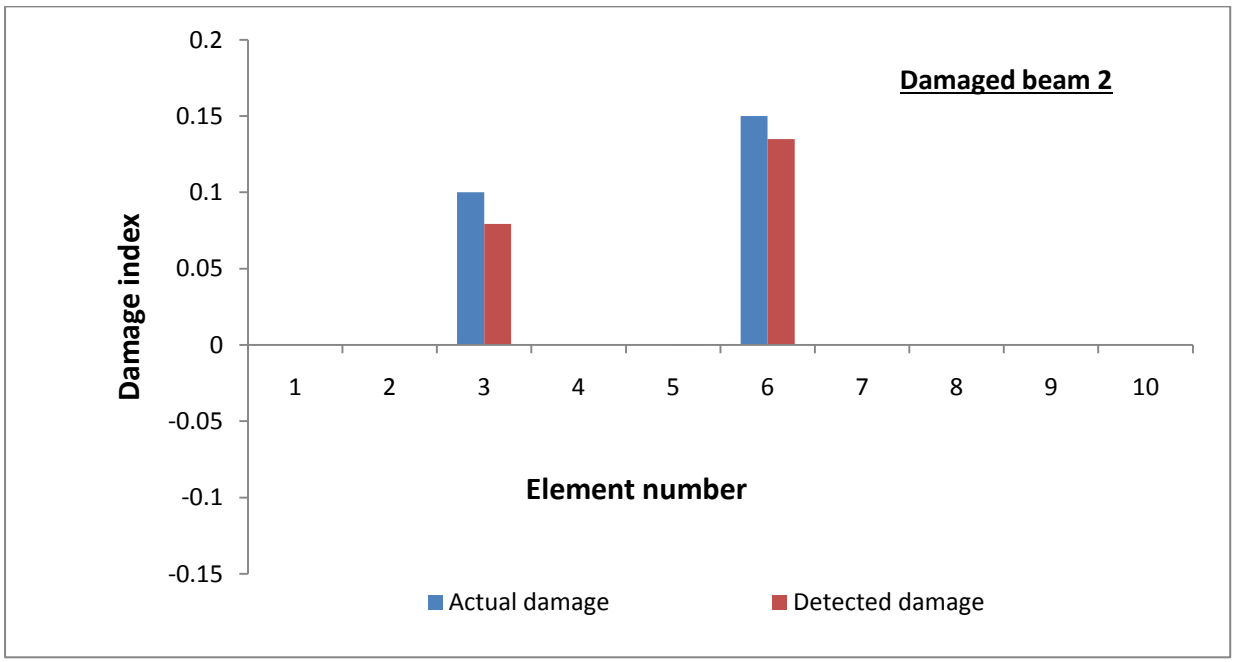


(b)

**Figure 6.7 Damage estimation for regularised case (a) for damaged beam 1 (b) for damaged beam 2**

From the results, it can be seen in all the cases that damage estimation from the regularization technique is more accurate than from SOO and MOO. The damage index for element No. 6 (actual damage index = 0.9) was found to be 0.93 for damage case 1. For damage case 2, damage index for the element No. 6 (actual damage index = 0.85) was found to be 0.86 and damage index for the element No. 3 (actual damage index = 0.9) was found to be 0.92. It was also found from Figure 6.7 that the regularised updating has good detection of damaged and undamaged elements when compared to SOO and MOO.

This proves that the proposed approach is more efficient in updating than both SOO and MOO. The regularization has improved the conditioning of the problem and thus leads to physically justifiable solutions. However, this regularization has assumed that the initial estimate of the model i.e. $x^0$ be considered as a good representative of the actual structure. This assumption may not be valid in all the cases as explained in Chapter 2 where a priori model realization may be significantly different from actual physical structure. A linear baseline model was adopted for model updating considering measured experimental frequencies and mode shapes. The initial linear SA model stays the same during the process of updating. In the case of high damage, the initial SA model will not be a true representation of the actual system and may result in a meaningless updated model.

In this research, natural frequencies and mode shapes extracted from vibrations of a structure are used for calibration of analytical models. Non-linearity in the actual structure would render it impracticable to extract natural frequencies and mode shapes. Therefore, the methods considered in this research will be applicable to low damaged structures up to the onset of non-linearity (Worden et al. 2008) as stated in the scope of this research.

## 6.6 Summary

This chapter presents a damage estimation method which simultaneously updates the undamaged as well as damaged structure model in a MOO process. The following is the summary and conclusions of this study:

1. Damage estimation via structural modal updating typically requires an updated baseline model of the undamaged structure. The associated errors may propagate when this baseline model is subsequently used for damage estimation. The use of multi-objective updating partly addresses these issues.
2. A simply supported beam has been used as an example problem and a noise level of 3% has been added to the identified mode shapes to assess the performance of the proposed procedure in accurate estimation of the damage. It has been found that the proposed method using MOO has been proved to be slightly better in updating both undamaged and damaged models than SOO.
3. Due to wrong detection of damage from both MOO and SOO, a simple regularization technique has been proposed using PSO. Improved results have been obtained when compared to both SOO and MOO. It was found that the proposed method is more efficient in accurately estimating damage severity and is less sensitive to experimental errors.

# Chapter 7. CONCLUSIONS AND RECOMMENDATIONS

## 7.1 Introduction

In this thesis, different GOAs have been applied to dynamic model updating problem to estimate the physical characteristics of built structures. This chapter summarises the conclusions of this work, and gives suggestions and recommendations for future research.

## 7.2 Conclusions

The following conclusions can be drawn from this research:

1. A laboratory structure is tested to find its dynamic response and three different GOAs namely PSO, GA and SiA have been applied for model updating. The results were compared in terms of accuracy and computational efficiency of the updated model. It was found that PSO has given the least error between the experimental and analytical frequencies, followed by GA and SiA. PSO also had the lowest standard deviation in the updated parameter values. A good agreement was found between the experimental and analytical results from PSO. The updated results obtained by GA and PSO match closely whereas SiA results differ from the other two. Also, PSO was found to be

computationally more efficient than GA and SiA because of the use of particle velocity, which makes PSO closer to the gradient-based methods. These attributes make it a more suitable candidate for its combination with other techniques. Important conclusions were drawn from the updated results. It was found that joints of the structure are mainly responsible for the reduction in the stiffness of the whole structure.

2- A systematic model updating study of a full scale cable stayed pedestrian bridge was carried out to check the effectiveness of the PSO and SM for model updating of full scale structures. PSO have proven to be effective in obtaining the least error between the experimental and analytical values of modal parameters. Important conclusions relating to the performance of the bridge were drawn from the updated results. The results indicate that the slab is not fully connected to the steel girder and the tensions in some cables are more than assumed in design. A technique combining SNT with PSO, which tried to systematically search the domain, was applied to solve this problem to give the user more certainty. SNT with PSO has successfully detected the minimum. The results show that the methodology proposed herein gave more information about the search space rather than applying blind independent runs and gave the user more confidence on the updating results.

3- A damage estimation method which simultaneously updates the undamaged as well as damaged structure model in a MOO process is investigated. Damage detection through model updating typically requires an updated baseline model of the undamaged structure and the associated errors may propagate when this baseline model is subsequently used for damage detection. The use of multi-objective updating alleviates these issues. A simply supported beam has been used as a numerical example and 3 % noise levels have been added to the identified mode shapes to assess the performance of the proposed procedure for an accurate estimation of damage. It has been found that the proposed

multi-objective method has been slightly better in concurrently updating both the undamaged and damaged models. A simple regularization technique using GOA is proposed and is found to be more accurate is damage estimation.

## 7.3 Recommendations for future research

The research work in this thesis revealed that the following are the recommended areas for further research:

1. Three GOAs have been investigated in this research on the dynamic model updating problem. Different variants of these algorithms can be explored by combining them together. Exploring other GOAs for this problem is also suggested.
2. The SNT technique enables finding different solutions in the search domain. A clustering technique can be applied on these solutions obtained by SNT to cluster physically similar and non-similar solutions. This can enable the user to select the best set of updating parameters for the inverse model updating problem.
3. The scope of this research is limited to low level damage. More research is suggested on non-linear model updating of damaged systems at different damage states where normal modes of vibrations no longer exist.
4. More work is suggested in effective error localization schemes which can guide the process of selecting susceptible regions, thus reducing the number of updating parameters effectively in the multi-objective model updating technique proposed in this research. Also, experimental validation of the multi-objective model updating would be useful at laboratory and possibly at full scale structure level. Moreover, the regularization techniques using GOAs can also be further explored.
5. The SA model updating is an inverse problem which is used to identify the physical properties of the built structure. The same concept can be used for other parameter

estimations such as wind pressure on structures. As a result, when the load acting on the structure is known, the stresses can be readily calculated.

6. Use of static measurements for SA model updating can also be explored for full scale structures. The local nature of these measurements can improve the SA model updating results. The effect of using objective functions related to, measured strain as compared to frequency and mode shapes, for example, can be investigated.
7. Most of the current literature addresses the model updating problem for linear systems with low excitation forces. However, the non-linear nature of the full scale structures can pose challenges in development of correct analytical models. Investigation of non-linear model updating should be attempted in future work.

# REFERENCES


Abdel-Ghaffar, A. M. and Khalifa, M. A. **(1991)**. Importance of cable vibration in dynamics of cable-stayed bridges. Journal of Engineering Mechanics, ASCE. 117(11): 2571-2589.

Abdel-Kader, R. F. **(2010)**. Genetically improved PSO algorithm for efficient data clustering. Machine Learning and Computing (ICMLC), Second International Conference, Banglore.

Abdel Wahab, M. and De Roeck, G. **(1999)**. Damage detection in bridges using modal curvatures: application to a real damage scenario. Journal of Sound and Vibration. 226(2): 217-235.

Abdul-Halim, M. F. and Abdul-Kader, A. F. **(2006)**. A new recombination scheme for diploid genetic algorithms. Computer Systems and Applications, IEEE International Conference, 274-280.

Ahmadian, H., Mottershead, J. E. and Friswell, M. I. **(1998)**. Regularization methods for finite element model updating. Mechanical Systems and Signal Processing. 12(1): 47-64.

Aktan, A. E., Catbas, F. N., Grimmelsman, K. A. and Tsikos, C. J. **(2000)**. Issues in infrastructure health monitoring for management. Journal of Engineering Mechanics, ASCE. 126(7): 711-724.

Aktan, A. E., Ellingwood, B. R. and Kehoe, B. **(2007)**. Performance-based engineering of constructed systems. Journal of Structural Engineering, ASCE. 133(3): 311-323.

Aktan, A. E., Farhey, D. N., Helmicki, A. J., Brown, D. L., Hunt, V. J., Lee, K.-L. and Levi, A. **(1997)**. Structural identification for condition assessment: experimental arts. Journal of Structural Engineering. 123(12): 1674-1684.

Aktan, A. E., Helmicki, A. J. and Hunt, V. J. **(1998)**. Issues in health monitoring for intelligent infrastructure. Smart Materials and Structures. 7(5): 674-692.

Alampalli, S. **(1998)**. Influence of in-service environment on modal parameters. Proceedings-SPIE the international society for optical engineering.

Allemang, R. J. and Brown, D. L. **(1982)**. A correlation for modal vector analysis. Proceedings of IMAC I : 1st International Modal Analysis Conference.

Alvin, K. F. and Park, K. C. **(1994)**. Second-order structural identification procedure via state-space-based system identification. AIAA Journal. 32(2): 397-406.

ANSYS **(1999)**. User's Manual, Revision 5.6, Swanson Analysis System, USA.

APSDynamics **(2012)**. Dynamic ElectroSeis shaker Model 400. http://www.apsdynamics.com/

Araki, Y. and Miyagi, Y. **(2005)**. Mixed integer nonlinear least-squares problem for damage detection in truss structures. Journal of Engineering Mechanics. 131(7): 659-667.

AS/NZS **(1996)**. AS/NZS 3679 Part-1 Structural steel hot rolled bars and sections, Jointly published by Standards Australia, Sydney and Standards New Zealand, Wellington.

Auweraer, H. V. d. and Peeters, B. **(2003)**. Sensors and systems for structural health monitoring. Journal of Structural Control. 10(2): 117-125.

Baker, T. and Marsh, E. **(1996)**. Error localization for machine tool structures. Proceedings-SPIE the international society for optical engineering.

Bakir, P. G., Reynders, E. and Roeck, G. D. **(2008)**. An improved finite element model updating method by the global optimization technique 'Coupled Local Minimizers'. Computers & Structures. 86(11): 1339-1352.

Baruch, M. **(1997)**. Modal data are insufficient for identification of both mass and stiffness matrices. AIAA Journal. 35(11): 1797-1798.

Beasley, D., Bull, D. R. and Martin, R. R. **(1993)**. A sequential niche technique for multimodal function optimization. Evolutionary Computation. 1(2): 101-125.

Beck, J. L. and Jennings, P. C. **(1980)**. Structural identification using linear models and earthquake records. Earthquake Engineering and Structural Dynamics. 8(2): 145-160.

Begambre, O. and Laier, J. E. **(2009)**. A hybrid Particle Swarm Optimization - Simplex algorithm (PSOS) for structural damage identification. Advances in Engineering Software. 40(9): 883-891.

Black, C. and Ventura, C. **(1999)**. Analytical and experimental study of a three span bridge in Alberta, Canada. Society for Experimental Mechanics, Inc, 17 th International Modal Analysis Conference.

Bodeux, J. B. and Golinval, J. C. **(2001)**. Application of ARMAV models to the identification and damage detection of mechanical and civil engineering structures. Smart Materials and Structures. 10: 479-489.

Brownjohn, J., Dumanoglu, A., Severn, R. and Blakeborough, A. **(1989)**. Ambient vibration survey of the Bosporus suspension bridge. Earthquake engineering & structural dynamics. 18(2): 263-283.

Brownjohn, J. M. W., Moyo, P., Omenzetter, P. and Lu, Y. **(2003)**. Assessment of highway bridge upgrading by dynamic testing and finite-element model updating. Journal of Bridge Engineering. 8(3): 162-172.

Brownjohn, J. M. W. and Xia, P. Q. **(2000)**. Dynamic assessment of curved cable-stayed bridge by model updating. Journal of Structural Engineering, ASCE. 126(2): 252-260.

Brownjohn, J. M. W., Xia, P. Q., Hao, H. and Xia, Y. **(2001)**. Civil structure condition assessment by FE model updating : methodology and case studies. Finite Elements in Analysis and Design. 37(10): 761-775.

Caicedo, J. M. and Yun, G. **(2011)**. A novel evolutionary algorithm for identifying multiple alternative solutions in model updating. Structural Health Monitoring. 10(5): 491-501.

Catbas, F., Lenett, M., Aktan, A., Brown, D., Helmicki, A. and Hunt, V. **(1998)**. Damage detection and condition assessment of Seymour bridge. Proceedings- SPIE the international society for optical engineering.

Catbas, F. N. and Aktan, A. E. **(2002)**. Condition and damage assessment: Issues and some promising indices. Journal of Structural Engineering, ASCE. 128(8): 1026-1036.

Catbas, F. N., Ciloglu, S. K., Hasancebi, O., Grimmelsman, K. and Aktan, A. E. **(2007)**. Limitations in structural identification of large constructed structures. Journal of Structural Engineering, ASCE. 133(8): 1051-1066.

Causevic, M. S. **(1987)**. Mathematical modelling and full-scale forced vibration testing of a reinforced concrete structure. Engineering Structures. 9(1): 2-8.

Center, J. S., Ricles, J. M. and Hamilton, D. A. **(1991)**. NONDESTRUCTIVE STRUCTURAL DAMAGE DETECTION IN FLEXIBLE SPACE STRUCTURES USING VIBRATION CHARACTERIZATION. William A. Hyman and Stanley H. Goldstein, Editors.

Chan, R. R. and Sudhoff, S. D. **(2010)**. An evolutionary computing approach to robust design in the presence of uncertainties. IEEE Transactions on Evolutionary Computation. 14(6): 900-912.

Chang, C. C., Chang, T. Y. P. and Zhang, Q. W. **(2001)**. Ambient vibration of long-span cable-stayed bridge. Journal of Bridge Engineering, ASCE. 6(1): 46-53.

Chen, G. **(2001)**. FE model validation for structural dynamics, University of London.

Chen, G. and Ewins, D. **(2004)**. FE model verification for structural dynamics with vector projection. Mechanical Systems and Signal Processing. 18(4): 739-757.

Chen, X. and Zhou, N. **(2007)**. Equivalent static wind loads on low-rise buildings based on full-scale pressure measurements. Engineering Structures. 29(10): 2563-2575.

Chopra, A. K. **(2007)**. Dynamics of structures : theory and applications to earthquake engineering, Prentice Hall,Upper Saddle River, NJ.

Clarence, W. D. S. and De Silva, C. W. **(2007)**. Vibration : fundamentals and practice, CRC/Taylor & Francis Boca Raton.

Clerc, M. and Kennedy, J. **(2002)**. The particle swarm - explosion, stability, and convergence in a multidimensional complex space. IEEE Transactions on Evolutionary Computation. 6(1): 58-73.

Clough, R. W. and Wilson, E. L. **(1999)**. Early finite element research at Berkeley. Proc. 5th US National Conf. Comp. Mech,, Boulder, CO.

Coello, C. A. C. and Lamont, G. B. **(2004)**. Applications of multi-objective evolutionary algorithms, World Scientific, Singapore.

CSI-Analysis-Reference-Manual **(2013)**. Computers and Structures, "Structural Analysis Program SAP-2000." CA.

De Lautour, O. R. **(2009)**. Assessment of seismic damage to civil structures using statistical pattern recognition techniques and time series analysis, PhD Thesis, The University of Auckland, New Zealand.

De Sortis, A., Antonacci, E. and Vestroni, F. **(2005)**. Dynamic identification of a masonry building using forced vibration tests. Engineering Structures. 27(2): 155-165.

Deb, K. **(1989)**. Genetic algorithms in multimodal function optimization, M.S. Thesis, The University of Alabama,Tuscaloosa, AL.

Deb, K. **(1998)**. Optimization for engineering design : algorithms and examples, Prentice-Hall of India, New Delhi.

Deb, K. **(2004)**. Multi-Objective Optimization using Evolutionary Algorithms, John Wiley & sons, Ltd.

Deb, K., Pratap, A., Agarwal, S. and Meyarivan, T. **(2002)**. A fast and elitist multiobjective genetic algorithm: NSGA-II. IEEE Transactions on Evolutionary Computation. 6(2): 182-197.

Dowsland, K. A. **(1993)**. Simulated annealing. Modern heuristic techniques for combinatorial problems, John Wiley & Sons, Inc.

Ecke, W., Peters, K. J. and Meyendorf, N. G. **(2008)**. Smart sensor phenomena, technology, networks, and systems, SPIE Bellingham

Ellis, B. R. **(1996)**. Full-scale measurements of the dynamic characteristics of buildings in the UK. Journal of Wind Engineering and Industrial Aerodynamics. 59(2-3): 365-382.

Ernst, H. and Der, E. **(1965)**. Der e-modul von seilen unter beruecksichtigung des durchhanges. Der Bauingenieur. 40(2): 52-55 (In German).

Ewins, D. J. **(2000)**. Modal testing : theory, practice, and application, Research Studies Press, Baldock, Hertfordshire, England.

Farrar, C. R., Cornwell, P. J., Doebling, S. W. and Prime, M. B. **(2000)**. Structural health monitoring studies of the Alamosa Canyon and I-40 bridges, Los Alamos National Lab., NM (US).

Farrar, C. R., Doebling, S. W., Cornwell, P. J. and Straser, E. G. **(1997)**. Variability of modal parameters measured on the Alamosa Canyon Bridge. Proceedings- SPIE the international society for optical engineering.

FEMtools **(2004)**. Theoretical Manual, Version 3.0.03, Dynamic Design Solutions, Leuven, Belgium.

Friswell, M. I. and Mottershead, J. E. **(1995)**. Finite element model updating in structural dynamics, Kluwer Academic Publishers, Netherlands.

Fujino, Y. and Abe, M. **(2002)**. Structural health monitoring in civil infrastructures and research on SHM of bridges at the University of Tokyo. Proceedings of the Third World Conference on Structural Control.

Gent, A. N. **(2012)**. Engineering with rubber - how to design rubber components (3rd Edition), Munich, Cincinnati, Hanser Publishers.

Geoffrey Chase, J., Leo Hwang, K., Barroso, L. and Mander, J. **(2005)**. A simple LMS- based approach to the structural health monitoring benchmark problem. Earthquake engineering & structural dynamics. 34(6): 575-594.

Gladwell, G. M. L. and Morassi, A. **(2011)**. Dynamical inverse problems : theory and application, Springer, Wien, New York.

Gola, M., Soma, A. and Botto, D. **(2001)**. On theoretical limits of dynamic model updating using a sensitivity-based approach. Journal of Sound and Vibration. 244(4): 583-595.

Goldberg, D. E., Deb, K. and Horn, J. **(1992)**. Massive multimodality, deception, and genetic algorithms. Parallel Problem Solving from Nature. 2(2): 37-46.

Grimmelsman, K. A. and Aktan, A. E. **(2005)**. Impacts and mitigation of uncertainty for improving the reliability of field measurements. 2nd international conference on structural health monitoring of intelligent infrastructure, Shenzhen.

Grimmelsman, K. A., Pan, Q. and Aktan, A. E. **(2007)**. Analysis of data quality for ambient vibration testing of the Henry Hudson bridge. Journal of Intelligent Material Systems and Structures. 18(8): 765-775.

He, R.-S. and Hwang, S.-F. **(2006)**. Damage detection by an adaptive real-parameter simulated annealing genetic algorithm. Computers & Structures. 84(31–32): 2231-2243.

Hester, D. and González, A. **(2012)**. A wavelet-based damage detection algorithm based on bridge acceleration response to a vehicle. Mechanical Systems and Signal Processing. 28(0): 145-166.

Hjelmstad, K. and Shin, S. **(1996)**. Crack identification in a cantilever beam from modal response. Journal of Sound and Vibration. 198(5): 527-545.

Holland, J. **(1975)**. Adaptation in natural and artificial systems, MIT Press, Cambridge, Mass.

Horst, R., Pardalos, P. M. and Thoai, N. V. **(2000)**. Introduction to global optimization, Springer, Netherlands.

Hu, N., Wang, X., Fukunaga, H., Yao, Z. H., Zhang, H. X. and Wu, Z. S. **(2001)**. Damage assessment of structures using modal test data. International Journal of Solids and Structures. 38(18): 3111-3126.

Hua, X. G., Ni, Y. Q. and Ko, J. M. **(2009)**. Adaptive regularization parameter optimization in output-error-based finite element model updating. Mechanical Systems and Signal Processing. 23(3): 563-579.

Huh, Y. C., Chung, T. Y., Moon, S. J., Kil, H. G. and Kim, J. K. **(2011)**. Damage detection in beams using vibratory power estimated from the measured accelerations. Journal of Sound and Vibration. 330(15): 3645-3665.

Ivanovic, S. S., Trifunac, M. D., Novikova, E. I., Gladkov, A. A. and Todorovska, M. I. **(2000)**. Ambient vibration tests of a seven-story reinforced concrete building in Van Nuys, California, damaged by the 1994 Northridge earthquake. Soil Dynamics and Earthquake Engineering. 19(6): 391-411.

Jaishi, B. and Ren, W. X. **(2005)**. Structural finite element model updating using ambient vibration test results. Journal of Structural Engineering, ASCE. 131(4): 617-628.

Jaishi, B. and Ren, W. X. **(2007)**. Finite element model updating based on eigenvalue and strain energy residuals using multiobjective optimisation technique. Mechanical Systems and Signal Processing. 21(5): 2295-2317.

Jang, J., Liu, J. F., Yue, C. P. and Sohn, H. **(2006)**. Development of self-contained sensor skin for highway bridge monitoring. Proceedings- SPIE the international society for optical engineering.

JE, M. and MI, F. **(1998)**. Regularisation methods for finite element model updating. Mechanical Systems and Signal Processing. 12(1): 47-64.

Kahraman, C., Birgün, S. and Yenen, V. Z. **(2008)**. Fuzzy multi-attribute scoring methods with applications, Springer Kahraman, Cengiz.

Kalyanmoy, D. **(2001)**. Multi-objective optimization using evolutionary algorithms, John Wiley & Sons, New York.

Kalyanmoy, D. and Deb, K. **(1998)**. Optimization for engineering design : algorithms and examples, New Delhi :Prentice-Hall of India.

Kalyanmoy, D. and Deb, K. **(2001)**. Multi-objective optimization using evolutionary algorithms, John Wiley & Sons, Chichester, New York

Kalyanmoy, D. and Deb, K. **(2007)**. Advances in computational optimization and its applications, Universities Press, New Delhi, India.

Kennedy, J. and Eberhart, R. **(1995)**. Particle swarm optimization. IEEE International Conference on Neural Networks.

Kirkpatrick, S. **(1984)**. Optimization by simulated annealing: Quantitative studies. Journal of Statistical Physics. 34(5): 975-986.

Knowles, J., Corne, D. and Deb, K. **(2008)**. Multiobjective problem solving from nature: from concepts to applications, Springer-Verlag, New York.

Konstantinos, E. P. and Vrahatis, M. N. **(2010)**. Particle swarm optimization and intelligence : advances and applications, Information Science Reference, Hershey, PA.

Koppen, M. and Yoshida, K. **(2007)**. Substitute distance assignments in NSGA-II for handling many-objective optimization problems. Artificial Intelligence and Computer Science, Lecture Notes in Computer Science. 4403 LNCS: 727-741.

Lee, H. S., Park, C. J. and Park, H. W. **(2000)**. Identification of geometric shapes and material properties of inclusions in two-dimensional finite bodies by boundary

parameterization. Computer Methods in Applied Mechanics and Engineering. 181(1): 1-20.

Levin, R. I. and Lieven, N. A. J. **(1998)**. Dynamic finite element model updating using simulated annealing and genetic algorithms. Mechanical Systems and Signal Processing. 12(1): 91-120.

Li, H. and Zhang, Q. **(2009)**. Multiobjective optimization problems with complicated pareto sets, MOEA/ D and NSGA-II. IEEE Transactions on Evolutionary Computation. 13(2): 284-302.

Li, H. L., Deng, X. and Dai, H. **(2007)**. Structural damage detection using the combination method of EMD and wavelet analysis. Mechanical Systems and Signal Processing. 21(1): 298-306.

Li, Q. S., Wu, J. R., Liang, S. G., Xiao, Y. Q. and Wong, C. K. **(2004)**. Full-scale measurements and numerical evaluation of wind-induced vibration of a 63-story reinforced concrete tall building. Engineering Structures. 26(12): 1779-1794.

Li, S. and Brown, D. L. **(1995)**. Application of a unified matrix polynomial approach (UMPA) to perturbed boundary condition (PBC) testing. Mechanical Systems and Signal Processing. 9(1): 77-84.

Lieven, N. A. J. and Ewins, D. J. **(1988)**. Spatial correlation of mode shapes, the Coordinate Modal Assurance Criterion (COMAC). Proceedings of IMAC VI: 6th International. Modal Analysis Conference, 690-695.

Lin, J. W., Betti, R., Smyth, A. W. and Longman, R. W. **(2001)**. On- line identification of non- linear hysteretic structural systems using a variable trace approach. Earthquake engineering & structural dynamics. 30(9): 1279-1303.

Link, M. **(1991)**. Comparison of procedures for localizing and correcting errors in computational models using test data. Proc. Of IMAC.

Link, M. and Conic, M. **(2000)**. Combining adaptive FE mesh refinement and model parameter updating. Proceedings of the 18th International Modal Analysis Conference.

Ljung, L. **(1987)**. System identification : theory for the user, Englewood Cliffs, NJ.

Luco, J., Trifunac, M. and Wong, H. **(1988)**. Isolation of soil- structure interaction effects by full-scale forced vibration tests. Earthquake engineering & structural dynamics. 16(1): 1-21.

Lundy, M. and Mees, A. **(1986)**. Convergence of an annealing algorithm. Mathematical programming. 34(1): 111-124.

Maia, N. M., Reynier, M., Ladeveze, P. and Cachan, E. **(1994)**. Error localization for updating finite element models using frequency-response-functions. Proceedings-SPIE the international society for optical engineering.

Marwala, T. **(2010)**. Finite element model updating using computional intelligence techniques, Springer-Verlag, London.

MathWorks **(2007)**. Matlab. The MathWorks, Natick, MA.

Metropolis, N., Rosenbluth, A. W., Rosenbluth, M. N., Teller, A. H. and Teller, E. **(1953)**. Equation of state calculations by fast computing machines. The Journal of Chemical Physics. 21: 1087.

Möller, P. W. and Friberg, O. **(1998)**. Updating large finite element models in structural dynamics. AIAA Journal. 36(10): 1861-1868.

Moon, F. L. and Aktan, A. E. **(2006)**. Impacts of epistemic (bias) uncertainty on structural identification of constructed (civil) systems. Shock and Vibration Digest. 38(5): 399-420.

Mottershead, J., Friswell, M. and Zhang, Y. **(1995)**. On discretisation error estimates for finite element model updating. Proceedings- SPIE the international society for optical engineering. 2460: 1289.

Mottershead, J. E. and Foster, C. D. **(1991)**. On the treatment of ill-conditioning in spatial parameter estimation from measured vibration data. Mechanical Systems and Signal Processing. 5(2): 139-154.

Mottershead, J. E. and Friswell, M. I. **(1993)**. Model updating in structural dynamics : a survey. Journal of Sound and Vibration. 167(2): 347-375.

Mottershead, J. E., Link, M. and Friswell, M. I. **(2011)**. The sensitivity method in finite element model updating: A tutorial. Mechanical Systems and Signal Processing. 25(7): 2275-2296.

Nazmy, A. S. and Abdel-Ghaffar, A. M. **(1990)**. Three-dimensional nonlinear static analysis of cable-stayed bridges. Computers and Structures. 34(2): 257-271.

Niknam, T. and Amiri, B. **(2010)**. An efficient hybrid approach based on PSO, ACO and k-means for cluster analysis. Applied Soft Computing Journal. 10(1): 183-197.

Ohba, R. **(1992)**. Intelligent sensor technology, Wiley Chichester, West Sussex, England ; New York

Okada, H. and Ha, Y.-C. **(1992)**. Comparison of wind tunnel and full-scale pressure measurement tests on the Texas Texh Building. Journal of Wind Engineering and Industrial Aerodynamics. 43(1-3): 1601-1612.

Overschee, P. V. and Moor, B. **(1996)**. Subspace identification for the linear systems : theory–implementation, Kluwer Academic Publishers, Netherlands.

Pan, Q., Grimmelsman, K., Moon, F. and Aktan, E. **(2010)**. Mitigating epistemic uncertainty in structural identification: case study for a long-span steel arch bridge. Journal of Structural Engineering. 137(1): 1-13.

Pavic, A., Miskovic, Z. and Reynolds, P. **(2007)**. Modal testing and finite-element model updating of a lively open-plan composite building floor. Journal of Structural Engineering, ASCE. 133(4): 550-558.

Pedersen, M. E. H. and Chipperfield, A. J. **(2010)**. Simplifying particle swarm optimization. Applied Soft Computing Journal. 10(2): 618-628.

Peeters, B. and De Roeck, G. **(1998)**. Stochastic subspace system identification of a steel transmitter mast. Society for Experimental Mechanics, Inc, 16 th International Modal Analysis Conference.

Perera, R., Fang, S.-E. and Huerta, C. **(2009)**. Structural crack detection without updated baseline model by single and multiobjective optimization. Mechanical Systems and Signal Processing. 23(3): 752-768.

Perera, R., Fang, S. E. and Ruiz, A. **(2010)**. Application of particle swarm optimization and genetic algorithms to multiobjective damage identification inverse problems with modelling errors. Meccanica. 45(5): 723-734.

Perera, R. and Ruiz, A. **(2008)**. A multistage FE updating procedure for damage identification in large-scale structures based on multiobjective evolutionary optimization. Mechanical Systems and Signal Processing. 22(4): 970-991.

Perera, R., Ruiz, A. and Manzano, C. **(2009)**. Performance assessment of multicriteria damage identification genetic algorithms. Computers and Structures. 87(1-2): 120-127.

Perera, R. and Torres, R. **(2006)**. Structural damage detection via modal data with genetic algorithms. Journal of Structural Engineering, ASCE. 132(9): 1491-1501.

Pimentel, R. L., Pavic, A. and Waldron, P. **(2001)**. Evaluation of design requirements for footbridges excited by vertical forces from walking. Canadian Journal of Civil Engineering. 28(5): 769-777.

Pintér, J. **(1996)**. Global optimization in action : continuous and Lipschitz optimization-algorithms, implementations, and applications, Kluwer Academic Publishers, Boston.

Price, K., Storn, R. M. and Lampinen, J. A. **(2005)**. Differential evolution : a practical approach to global optimization, Springer-Verlag, New York.

Proakis, J. G. and Manolakis, D. G. **(1996)**. Digital signal processing : principles, algorithms, and applications, Prentice-Hall, Upper Saddle River, NJ.

Raich, A. M. and Liszkai, T. R. **(2007)**. Improving the performance of structural damage detection methods using advanced genetic algorithms. Journal of Structural Engineering, ASCE. 133(3): 449-461.

Rayward-Smith, V. J., Osman, I. H., Reeves, C. R. and Smith, G. D. **(1996)**. Modern heuristic search methods, Wiley Chichester, Jogn Wiley and Sons.

Ren, W.-X., Blandford, G. E. and Harik, I. E. **(2004)**. Roebling suspension bridge. I: Finite-element model and free vibration response. Journal of Bridge Engineering. 9(2): 110-118.

Ren, W. X. and Peng, X. L. **(2005)**. Baseline finite element modeling of a large span cable-stayed bridge through field ambient vibration tests. Computers and Structures. 83(8-9): 536-550.

Robert Nicoud, Y., Raphael, B., Burdet, O. and Smith, I. **(2005)**. Model identification of bridges using measurement data. Computer-Aided Civil and Infrastructure Engineering. 20(2): 118-131.

Saada, M. M., Arafa, M. H. and Nassef, A. O. **(2008)**. Finite element model updating approach to damage identification in beams using particle swarm optimization. 34th Design Automation Conference, ASME.

Salawu, O. S. and Williams, C. **(1995)**. Review of full-scale dynamic testing of bridge structures. Engineering Structures. 17(2): 113-121.

Sanayei, M., Arya, B., Santini, E. M. and Wadia-Fascetti, S. **(2001)**. Significance of modeling error in structural parameter estimation. Computer- Aided Civil and Infrastructure Engineering. 16(1): 12-27.

Sanayei, M. and Onipede, O. **(1991)**. Damage assessment of structures using static test data. AIAA Journal. 29(7): 1174-1179.

SAP2000 **(2009)**. Structural Analysis Program, Computers and Structures, CA.

Schlune, H., Plos, M. and Gylltoft, K. **(2009)**. Improved bridge evaluation through finite element model updating using static and dynamic measurements. Engineering Structures. 31(7): 1477-1485.

Schnur, D. and Zabaras, N. **(1990)**. Finite element solution of two- dimensional inverse elastic problems using spatial smoothing. International Journal for Numerical Methods in Engineering. 30(1): 57-75.

Shah, A. A., Alsayed, S. H., Abbas, H. and Al-Salloum, Y. A. **(2011)**. Predicting residual strength of non-linear ultrasonically evaluated damaged concrete using artificial neural network. Construction and Building Materials. 29(6): 42-50.

Shah, A. A. and Ribakov, Y. **(2009)**. Non-linear ultrasonic evaluation of damaged concrete based on higher order harmonic generation. Materials and Design. 30(10): 4095-4102.

Singh-Levett, I. **(2006)**. Real-time integral based structural health monitoring, Master's thesis, Mechanical Engineering, University of Canterbury, New Zealand.

Skolnik, D., Lei, Y., Yu, E. and Wallace, J. W. **(2006)**. Identification, model updating, and response prediction of an instrumented 15-story steel-frame building. Earthquake Spectra. 22(3): 781-802.

Srinivas, M. and Patnaik, L. M. **(1994)**. Adaptive probabilities of crossover and mutation in genetic algorithms. IEEE Transactions on Systems, Man and Cybernetics. 24(4): 656-667.

Stoica, P. and Moses, R. L. **(1997)**. Introduction to spectral analysis, Upper Saddle River, N.J. : Prentice Hall, c1997.

Storn, R. and Price, K. **(1997)**. Differential evolution - a simple and efficient heuristic for global optimization over continuous spaces. Journal of Global Optimization. 11(4): 341-359.

Tebaldi, A., Dos Santos Coelho, L. and Lopes Jr, V. **(2006)**. Detection of damage in intelligent structures using optimization by a particle swarm: Fundamentals and case studies. Controle & Automação Sociedade Brasileira de Automatica. 17(3): 312-330.

Teughels, A., De Roeck, G. and Suykens, J. A. K. **(2003)**. Global optimization by coupled local minimizers and its application to FE model updating. Computers and Structures. 81: 2337-2351.

Tikhonov, A. N. **(1963)**. Regularization of incorrectly posed problems. Soviet Mathematics. 4(1): 1624–1627.

Titurus, B. and Friswell, M. I. **(2008)**. Regularization in model updating. International Journal for Numerical Methods in Engineering. 75(4): 440-478.

Trelea, I. C. **(2003)**. The particle swarm optimization algorithm : convergence analysis and parameter selection. Information Processing Letters. 85(6): 317-325.

Tu, Z. and Lu, Y. **(2008)**. FE model updating using artificial boundary conditions with genetic algorithms. Computers and Structures. 86(7-8): 714-727.

Udwadia, F. E. **(2005)**. Structural identification and damage detection from noisy modal data. Journal of Aerospace Engineering. 18(3): 179-187.

Van Overschee, P. and De Moor, B. **(1994)**. N4SID : subspace algorithms for the identification of combined deterministic-stochastic systems. Automatica. 30(1): 75-93.

Ventura, C. E., Liam Finn, W. D., Lord, J. F. and Fujita, N. **(2003)**. Dynamic characteristics of a base isolated building from ambient vibration measurements and low level earthquake shaking. Soil Dynamics and Earthquake Engineering. 23(4): 313-322.

Wada, B. K. **(1980)**. Correlation of Modal and Test Analysis, Technical Report, Jet Propulsion Laboratory.

Ward, H. and Heylen, W. **(1997)**. Modal analysis theory and testing, Katholieke Universiteit Leuven, Belgium.

Weber, B., Paultre, P. and Proulx, J. **(2007)**. Structural damage detection using nonlinear parameter identification with Tikhonov regularization. Structural Control and Health Monitoring. 14(3): 406-427.

Weber, B., Paultre, P. and Proulx, J. **(2009)**. Consistent regularization of nonlinear model updating for damage identification. Mechanical Systems and Signal Processing. 23(6): 1965-1985.

Wenzel, H. **(2005)**. Ambient vibration monitoring / Helmut Wenzel, Dieter Pichler, Chichester, England : John Wiley, 2005.

Wilson, J. C. and Liu, T. **(1991)**. Ambient vibration measurements on a cable- stayed bridge. Earthquake engineering & structural dynamics. 20(8): 723-747.

Wilson, J. S. **(2005)**. Sensor technology handbook, Elsevier Amsterdam ; Boston.

Wolpert, D. H. **(1996)**. The lack of a priori distinctions between learning algorithms. Neural computation. 8(7): 1341-1390.

Worden, K., Farrar, C. R., Haywood, J. and Todd, M. **(2008)**. A review of nonlinear dynamics applications to structural health monitoring. Structural Control and Health Monitoring. 15(4): 540-567.

Wu, J. R. and Li, Q. S. **(2004)**. Finite element model updating for a high-rise structure based on ambient vibration measurements. Engineering Structures. 26(7): 979-990.

Wu, Y.-X. **(1999)**. Sensitivity-based finite element model updating methods with applications to electronic equipments. Ph.D. thesis, : Faculte polytechnique de Mons, Belgium.

Yang, X., Zhao, Y., Chen, Y. and Zhao, X. **(2011)**. A multi-swarm cooperative perturbed particle swarm optimization. 225-226**:** 619-622.

Yeo, I., Shin, S., Lee, H. S. and Chang, S.-P. **(2000)**. Statistical damage assessment of framed structures from static responses. Journal of Engineering Mechanics. 126(4): 414-421.

Yu, E., Taciroglu, E. and Wallace, J. W. **(2007)**. Parameter identification of framed structures using an improved finite element model-updating method - Part I: Formulation and verification. Earthquake Engineering and Structural Dynamics. 36(5): 619-639.

Zang, C., Chen, G. and Ewins, D. **(2006)**. Finite element model updating with modal data. The 24th Internation-al Modal Analysis Conference. Saint Louis, USA z The Printing House Inc.

Zapico, J. L., González, M. P., Friswell, M. I., Taylor, C. A. and Crewe, A. J. **(2003)**. Finite element model updating of a small scale bridge. Journal of Sound and Vibration. 268(5): 993-1012.

Zárate, B. A. and Caicedo, J. M. **(2008)**. Finite element model updating : Multiple alternatives. Engineering Structures. 30(12): 3724-3730.

Zhan, Z. H., Zhang, J., Li, Y. and Chung, H. S. H. **(2009)**. Adaptive particle swarm optimization. IEEE Transactions on Systems, Man, and Cybernetics, Part B: Cybernetics. 39(6): 1362-1381.

Zhang, Q., Chang, C. and Chang, T. **(2000)**. Finite element model updating for structures with parametric constraints. Earthquake engineering & structural dynamics. 29(7): 927-944.

Zhang, Q. W., Chang, T. Y. P. and Chang, C. C. **(2001)**. Finite-element model updating for the Kap Shui Mun cable-stayed bridge. Journal of Bridge Engineering. 6(4): 285-294.

Zhao, X. and Wang, W. **(2010)**. An AntiCentroid-oriented Particle Swarm Algorithm for Numerical Optimization. Artificial intelligence and computer science, Lecture Notes in Computer Science. 6320 LNAI: 302-309.

Zheng, Y. L., Ma, L. H., Zhang, L. Y. and Qian, J. X. **(2003)**. On the convergence analysis and parameter selection in particle swarm optimization. International Conference on Machine Learning and Cybernetics.

Zivanovic, S., Pavic, A. and Reynolds, P. **(2007)**. Finite element modelling and updating of a lively footbridge : the complete process. Journal of Sound and Vibration. 301(1-2): 126-145.